# The Everglades Landscape Model:

## *Summary Report of Task 2, Model Development*

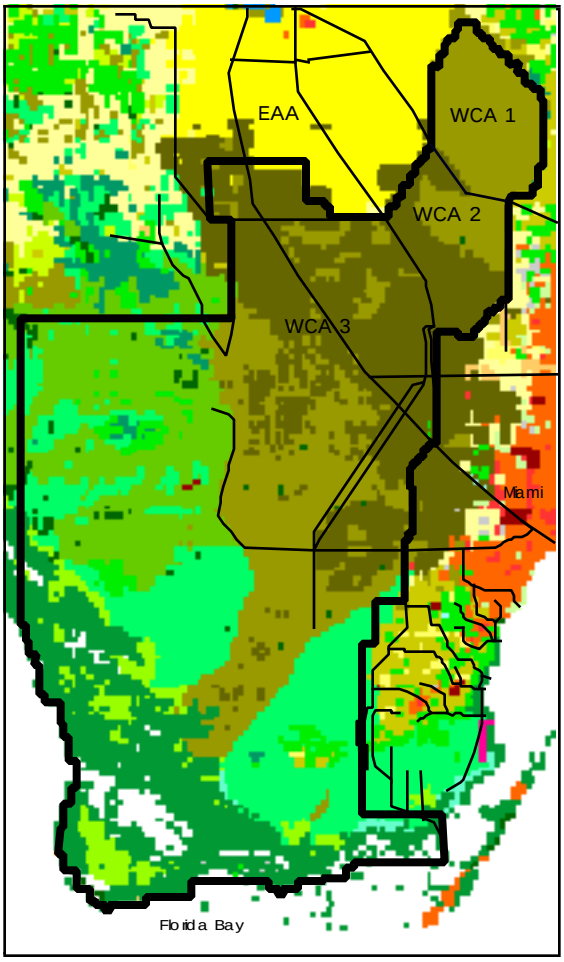


H. Carl Fitz
Robert Costanza
Enrique Reyes

Institute for Ecological Economics
Center for Environmental and Estuarine Studies
University of Maryland System
Box 38, Solomons, MD 20688-0038 USA

September 30, 1993

# CONTENTS

Blank Page

# EXECUTIVE SUMMARY

## Objectives

A regional landscape simulation model that can address the effects of different management scenarios on the ecosystems in the Everglades is being developed as part of the integrated Everglades Research Plan of the South Florida Water Management District (SFWMD). The Everglades Landscape Model (ELM) will be one of the principal tools in a systematic analysis of the varying options in managing the distribution of water and nutrients in the Everglades. It will:

1) provide a *tool to estimate the water demands* of the Everglades in terms of adequacy of water flow and water levels to achieve user-defined landscape/ecosystem characteristics;
2) *predict changes in vegetation* that result from specific hydrology and water quality regimes, simulating the inter-relationships among water quality, hydrology, and vegetation, and thus the influence of these relationships on habitat quality; and
3) take advantage of sophisticated hardware/software, allowing the model to be *easy to use and modify*.

## Model structure

Central to the ELM structure is the division of the landscape into square grid cells (10,178 in this implementation) that are used to identify components of the landscape in digital form. Superimposed on this grid network are the vector lines of canals that cross the region. Using a variety of state-of-the-art software tools and hardware, the ELM is a regional scale, spatially articulated simulation model that incorporates four fundamental pieces.

- First, the model parameters that are constant within a given habitat (such as maximum specific rate of plant primary production), and the time series data (such as rainfall) that drive the model are contained in customized data bases for input to the model.
- Secondly, spatial data of attributes such as habitat type and elevation that may vary significantly within the landscape are contained in digital map files.
- The third principal component of the ELM structure is the "unit" model. It is the most basic building block of the ELM, simulating the temporal dynamics of important biological and physical processes within ecosystems found in the Everglades. Different habitats within the model have unique parameter sets determined within the databases, but all habitats run with the same general unit model structure.
- The cells are linked by the spatial articulation of the ELM, providing the mechanism for water, and its dissolved and suspended matter, to flow between cells and through canals. This is the fourth component of the ELM: this spatial modeling code drives the ELM by integrating all of the components, providing the mechanism for changing the landscape with time (succession), and coordinating input/output.

The computer platform that the ELM optimally uses is that of a parallel processing environment. We currently are running the model on 24 transputers that are installed in a high-end Macintosh computer serving as the front end, providing an interface that greatly facilitates the use of the model. We also have the capability to use a massively parallel supercomputer (CM-5) or, less optimally, the drivers are available to run the code on Unix workstations.

## Model boundaries and scales

Figure 1 and the cover of the report indicate the ELM boundaries, which basically encompass the natural system of the Everglades and Big Cypress, omitting the urban areas of the lower East Coast and the agricultural regions. These boundaries alleviate the need to model the significant complexity of the latter areas, yet provide a simulation tool to analyze the response of the natural system to altered hydrologic and nutrient regimes due to management decisions.

Also shown in Figure 1 is the 1 $km^2$ grid cell size in relation to the model area. We currently make the assumption that each cell is homogenous in its vegetation composition and

other characteristics, but will be incorporating statistically weighted model parameters (such as plant primary production rates) in proportion to the area of different habitat types in each cell. The model runs with a daily time step, and is scaled to exhibit monthly or seasonal changes in model results such as plant biomass or species composition. Typical scenario simulations will encompass several decades, perhaps as many as 50 years depending on the objective.

## Processes simulated

The ELM simulates fundamental ecological processes with the objective of quantifying the response of vegetation to the varying environment. Hydrology is fundamental to the model, with 3-dimensional flow of water within the landscape. Many of the hydrologic algorithms are based on those developed for the South Florida Water Management Model, but with some changes towards finer scales and in some aspects of the mass balance accounting. The growth of the macrophyte and periphyton communities responds to available nutrients, water, sunlight and temperature using documented algorithms. The hydrology in the model responds directly in turn to the vegetation via linkages such as the Manning's roughness coefficients' dependence on dynamic plant density and composition, and transpiration losses being dependent not only on physical heat flux but on plant canopy conductance and response to water limitation. The nutrient cycles of both phosphorus and nitrogen are simulated so that a basic, but realistic, portrayal of the availability of nutrients is possible. Fire is an important part of the simulation and is based on a variety of habitat characteristics such a fuel quality and moisture. By keeping track of the historical nutrient availability, hydroperiod, and fire severity of the cells in the model, a (developing) habitat transition algorithm alters the habitat pattern and associated model parameters.

## Utility

The ELM is a tool to analyze the interaction of hydrology, nutrients, and vegetation growth on a systematic, landscape level scale. The degree of complexity associated with its development has been incrementally increasing as the model development process continued. One of the key issues that has slowed some development has been obtaining appropriate hydrologic data, including exact canal and levee locations and attributes, soil types, and accurate elevation data. Similarly, one of the principal issues that needs addressing in the near and long term for a more accurate ELM is that of strengthening the available ecological dataset. Though there are data that can support the ELM for a reasonable degree of utility, a more systematic research program is desirable to obtain better estimates for elevation, rainfall and evaporation throughout the region. Biological processes such as nutrient requirements by plants and succession are incompletely known, as are estimates of plant growth, senescence and mortality over time.

As the ELM stands, the major model developmental steps and their implementation have been achieved. We have all of the major structural attributes in place in the model, with the associated computational algorithms. At this point, we will be beginning the extensive calibration and verification stages, then completing the project by producing specific scenario analyses and making the model available for use by the District.

## Code/databases delivered

In addition to various documents (including this one) that report on descriptions of the model development and initial results, the following components of the ELM have been transferred to the District. Integration of all of these components is the ELM.

### Unit model

- A 20[1] state variable, ecosystem-level model. Written and debugged using STELLA® dynamic simulation software package. Calibrated to a low/moderate level of confidence depending on the habitat involved.

---

[1] 25 state variables appear in the unit model diagram, but 5 of those have that designation due to specific characteristics of the STELLA™ modeling program and do not represent standing stocks.

**STELLA®-to-C code Translator**

• Translates equations output from debugged STELLA® model into C code for running simulation without STELLA®. An executable program that runs on Macintosh computers, it was written in the C programming language using ANSI standards.

**Spatial Modeling Package**

• Code that integrates data (spatial and non-spatial), the unit model, and interface(s) to run a simulation in space and time. Written in ANSI C code, the drivers are written for transputers installed in Macintosh computers, a massively parallel CM-5 supercomputer, and Sun workstations.

**Canal routing algorithms**

• Algorithms (and explanatory text) to place canal vectors over a raster grid of landscape cells, determining the exact area of interaction between canals and the cells. These algorithms (mostly developed) also allow the implementation of the SFWMD's (serial) canal flux algorithm into a form that runs in the parallel processing environment that the ELM uses.

**Habitat-specific databases**

• Series of linked, pseudo-relational databases for the ecological/hydrologic data in the habitats simulated in the ELM. Developed using Filemaker® Pro for the Macintosh, each contains the numeric data and comments, citations, and other data attributes. These habitat databases are linked into one Central database which exports one datafile to the Spatial Modeling Package.

**Spatial databases**

• Set of Geographic Information System (GIS) databases including land use in 1900, 1953 and 1973, elevation, permeability, and other spatial data for direct input to the spatial model. All are in 1 $km^2$ raster format using MAP II® on the Macintosh, and can be exported to other GIS packages such as GRASS and ARC/INFO.

**Unit model interface**

• Guide to the model structure, simulation capabilities, and assumptions. Developed using HyperCard, which is a graphical based, hypertext language for the Macintosh computer. This interface enables more effective communication and understanding of the processes that are incorporated into the unit model.

**Database interface**

• Guide to the databases for each biological habitat simulated in the ELM. Developed using HyperCard for the Macintosh, this provides an overview of the structure of the databases and their linkages.

**Spatial model interface**

• Guide to editing the runtime parameters, including input data and output data needs. Developed using HyperCard for the Macintosh, this provides a user friendly means of implementing a spatial simulation run for varying scenarios.

INSERT .i.Figure 1;

# INTRODUCTION

## Scope of report

We have previously (Costanza et al., 1992a; Costanza et al., 1992b; Costanza et al., 1992c) provided reports on: a) the steps in conceptualizing the Everglades Landscape Model (ELM) via a workshop process; and b) significant aspects of the model structure and processes that were to be simulated. With approval from the South Florida Water Management District, we then proceeded with full model development, and have designed and implemented the large number of components of the spatially articulated ELM. Because our feasibility assessment report (Costanza et al., 1992c) described many of the fundamental attributes of the model, we will not repeat such information in detail within the current report. This report describes many of the algorithms and development steps that were previously outlined. This includes the algorithms for simulating ecological processes, the logic of water flow within canal networks and the canal-cell interactions, our means of data organization, the steps in map processing, means of evaluating scale-dependent issues, and the software that integrates most of these model components. In a model of this large areal extent and process complexity, compromises between decreasing computational complexity and increasing realism are necessary. Many of the issues associated with this tradeoff were discussed in the series of workshops described in the referenced reports. In the current report, the arguments behind various decisions are not reiterated. Thus, for the reader to understand much of the rationale behind the ELM conceptualization, a perusal of the prior feasibility assessment report (Costanza et al., 1992c) is recommended.

The scope of the current report is of a more technical nature, wherein we show how the concepts have been implemented into working algorithms and models. At this point, we have developed virtually all of the components of the ELM, and are about to integrate them into the ELM for calibration. However, we believe that improvements in some of the modules will occur as we run the model in the calibration process. In particular, we hope that this report may allow others involved in the prior stages of development to point out aspects of the model that could benefit from either simpler or more sophisticated structure. We present this report as a more detailed representation of how the ELM is being implemented, but NOT as the final version that will be presented in the final report of Task 3. The contents of this report represent working versions of the model and carefully designed algorithms that are about to be fully integrated into the working, spatially explicit ELM. We welcome feedback in the very near future.

## ELM function

The ELM is to serve as one of the principal tools in a systematic analysis of the varying options in managing the distribution of water and nutrients in the Everglades. Water quantity, and the associated hydroperiod, has been a central issue in understanding the ecosystem health (Costanza et al., 1992) of the Everglades. Nutrients from agricultural areas also appear to be important in understanding vegetation succession (Davis, 1991) in this historically oligotrophic system (Steward and Ornes, 1975). The interaction of these factors, including the frequency and severity of fires, appears to drive the succession of the plant communities in the Everglades (Duever, 1984; Gunderson, 1989). Thus this system has myriad indirect interactions, constraints and feedbacks that result in complex ecosystem structure (biotic and abiotic components and their flow pathways) and function (the modes of interaction and their rates). For this reason, it is critical to develop a systems viewpoint towards understanding the dynamics inherent in that ecosystem structure and function. Part of this process is the development of a dynamic spatial simulation model. The ELM will provide that analytic tool.

In this model, the important ecosystem processes that shape plant communities are simulated within the varying habitats distributed throughout the landscape. The principal dynamics within the model are: plant growth in response to available sunlight, temperature, nutrients, and water; flow of water plus dissolved nutrients in three dimensions; fire initiation

and propagation; and succession in the plant community in response to the historical environment. Using a mass balance approach in incorporating process-based data of a reasonably high resolution within the entire Everglades landscape, changing spatial patterns and processes can be analyzed within the context of altered management strategies. Only by incorporating spatial articulation can an ecological model realistically address large scale management issues within the vast, heterogeneous system of the Everglades.

## ELM structure

For the spatially explicit ELM, the modeled landscape will be partitioned into a spatial grid of 10,178 square unit cells, each having 1 $km^2$ surface area. The ELM is hierarchical in structure, incorporating an ecosystem-level "**unit**" model that is replicated in each of the unit cells representing the Everglades landscape (Figure 2). The unit model itself is divided into a set of model sectors that simulate the important ecological (including physical) dynamics using a process oriented, mass balance approach. The hydrologic sector of the unit model is a fundamental driving force, simulating water flow vertically within the cell . Hydrology and hydrodynamics, nutrient, plant, consumer, fire, detritus, and sediment dynamics are some of processes that are simulated within sectors of the unit model. While the unit model simulates ecological processes within a unit cell, horizontal fluxes across the landscape will occur within the domain of the broader **spatial** model of the ELM. Such fluxes will be driven by cell-cell head differences of surface water and of ground water in saturated storage. Within this spatial context, the water fluxes between cells carry dissolved and suspended materials, determining water quality in the landscape.

Whereas the same generic unit model structure will be run in each cell, there is a suite of parameter sets that will serve as input to the model to accommodate the different habitat types within the landscape. As indicated in Figure 2, a set of values of standing stocks, rate parameters, etc. that are specific to the cell's habitat type will be input to the unit model for each unit cell. The vegetation communities in the cells will respond to changing hydrologic, nutrient and fire regimes via successional switching algorithms which are defined by current ecological knowledge. Thus, when run within the spatial framework of the overall ELM, the landscape response to hydrology and water quality will be effectively simulated as flows of material occur between adjacent cells.

This modeling project encompasses the interactions of a wide range of biological and physical processes to simulate ecosystem dynamics over a large landscape. Therefore this model has a fairly high degree of complexity, both conceptually in the detail of processes, and computationally in the implementation of fine scale process equations over a large spatial extent. For a complex model such as this, it is important that its design and results be effectively communicated to others; i.e., the model would be less useful if it were not well-understood for evaluation. In order to communicate the model's design and assumptions, we employed software tools that we have developed and that are available commercially. While the ELM is complex, its focus and assumptions are more easily understood than would be the case using standard software tools. For running the model, we are using state-of-the-art transputers that are ideally suited to grid based spatial modeling, yet are economical enough to be practical for desktop computing[2]. The ELM is running approximately 10,000 ecosystem level models at once, each communicating results to neighboring cells. Because the same problem (unit model) can be distributed across many processors, a parallel (distributed) processing environment is an efficient architecture for running the spatial model. We believe that the hardware and easy to use software components of the ELM will aid in making it more available and usable to the research and management community.

---

[2] The ELM is not limited to a transputer-based architecture. See the Spatial Model Hardware section for information on the other computer platforms that may be used to run the ELM.

# UNIT MODEL

## Overview

Because of the heterogeneity of the habitat types, ranging from mangroves to fresh marshes to hardwood forests, it was necessary that the unit model be generalized enough so that the ecological processes for all different habitats could be accommodated in a given landscape simulation. During the model feasibility assessment stage, we discussed preliminary versions of the unit model with the participants in a workshop process (Costanza et al., 1992a; Costanza et al., 1992b; Costanza et al., 1992c). Those developmental "beta" versions served as a focus of discussion of the types of ecological processes that the total ELM should be able to simulate. The consensus from those discussions was that certain aspects of the original, simplified unit model needed enhancement, resulting in a model that was significantly more complex than originally envisioned. The version of the ELM unit model that we are implementing is the Generic Ecosystem Model, or GEM v. 1.1, and a manuscript version of its description has been submitted for review (DeBellevue et al., submitted).

The unit model itself is divided into a set of model sectors that simulate the important ecological (including physical) dynamics using a process oriented, mass balance approach. This approach is particularly important in developing a generic ecosystem model, due to the need to simulate the underlying mechanisms associated with water flows, nutrient cycling, plant growth, etc. Using this approach, responses to inter-related control functions provide the mechanisms to initiate/terminate material flows among variables, avoiding any physical unrealities of "creating" matter in order to increase the mass of a state variable. Moreover, if a statistical, best-fit approach was the fundamental means to produce simulation output of a process such as macrophyte growth, the model would need to be modified for each of the vast set of different environmental conditions that are encountered both temporally and spatially. Such a model would be impractical for the range of conditions that will be included in ELM simulations. Importantly, the constraints and feedbacks associated with varying environmental conditions would not be operative in a statistically-oriented model and unrealistic output would invariably result. For example, macrophytes could "take up" nutrients associated with their statistically-defined carbon growth in a simulation, but phosphorus may be unavailable or limiting in reality due to slow decomposition of available organic material. In that instance, the nonsensical result would be that "non-existent" phosphorus would be taken up by plants as a result of unconstrained growth, thus ignoring mass conservation laws.

The unit model, however, maintains bookkeeping algorithms for the availability of various types of matter, including system inputs, outputs, and internal cycling. In the instance of plant growth in the presence of low nutrient concentration, that concentration of available nutrients limits carbon uptake by the macrophyte. Thus the plant growth, and its associated nutrient uptake, would be constrained by nutrient availability, and nutrient mass would be conserved (as opposed to uptake of non-existent nutrient mass). In all aspects of the ELM, i.e. in the unit model and in the spatial model, the conservation of mass of carbon, water, nutrients, sediments and salts is maintained by the structure of the model with its cycling and feedbacks, and indeed is fundamental to the process-driven foundation of the ecological modeling.[3]

Hydrology and hydrodynamics, nutrient, plant, consumer, fire, detritus, and sediment dynamics are some of processes that are simulated within sectors of the unit model (Figure 3 and Figure 4). The hydrologic sector of the unit model is an important driving force, simulating water flow vertically within the cell. While the unit model simulates ecological processes within a unit cell, horizontal fluxes across the landscape will occur within the domain of the broader spatial model of the ELM. Such fluxes will be driven by cell-cell head differences of surface water and of ground water in saturated storage. Within this spatial

---

[3] The calibration step is still extremely important, and involves a statistically derived fit of the model to observed data. However, a well-calibrated ecological/physical model that incorporates responses to underlying constraints and/or feedbacks will eliminate the need to recalibrate a response to the many variations in the inputs.

context, the water fluxes between cells carry dissolved and suspended materials, determining water quality in the landscape.

We are using this version of the unit model to implement the first version of the spatially articulated ELM. We emphasize that this is not the final version for the project. Sensitivity analyses and other model evaluations (see the Sensitivity Analysis Section) indicated that several of the biotic modules, including the hydrologic sector, should be improved upon. We will be performing more extensive evaluations of the model's code and make corrections/refinements in the future during the continued calibration process.

## Unit model use

The unit model can be run using STELLA® II 2.2.2 on a Macintosh computer. We recommend that the model is run on a Macintosh with at least a 68030 microprocessor, such as a Macintosh IIci with at least 3 free megabytes RAM allocated to run the application. Different scenarios may be simulated by varying the inputs, boundary conditions, or model parameters. Table 1 is a very basic example of only a small subset of the model parameters that can be changed for varying scenarios. The large number of model interactions can not be adequately portrayed in a simple table; however, we provide a few examples of some of the more obvious results of manipulating parameters associated with macrophytes and hydrology. A thorough understanding of the interactions and feedbacks within the model is necessary before extensive scenario alterations are made, but a small number of minor adjustments to the model should be possible without extensive study. (Most of the model equations are reasonably-well documented at this point. More extensive documentation will be added during Task 3 documentation).

| Description | Name | Direct/Indirect results |
|---|---|---|
| Rainfall | sf_wt_from_rain | Many, particularly influencing the amount of water available for plant uptake, ... |
| Surface water head in surrounding cells | Sf_wt_W_head, Sf_wt_E_head | Many, particularly influencing the amount of water available for plant uptake, ... |
| Ground water head in surrounding cells | Sat_wat_West_head Sat_wat_East_head | Many, particularly influencing the amount of water available for plant uptake, ... |
| Hydraulic (saturated and unsaturated) conductivity, infiltration rate | sat_hydrol_conduct rc_unsat_Hyd_cond rc_sf_wt_infilt | Many, particularly influencing the amount of water available for plant uptake, ... |

Due to the large number of interactions and cascading effects of different actions within the model, GEM is structured to include various threshold responses and maximum attainable rates and stocks. In this fashion, a complex model can be maintained within the ranges of observed, or reasonable, values. Thus, even though there are a large number of interactions and possibilities for the propagation of error through the simulation, when the model is effectively calibrated it can be trusted to stay within appropriate bounds of output due to these constraints. Maximum attainable standing stocks, minimum threshold responses, etc. are all easily changed by the user, based on appropriate data.

The unit model was developed using STELLA® to allow the user to most easily discern the linkages among the model sectors. The initialization of state variables and the modification of rate constants and model parameters is facilitated by placing aliases (=copies or "ghosts") of those parameters in central locations within each sector. Figure 5 is a "map" of the sector locations for user navigation within the model diagram.

## Unit model structure/equations

### Conventions

The following descriptions of the different sectors of the model incorporate many of the principal equations that describe the fluxes associated with state variables and the functions that provide feedbacks to some of the biological and/or physical processes. In the text body we present the logic of many of the algorithms used in the model to generate the flow of material or information. In order to maintain a seamless link between the model and the text, we maintain the full variable names in accordance with their use in the STELLA® model. A generalized schematic diagram of the model is provided in Figure 4.

We assume that the area included in the model boundaries is homogenous in most respects. Text in ALL_CAPS indicates a state variable, and is given in this format when first defined in the text and in all tables and equations. Text that is *italicized* represents auxiliary variables and parameters when first defined within a sector and when used in equations and lists. Otherwise, variables and parameters will be spelled out completely, unitalicized, when used in other contexts within the text. Within the equations in the text, variables and parameters given in **bold,** standard text represent Boolean statements and intrinsic functions. Parameters preceded by *rc_* are rate constants; variables appended by *_fb* are feedback control functions.

### Global Inputs Sector

Daily solar radiation is simulated by an algorithm based on that by Nikolov and Zeller (1992). This procedure uses standard calculations for determining daily solar radiation at the top of the atmosphere based on julian date, latitude, solar declination, and other factors. Nikolov and Zeller (1992) developed a regression relationship of mean monthly cloud cover that was based on precipitation, humidity, and temperature data. For the unit model, we developed a data input file of simulated monthly cloudiness based on the Nikolov and Zeller (1992) algorithm, requiring only the three (daily) data sets listed above. We used these monthly atmospheric input data in an algorithm that determined the average daily irradiance at a altitude of 274 m above MSL. Finally, a Beer's law relationship was used to account for attenuation through the atmosphere at different altitudes/solar elevations, thus determining the daily radiation (*SolRadGrd* in $cal*cm^{-2}*d^{-1}$) received at the earth surface at any elevation, latitude, or time of year in the northern hemisphere.

### Hydrology Sector

Water is held in three state variables, with potential flux among the variables dependent on a variety of simulated processes. 1) SURFACE_WAT is water that is stored above the sediment/soil surface; 2) UNSAT_WAT is stored in the pore spaces of the sediment/soil complex, but not saturating that zone; 3) SAT_WAT is water saturating the pore spaces of the sediment/soil complex. Daily precipitation values are input data to the model. Surface water **r**unoff, evaporation, and infiltration, and saturated/unsaturated water transpiration are some of

the more critical fluxes for accurate simulation of water storages (at daily time scales) in most systems to be considered. In general, we ignore some of the details of processes that occur on a time scale faster than the daily time step used in the unit model. Thus, the longer term results of storage in a small landscape can be effectively captured within the day-to-weekly time scale.
*Surface water flows* -- Runoff is first in calculation dependencies, in that the volume that can runoff in one time step is calculated before infiltration and evaporation fluxes. Runoff is determined by the use of Manning's equation for overland flow, based on the hydraulic head difference between cells. Whereas the unit model is designed to work as 1) a unit model in a spatial model context or 2) as a single ecosystem model, we provide only two directional pathways of flow (east and west) for simplicity. In the spatial modeling context, the flux equations would operate in the four directions of the compass. While input and output flows can occur in two compass directions, an example equation of potential flow from the current cell to the eastern boundary is:

if ( $Sf\_wt\_E\_head < Sf\_wt\_Head$ ) then

$$Sf\_wt\_E\_out = \sqrt{\frac{Sf\_wt\_Head - Sf\_wt\_E\_head}{\sqrt{sf\_wt\_area}}} \quad \frac{Sf\_wt\_depth^{5/3}}{Mannings\_coef}$$

$$pot\_pan\_evap = (0.00482 * C_T * C_W * C_H) * SolRadGrd / 585$$
$$C_T = 0.463 + 0.425(T / T_0) + 0.112(T / T_0)^2$$
$$C_W = 0.672 + 0.406(W / W_0) - 0.078(W / W_0)^2 \quad \textbf{(3)}$$
$$C_H = 1.035 + 0.240(H / H_0) - 0.275(H / H_0)^3$$

where 585 cal/g latent heat of vaporization is used in conversion of solar radiation from cal · $cm^{-2}$ · $d^{-1}$ to it's water equivalent of cm/d. $C_T$, $C_W$, and $C_H$ are coefficients related to temperature ($T$ in ˚C), wind speed ($W$ in km/hr), and humidity ($H$, proportion from 0-1), respectively. Parameters subscripted with 0 (such as $T_0$) are reference values in Christiansen's (1968) model. If adequate pan evaporation data are available, actual evaporation is determined by the reduction of the pan evaporation flux by a temperature dependent pan evaporation coefficient.

*Saturated and Unsaturated water* -- Loss of water by plant transpiration occurs either from the unsaturated or saturated water storages depending on the presence/absence of roots in saturated zone. We have a gradation between physical and biological controls on this flux term, with the choice dictated by the vegetation type, water availability, and model scale. There are two basic mechanisms controlling evaporative losses through the plant canopy. First, the degree of coupling between the canopy and atmosphere influences the degree to which purely physical processes drive the transpirative loss. Secondly, the degree to which water is limiting, and thus stressing plants, simulates the reduction in transpiration (and thus primary production at some point) due to stomatal closure and changed canopy conductance. Because of the importance of evaporation and transpiration to this wetland model, we analyze the effects of this parameterization closely in the unit model Sensitivity Analyses section, where a thorough description of the evaporation and transpiration algorithms is provided.

Horizontal flow of water in saturated storage was determined using the simplifying assumptions of steady, unidirectional flow in an unconfined aquifer. The basic Darcy equation was then applied for groundwater flow for each of two directions (as explained above), with the following example for flux to the east:

**if** $tot\_water\_head > SAT\_wat\_East\_head$ **then**

$$Sat\_wt\_E\_out = \frac{(tot\_water\_head - SAT\_wat\_East\_head)}{\sqrt{cell\_size}} \quad \textbf{(4)}$$
$$sat\_hydrol\_conduct \ \sqrt{cell\_area} \ \ sat\_water\_hd$$

**else** 0

where *tot_water_head* is the total water head (m), the sum of the saturated water head plus the surface water height (if the saturated water height reaches the sediment/soil surface); *SAT_wat_East_head* is the hydraulic head (m) outside the cell to the east; *sat_hydrol_conduct* is the saturated hydraulic conductivity (m · $d^{-1}$); and s*at_water_hd* is the hydraulic head of the saturated water (m).

Vertical fluxes of water occur between all three of the water storage compartments. If surface water is present, and there is available storage in the unsaturated storage, a volume water infiltrates into the unsaturated zone at a rate determined by the (daily) infiltration rate (m · $d^{-1}$) for the habitat type. When the sediment/soil is fully saturated, surface water may flow into the saturated layer to replace outflow from the saturated storage at a rate determined by the loss of saturated water. Thus, we assume that the rate of vertical movement of water from the surface to the saturated zone is at least as fast as that of losses from saturated storage via horizontal flow plus transpiration. Similarly, water in saturated storage flows into surface

water storage when the total capacity of the sediment/soil is exceeded, determined by the rate of horizontal saturated water flow into the cell.

Percolation from the unsaturated storage to saturated storage is determined by the hydraulic conductivity of the sediment/soil for unsaturated conditions. We make the simplifying assumption that the water in unsaturated storage is distributed homogeneously within that zone, again ignoring the presence of any wetted front and the heterogeneities associated with processes occurring on faster time scales than the daily time step used in the unit model. A maximum unsaturated hydraulic conductivity is determined for each habitat (soil/sediment) type, and the actual conductivity is mediated by the soil moisture. This determination is an empirically derived function, ranging sinusoidally from 0 to maximum (Dominico and Schwartz, 1990) as shown in Figure 6.

Percolation flow ($m^3 \cdot d^{-1}$) is simply the saturated (vertical) hydraulic conductivity (m/d) multiplied by the surface area in the system. With a rising water table, water in the lower part of the unsaturated zone becomes part of the saturated water storage, and thus the moisture within the unsaturated zone is added to saturated storage (for accounting purposes). Then the total volume allocated from the unsaturated to saturated zone ($m^3 \cdot d^{-1}$) is:

$$unsat\_to\_sat\_fl = \textbf{if } unsat\_moist\_prp < 1.0 \textbf{ then } unsat\_perc + sat\_add\_fm\_rise \textbf{ else } UNSAT\_WATER / DT \quad \textbf{(5)}$$

where *unsat_moist_prp* is the dimensionless proportion of water to pore space in the unsaturated zone, *unsat_perc* is the flux of water ($m^3 \cdot d^{-1}$) percolating from unsaturated storage to saturated, and *sat_add_fm_rise* is unsaturated water ($m^3 \cdot d^{-1}$) that is allocated to saturated storage with a rise in the saturated water table. At the point that surface water infiltrates into the unsaturated storage such that it becomes completely saturated, all of the unsaturated water is allocated to saturated storage in one time step, (a discontinuity that is a relatively small "flux" under normal conditions).

**Hydrodynamics Sector**

In shallow surface water (<3 m?), the unit model will simulate the hydrodynamics associated with the transfer of wind energy to water, calculating the stress effect of wave and current induced turbulence near the bottom sediments. This energy drives the suspension and deposition of sediments, which in turn affects water clarity within the system. In the spatial modeling context, sediments can be transported while in suspension. For the purposes of the unit model, we assume that 1) water density is constant; 2) surface tension is negligible; 3) Coriolis force is negligible; 4) only one set of waves is considered at a time; 5) the sediment surface is a horizontal, fixed boundary that does not absorb energy; and 6) wave amplitude is small and the waveform invariant within the time and space scales considered. While the first three assumptions are reasonable for most situations that the unit model is applied to, assumptions 4-6 involve issues of the area considered in the model, and can be considered reasonable in most situations if sufficiently small cells are used in a spatial model.

*Wave and current simulation* -- The wave dynamics in the unit model are estimated by wave prediction equations for transitional depth water, where the depth:wavelength ratio is between 1:25 and 1:2 (USACOE, 1984). The unit model will not necessarily predict wave erosion accurately when waves are limited by the duration of wind events. Wave development that is duration-limited occurs in water bodies exceeding several square kilometers, whereas fetch-limited conditions are more typical for smaller areas. We use USACOE (1984) for determining the wave height and period in the following series of equations. After determining the fetch distance for a given wind direction within the cell, a series of algorithms calculate a local wave height using information on wind speed, fetch distance and water depth. Both of the latter corrections convert distances into dimensionless parameters using the gravitational constant. For instance, the dimensionless depth parameter used in determining local wave height is determined by:

$$D\_less\_depth = \frac{Sf\_wt\_depth * G}{Wind\_speed^{2}} \quad \textbf{(6)}$$

where *D_less_depth* is the dimensionless fetch parameter, *Sf_wt_depth* is the distance of open water over which waves travel (m), *G* the gravitational acceleration ($m \cdot sec^{-2}$), and *Wind_speed* is in $m \cdot sec^{-1}$. The STELLA® software does not support an intrinsic hyperbolic tangent function needed in the calculation of wave height. Therefore we developed a graphical algorithm to approximate tanh(X), where X is any expression. This algorithm is then used in calculating intermediate parameters involving depth and fetch parameters, solving the following relationship:

$$depth\_H\_corr = \mathbf{tanh}\left(0.530 \quad D\_less\_depth^{0.75}\right) \quad \textbf{(7)}$$

where *depth_H_corr* is the intermediate result involving the hyperbolic tangent of the dimensionless depth parameter, **tanh** the hyperbolic tangent function, and 0.530 an empirical constant. A similar technique is used to determine a second intermediate result involving fetch, *fetch_H_corr*. These intermediate results are then used in solving the following equation for local wave height:

$$Loc\_Wave\_height = \frac{0.283 \quad Wind\_speed^{2} \quad depth\_H\_corr \quad fetch\_H\_corr}{G} \quad \textbf{(8)}$$

where 0.283 is a dimensionless empirical constant.

This waveheight is then expressed as wave energy (USACOE, 1984 pgs 2-26) Energy can be added to the cell when the unit model is applied in a spatial context and wave energy is propagated from outside the cell. Energy is also dissipated due to bottom friction as waves travel within the cell. From the combined energy of such inputs/outputs, the actual wave height *(Wave_height)* within the system is calculated from this total energy.

The wave period is determined from algorithms similar to those used in wave height calculations (USACOE, 1984), wherein intermediate results are found involving the hyperbolic tangent function and empirical constants (see above). The wave period is determined by:

$$Wave\_period = \frac{7.54 * Wind\_speed * depth\_T\_corr * fetch\_T\_corr}{G} \quad \textbf{(9)}$$

where *depth_T_corr* and *fetch_T_corr* are the intermediate results involving depth and fetch. Likewise, the *wave_Length* is calculated following the USACOE (1984). We then determine the wave orbital velocity for waves in water of transitional relative depth using Linear (Airy) theory (USACOE, 1984).

$$Wave\_orbit\_velo = \frac{Wave\_height * G * Wave\_periodt}{2 * Wave\_Length} * \frac{2}{\mathbf{EXP}\left(\frac{2 * PI * Sf\_wt\_depth}{Wave\_Length}\right) + \mathbf{EXP}\left(\frac{-2 * PI * Sf\_wt\_depth}{Wave\_Length}\right)} \quad \textbf{(10)}$$

where *Wave_height* is the actual wave height (m), and *Sf_wt_depth* is the depth of the surface water (m).

*Shear stress* -- The unit model calculates shear stress in streams differently than in open water such as a lake. We calculate a shear stress that is a function of the interaction of wind-induced wave motion and currents (Grant and Madsen, 1979):

$$\begin{aligned} Shear\_stress = {} & 0.5 * fric\_coef * Fluid\_density \\ & * [1.0 + current\_corr^2 + 2.0 * current\_corr \\ & * \mathbf{COS}((\mathbf{ABS}(Current\_direction - Wind\_direction) * 0.8))] \\ & * \mathbf{ABS}(Wave\_orbit\_velo) \end{aligned} \quad \textbf{(11)}$$

where *fric_coef* is the friction coefficient that varies with the extent to which the turbulence is due to wave vs. current velocities, *Fluid_density* is the density of water ($kg \cdot m^{-3}$), and *current_corr* is the ratio of current velocity to wave orbital velocity. The shear stress is used in the Inorganic Sediments Sector and the Deposited Organic Matter Sector, where it is used to suspend sediments above threshold resistances.

**Inorganic Sediments Sector**

The inorganic (mineral) sediments sector is the foundation for the terrestrial and wetlands soil and open water sediment submodels. It includes two state variables that represent an aggregate of all sizes of mineral particles. One state variable represents those sediments that are part of the deposited sediment (DEP_INORG_SEDS). The other represents suspended sediments (SUS_INORG_SEDS).

Deposited inorganic sediments are suspended in the presence of surface water as a function of the shear stress calculated in the hydrodynamic sector. Erosion occurs by first suspending sediments, then exporting them in runoff water. As described in the Hydrodynamics sector, a shear stress due to waves/currents is determined each time step. This shear stress on the sediment is compared to the shear resistance, which is an empirical function of the root density of macrophytes and the inverse of the proportion of organic material in the sediments. Sediment suspension occurs in layers that depend on the extent of erosion during the prior time step, wherein if the potential erosion at time $t_i$ is less than that which occurred one time unit previously $t_{i-1}$ then no erosion will occur because it is assumed that the sediments underlying the eroded material are more consolidated (less fluffed), and thus will not erode as readily. However, that layer is subject to erosion if the potential for erosion is greater than during the prior time step:

$$eros = \mathbf{MAX}[Pot\_Eros - \mathbf{DELAY}(Pot\_Eros, 1), 0] * cell\_area \quad \textbf{(12)}$$

where *eros* is the volume ($m^3$) of (organic and inorganic) sediment that is actually eroded in one time unit, *Pot_Eros* is the depth (m) of (organic and inorganic) sediment that may be potentially eroded due to the difference between shear stress and shear resistance, and *cell_area* is the surface area ($m^2$) of the cell. In this example, the **DELAY** function is an intrinsic function in STELLA® that returns the value of *Pot_eros* from the prior (1) time unit. The actual mass of inorganic sediments eroded are determined by multiplying the volume of eroded sediments by the proportion of sediments that are inorganic and their bulk density.

Suspended inorganic sediments many enter/leave the cell as a function of surface water inflow/outflow as calculated in the hydrologic sector. Sediments are deposited from the suspended stock under low shear stress conditions, i.e., when shear stress is less than fluid mud yield. Another input is the precipitation of calcite by periphyton photosynthesis, forming a calcite mud substrate which forms a major soil type in some regions, e.g. where we are applying the model in south Florida (Browder, in press). This is an example of a flux that may easily be rendered inoperative (deleted or zeroed out) without other effects on the model, if it is deemed unimportant to the system of interest.

The sediment depth may change due to decomposition of organic material and the suspension/deposition of sediment/soil. We dynamically determine sediment elevation depending on the masses of the sediment block, using a function of the volumes of pore space and the inorganic and organic sediments. The block volume of the organic and the inorganic sediment masses (without pore space) is determined from the mass and the standard density of

the organic and of the inorganic constituents. The total sediment volume is then the sum of the block volume of inorganic sediment/soil plus the block volume of the organic component plus the pore space volume. Sediment elevation is then determined from the volume and the total cell area. Over long time scales, sediments can also downwarp, moving part of the sediment/soil block down below the base datum of reference, thus effectively being lost from the system. We describe them as a function of simple constant rate:

$$DIS\_dn\_warp = rc\_downwarp \;\; cell\_area \;\; (1 - Porosity) \;\; DIS\_part\_density \qquad \textbf{(13)}$$

where *rc_downwarp* is the rate of geologic downwarping (m/d), *porosity* is the proportion of sediment/soil structure that is occupied by pore space, and *DIS_part_density* is the average density of inorganic material in the sediments ($kg \cdot m^{-3}$). These dynamics of sediment elevation are most important in Florida Bay coastal areas in relation to the height of the surface (sea) water.

**Chemical sectors: general dynamics**

Chemical state variables include inorganic nitrogen, phosphorous, oxygen, and salt, each within a separate sector. The chemical sectors have certain common structures and dynamics which will be discussed here and not repeated for individual sectors. Nitrogen, phosphorus, and salt are divided into those that are dissolved in surface water and those that are dissolved in sediment pore water, the latter being the total of saturated and unsaturated water storage stocks. Oxygen is explicitly considered only within the surface water. Concentrations of each dissolved chemical are calculated from the mass of the chemical and the water volume of its storage stock. Whereas a vertical oxygen profile is simulated within the surface water, the other chemicals are assumed to be homogenous within its storage volume. Thus, the concentration of chemicals in the sediment water are assumed to be distributed evenly throughout the water of *both* the saturated and the unsaturated zones of water.

All chemicals dissolved in surface water can move in and out of the cell with the horizontal flows that are calculated in the hydrologic sector. Chemicals may also enter from precipitation, and some atmospheric exchanges can occur via diffusion and biologically-mediated processes. All chemicals that are simulated in the sediment water can flow across the sediment/water interface as a function of simple diffusion across a concentration gradient, or with the vertical water flows of upwelling or percolation/infiltration.

All chemicals dissolved in sediment water can enter and leave as constituents of saturated water flow that is calculated in the hydrologic sector. Because of the assumed homogeneity of concentration in both the saturated and unsaturated water components, a loss of chemicals (such as nutrients) via saturated (groundwater) flow also decreases the concentration in the unsaturated water zone. Similarly, mineralization or biotic uptake of nutrients in the aerobic zone are vertically stratified processes. We assume that the vertical fluxes of chemicals between the unsaturated and saturated zones is rapid enough to allow this equilibrium to occur between the different dissolved components in the vertical profile. This assumption appears reasonable where most of the dynamic processes that are being simulated occur within the shallow, upper zone of the profile, which is the case for the wetland systems in the Everglades. Chemicals dissolved in the sediment water can leave the system with recharge to the aquifer below the base datum.

**Salt (Conductivity) Sector**

Salts are not actively taken up or released by the biotic components, but the salinity (concentration of NaCl and potentially other "tracer" chemicals of interest) affects certain biological processes and the habitat type. In the current version of the unit model, the structural dynamics are established for salinity, but salinity does not directly affect biotic components. This is one example of where a module structure is established for future use. The structure and dynamics of the Salt Sector follow the above general discussion, but an accounting system is developed to allow salt to precipitate in crystalline form (SALT_CRYST).

This module allows salts to accumulate in the sediment with evaporation. Conductivity can also be estimated when this value is needed to affect certain chemical reactions.

**Dissolved Phosphorus Sector**

Available inorganic phosphorus is considered to be soluble orthophosphate in all of its forms, here simply designated as $PO_4$. Phosphorus is one of two nutrients that can potentially limit the growth of plants in a unit model simulation. The general chemical dynamics follow the outline above, but also includes losses due to plant uptake and gains due to mineralization of organic material.

Whereas phosphorus dissolved in surface water (PO4_SF_WT) may increase from precipitation or general atmospheric deposition, it is not lost to the atmosphere. Uptake of phosphorus in this module by algae is determined by a simple ratio of carbon to phosphorus (C:P) and is thus phosphorus uptake is determined by the amount of carbon fixed by the algae. Likewise, the rate of decomposition of organic material determines the rate of mineralization of this nutrient via the C:P ratio of the organic material suspended in the surface water column. Currently, the C:P ratio does not vary with time, only with the habitat type.

Uptake and mineralization of phosphorus in the sediment water (PO4_SED_WT) are determined in the same manner as described for the surface water phosphorus, with the replacement of algae by macrophytes for uptake. Adsorption-desorption of phosphorus to clays and other sediment particles in the sediment is another process determining the availability of phosphorus.

**Dissolved Nitrogen Sector**

In addition to phosphorus, nitrogen is considered in the unit model to be a potentially limiting nutrient. Dissolved inorganic nitrogen is stored in surface water (DIN_SF_WT) and sediment water (DIN_SED_WT), with dynamics that generally follow those of the equivalent phosphorus modules. For the simulation we aggregate $NO_2^-$, $NO_3^-$, and $NH_4^+$ into one mass value of nitrogen to represent the inorganic forms of nitrogen that are most readily available for plant uptake. There are a number of oxidation and reduction reactions that determine the species of nitrogen present in a given type of environment, and thus the extent to which the inorganic nitrogen is readily available for plant uptake. However, we make the simplifying assumption that a certain proportion of the total inorganic nitrogen is in an available form within different environmental conditions (anaerobic sediments, aerobic water column, shallow aerobic sediments, etc.). Thus, the detailed kinetics of nitrification and other processes are not simulated, with an assumed equilibrium (over the daily time steps) of $NO_3$-N in the surface water for algal uptake and $NH_4$-N in the sediment water for macrophyte uptake.

The differences between simulated dynamics of phosphorus and nitrogen are in the addition of denitrification losses from the sediment water storage and the lack of explicit sorption/desorption to clay particles. Denitrification losses to $N_2O$ and $N_2$ occur in the anaerobic portion of the sediment profile, the depth of which is determined in the Deposited Organic Matter Sector. Denitrification is determined by:

$$din\_sed\_wt\_denitrific = sed\_anaerob\_depth \;\; cell\_size \;\; DIN\_SED\_WT \;\; rc\_DIN\_denit \cdot \mathbf{exp}^{(Air\_temp - T_C)} \quad \textbf{(14)}$$

where *sed_anaerob_depth* is the depth (m) of the anaerobic layer in the sediments, *cell_area* is the surface area ($m^2$) of the system (or cell), *rc_DIN_denit* is the specific rate ($1 \cdot d^{-1}$) of denitrification, *air_temp* is the air temperature, and $T_C$ is the critical temperature, at which denitrification is near its maximum rate. Whereas sorption/desorption is not explicitly determined, a proportion of total inorganic nitrogen $NH_4$-N is assumed available for uptake by plants within the sediment water. Thus, concentration of available nitrogen in the sediment water is decreased by a factor representing the proportion of $NH_4$ that is not bound to sediment particles, which is determined by the habitat type.

**Dissolved Oxygen Sector**

Dissolved oxygen (O2_SF_WT) is only calculated for surface water. Estimates of bottom water oxygen concentration are a function of the dissolved oxygen, percent sediment organic mater, and surface water depth. Dissolved oxygen may be contributed by plant photosynthesis and removed by plant and animal respiration, in addition to atmospheric diffusion. This sector is used to simulate anoxic and hypoxic conditions for animal consumers.

**Algae Sector**

This sector contains one module which may be used to represent all species of both phytoplankton and periphyton. Thus its parameters are empirically derived values which approximate weighted averages of individual species. It is possible within the model framework to replicate the algal modules, assigning specific values for all major species. An aggregate value for organic carbon in algal biomass (ALGAE) is increased by carbon fixation in primary production. A state variable is used in STELLA® to maintain an accounting of the ratio of phytoplankton to benthic algae. Both stocks are assumed to have identical growth and loss dynamics, with the exception that only phytoplankton can be transported into/from the cell with horizontal surface water fluxes.

*Inputs* -- Growth of the standing stock of algae is described by a maximum growth rate multiplied by the standing stock, a density-dependent logistic feedback, and a control function involving several environmental parameters:

$$Alg\_gross\_PP = rc\_alg\_prod \quad ALGAE \quad 1 - \frac{ALGAE}{alg\_max}$$

$$Alg\_temp\_fb = \mathbf{exp}\left[C\left(H2O\_temp - T_{op}\right)\right]^{C\left(T_{mx} - T_{op}\right)} \left(\frac{T_{mx} - H2O\_temp}{T_{mx} - T_{op}}\right) \quad \textbf{(17)}$$

where $C$ is a curvature parameter, *H2O_temp* the water temperature, $T_{mx}$ the maximum temperature (˚C), and $T_{op}$ the optimal temperature (˚C). This feedback rises to 1 at the optimal temperature at an exponential rate which depends on a curvature parameter; the interval width between the optimal temperature (response=1) and maximum temperature (response=0) determines the rate at which the function decreases to 0.

Nutrient limitation is based on the most limiting nutrient, using standard Michaelis-Menten relations for nitrogen and for phosphorus and field- or literature- derived half saturation constants. The formulation assumes limitation by the one nutrient that is most limiting:

$$Algal\_nut\_fb = \mathbf{min} \quad \frac{DIN\_sf\_wt\_conc}{DIN\_sf\_wt\_conc + DIN\_half}$$

The nutrient feedback control function is the same form as Equation 18 for algae, with the replacement of nutrients in the surface water by nutrients in the sediment water. Likewise, the temperature feedback is the same form as that used in the algal sector, Equation 17 but air temperature is used instead of water temperature.

Water availability feedback is an empirically derived function of the soil moisture available to the plants. If roots penetrate to the depth of the saturated water storage, no limitation occurs (feedback=1.0). If roots are only within the unsaturated zone, the feedback decreases sinusoidally down to near 0 at the wilting point, which is the moisture proportion at which plants lose their turgor pressure.

Whereas the carbon biomass that is fixed by the photosynthetic pathway is calculated using the above algorithms, the rate of growth of carbon stocks *only* in new shoots and leaves is compared to the rate of carbon fixation. Shoot growth depends on a maximum specific rate that depends on the nonphotosynthetic biomass, the seasonal control function, and a density dependent feedback:

$$PhBio\_shoot\_grow = rc\_PhBio\_shoot\_grow \;\; MAC\_NOPH\_BIOMAS$$

$$PhBio\_shoot\_seas \quad 1 - \frac{MAC\_PH\_BIOMAS}{PhBio\_max}$$

**Suspended Organic Matter Sector**

The organic matter stock in this sector includes the mass of non-living organic matter and of living microscopic decomposers that are suspended in surface water. The non-living portion of this stock includes organic material ranging in size from dissolved organic compounds to particulate detritus such as leaves that are in the surface water volume. (Thus, here we use the term suspended to include material which is dissolved, or "suspended in solution"). As indicated in the Inorganic Sediments Sector, we simulate the dynamics of suspension and deposition of both organic and inorganic material in the unit model. Thus, for the purposes of tracking such changes in the sediment/soil depth (mass) via suspension and deposition, our units for the suspended (and deposited) organic material stocks are in mass of total organic matter, as opposed to only organic carbon. We currently assume that the stock of suspended organic matter is homogeneously distributed throughout the water column, and is parameterized such that organic material of all size fractions have the same characteristics in the input-output dynamics discussed below.

The model structure is such that some inputs to this sector will occur during one time step, even if no surface water is present. However, that same material is "deposited" to the deposited organic material during the same time step.

*Inputs* -- Mortality of algae, macrophytes, and consumers, along with consumer egestion/excretion, are inputs from the biotic components of the unit model. Being entirely donor dependent, the flux rate of carbon is calculated in the appropriate living biotic sector. The ratios of carbon to organic matter for these living carbon stocks determine the mass of total organic material associated with each input. Depending on the habitat and thus the type of living plants and organisms, specific proportions of the mortality are then allocated to either suspended, deposited, or (in the case of macrophytes), standing dead detritus. Suspended organic matter input to this stock from consumers (kg OM· $d^{-1}$) is given simply by:

$$SOM\_fr\_consum = Cons\_prop\_to\_SOM * \frac{(cons\_mort\_biom + cons\_egest)}{Cons\_C\_to\_OM} \quad \textbf{(22)}$$

where *Cons_prop_to_SOM* is the dimensionless proportion of consumer losses that is directly allocated to the suspended stock, *cons_mort_biom* is consumer mortality (kg C· $d^{-1}$), *cons_egest* is the egestion by consumers (kg C· $d^{-1}$), and *Cons_C_to_OM* is the ratio of carbon to total organic matter of consumers (kg C · kg $OM^{-1}$). The complement of *Cons_prop_to_SOM* is the proportion that is allocated to the deposited organic matter stock (described below). A similar relationship of allocations is used to determine the flux of total organic matter to this organic matter stock for the flux of carbon due to mortality of macrophytes and algae and due to degradation of standing dead detritus.

Inputs to this stock from suspension of organic matter from the sediments is described in the sector concerning deposited organic material. Suspended material can flow into the system with surface water flux determined in the Hydrology Sector, and is merely the mass of organic material suspended in the water volume that is input to the cell.

*Outputs* -- Outflows from this stock include decomposition, deposition, consumer ingestion, and export with surface water. Decomposition is implicitly driven by the microbial community, with no internal feedback mechanism or recycling within the module. This mineralization of organic material is assumed to be an aerobic process in the water column, and thus there are simply two control functions constraining this flux of organic material.

$$SOM\_decomp = rc\_decomp * SUS\_ORG\_MAT * decomp\_temp\_rel * \mathbf{min}\left(\frac{SOM\_NC}{SOM\_NC_{opt}}, 1\right) \quad \textbf{(23)}$$

where *rc_decomp* is the maximum specific rate of decomposition in aerobic conditions. The *decomp_temp_rel* is a temperature control function that increases in a sigmoid fashion, ranging

from near-zero response when the temperature is 0 ˚C to 1.0 at 30 ˚C. This is a hypothetical temperature relationship that can be modified for alternative responses to temperature. The other control function involves substrate quality, and is simply the linear relation of the nitrogen:carbon ratio of the suspended organic material (*SOM_NC*) divided by the optimal nitrogen:carbon ratio ($SOM\_NC_{opt}$).

Export with surface water is driven entirely by the flux of water determined in the Hydrology Sector, carrying the mass of organic material suspended in the water column. Likewise, ingestion of suspended organic matter is controlled by the consumption rate determined in the Consumer Sector (below). Deposition of organic matter is controlled by the shear stress calculated in the Hydrodynamics Sector. If the shear stress is below a threshold value, then all of the suspended organic material is deposited in one time step. Above the threshold, a constant proportion of the organic material is deposited each time step.

**Deposited Organic Matter Sector**

The organic matter (DEPOS_ORG_MAT) stock in this sector includes the mass of non-living organic matter and of living microscopic decomposers that are deposited as part of the sediment/soil complex. All non-living organic material is included within this sector, from particulates to dead plant roots. Thus, changes in sediment organic biomass are part of the sediment elevation that is calculated in the Inorganic Sediment Sector. Inputs to this stock are from deposition of Suspended Organic Matter, mortality of macrophyte non-photosynthetic biomass, and from a portion of consumer mortality and egestion. Outputs occur via suspension, fire, decomposition, and ingestion by consumers.

Suspension and deposition are driven by the shear stress calculated in the Hydrodynamics Sector; deposition was described in the Suspended Organic Matter Sector. The erosion process was described in the Inorganic Sediment Sector, with the amount of organic sediments that erode being a proportion of the mixed sediments (as previously shown). However, decomposition in sediments differs from that in the water column due to the extent of the aerobic zone of the sediments. Decomposition in the sediments takes the same basic functional form as decomposition in the water column, but with fluxes described separately for the aerobic and the anaerobic zones. For the aerobic zone, Equation 23 was further constrained by:

*sed_aerob_depth*

*sed_elevË (teri50 È)Tj -43Ô3 0 T-00 TD (tby )Tj 23*

carbon to organic matter ratio for the sediment type. As with the inorganic sediments, we allow for the downwarping of sediments past the base datum of measurement, with the entire sediment/soil mass to subside based on a simple measured rate.

**Standing Detritus Sector**

Dead organic matter that is attached to a living plants or to the earth, and can not be moved because of this attachment under normal hydrologic flows, is defined as Standing Detritus. This stock includes dead standing marsh grass leaves, snags, dead brush, matted leaf litter, and fallen stems and trunks. The stock is increased by plant mortality and decreased by combustion, consumer ingestion, and decomposition to the Above Sediment Organic Matter stock.

Standing detritus (STAND_DETRITUS) represents the above-ground carbon mass of macrophytes that has died and is still rooted in the sediment/soil or otherwise massive enough that it does not move under normal hydrologic flows. This represents dead standing grasses, large connected mats of plant litter, and large fallen stems and trunks, etc.

Mortality of macrophytes is the only input to this stock, with the rate determined in the macrophyte sector. The flux from nonphotosynthetic biomass is partitioned between deposited organic material and standing detritus, whereas the flux of dead photosynthetic biomass is partitioned between suspended organic matter and standing detritus.

Decomposition of this stock is aerobic, controlled by temperature and the nitrogen:carbon ratio as described for decomposition in other sectors above. We make the simplifying assumption that standing detritus is dry, and thus the rate is reduced to that of low moisture conditions.

Wind and animal consumers contribute to the fragmentation and shredding of standing detritus, whereby the detritus is converted to fragments/particles that are more available to surface water inundation and can be transported by surface water flows. This material becomes part of the suspended organic material. We determine the rate of this loss of standing detritus to suspended organic matter by:

$$St\_\det\_to\_SOM = cons\_ingest\_std\_\det r \;\; StDet\_shred\_to\_ingest$$
$$+ STAND\_DETRITUS \;\; 0.9 \;\; \mathbf{max}\left(1 - \frac{\mathbf{max}(wind\_storm - Wind\_speed, 0)}{wind\_storm - wind\_thresh}, 0\right) \quad \textbf{(26)}$$

where *cons_ingest_std_detr* is the flux of standing detritus to consumer ingestion (kg C·d$^{-1}$), *StDet_shred_to_ingest* is the ratio of mass shredded to mass ingested, 0.9 is a calibrated rate constant (1/d), wind_storm is the wind speed (m/sec) at which maximal damage to standing detritus occurs, and wind_thresh is the threshold wind speed (m/sec) below which wind does not affect the standing dead detritus. For simplicity, the wind effects are linear between two extremes, but other relations can easily be incorporated.

The other two losses from this detrital stock are ingestion by consumers and oxidation by fire. Both are described in their appropriate sector description. The availability of standing detritus to consumers, and the refuge level (see the Consumer Sector) are determined as proportions of the initial conditions in this sector.

**Consumers Sector**

The basic consumer module represents an aggregate carbon mass of all consumers (CONS), both herbivores and predators. At this level of aggregation it is used primarily as a mass-balance processor of detritus and living/dead plant material. The consumer is omnivorous, ingesting all carbon stocks in the model with equal preference. The consumer has a maximum rate of ingestion which is applied to all equations of ingestion of resources. For each carbon food source, the realized ingestion rate is constrained by functions of 1) temperature, 2) the availability of that resource, and 3) density dependent regulation of the

consumption and maintain the consumers within biomass densities that are reasonable compared to observed values.

The availability control function determines the biomass of a particular resource that is available for ingestion by the consumer. Its general form for availability of resource X follows that of Wiegert (1979):

$$X\_avail = \mathbf{max}\left[1 - \frac{(X_s - X)}{(X_s - X_r)}, 0\right] \quad \textbf{(27)}$$

where $X_S$ is the saturation density of resource X at which ingestion by consumers is maximal, X is the current density of the food resource, and $X_r$ is the density of the resource at which consumption does not occur. The **max** function constrains the result to be non-negative, ranging from 0 to 1. This ratio is then multiplied by the standing stock of the resource, resulting in the mass of (carbon) biomass of that resource that is available for consumption.

The third control function is the density dependent feedback, constraining ingestion to 0 when a maximum biomass density is attained. Thus, the following is the general form of the equation for consumer ingestion, using ingestion of the nonphotosynthetic portion of macrophytes as an example:

$$Cons\_ingest\_NPhBio = \frac{NPhBio\_avail}{OM\_tot\_carbon} \; Cons\_temp\_fb \; CONS \; rc\_cons\_ingest * \left(1 - \frac{CONS}{cons\_\max}\right) \quad \textbf{(28)}$$

where *OM_tot_carbon* is the total carbon biomass of all organic matter stocks in the model.

Losses to consumer stock include respiration, egestion, mortality, and emigration. Respiration and mortality use the same form of temperature feedback as that used in the algae and photobiomass state variables. Egestion is a proportion of the material egested, or the complement of an average (carbon) assimilation efficiency.

**Fire Sector**

Fire can burn living and non-living plant biomass in the unit model, whether the material is emergent vegetation, peat or other organic material in the soil. The probability of a lightning strike is a random function of time, using a pseudo random number generator in STELLA®. However, the threshold probability of a strike occurrence varies seasonally or otherwise, allowing for varying probability distributions of fire source. The distribution of threshold values for a lightning strike is:

$$lightn\_strike\_thresh = 0.02 * \mathbf{COS}(DayJul / 365 * 2 * PI) + 0.98 \quad \textbf{(29)}$$

which ranges from 1.0 in January and December (julian dates 1 and 365), to 0.96 in July. If the random number generator returns a value larger than the threshold, a lightning strike is generated. A fire could also be generated from other, nonrandom, sources as necessary.

Ignition from a fire source and the rate of fire propagation within the system are calculated using a formulation similar to Kessell's (1977) fire model. A state variable is used to store the attribute of a new lightning strike or a continued fire presence. If this FIRE_ORIG value is non-zero, then the fire spread rate across the horizontal area of the system (m/d) is described by:

$$fire\_spread\_rate = \frac{fuel\_heat\_content \;\; fuel\_loading \;\; fire\_rx\_veloc \;\; Oxyd\_moist\_exp \;\; fuel\_ash\_free}{fuel\_bulk\_dens \;\; fire\_heat\_for\_ignit} \quad \textbf{(30)}$$

where *fuel_heat_content* is the potential heat content of the fuel type (kcal/g), *fuel_loading* is the biomass of available fuel ($g \cdot m^2$), *fire_rx_veloc* is the consumption rate of the fire (1/d), *Oxyd_moist_exp* is a dimensionless function of the moisture of the fuel, *fuel_ash_free* is the dimensionless proportion of the fuel that is organic material, *fuel_bulk_dens* is the effective bulk density of the fuel ($kg \cdot m^{-3}$), and *fire_heat_for_ignit* is the threshold heat required to ignite the given fuel (kcal/g).

Vegetation height and root depth modify the bulk density, with the effective bulk density being equal to the biomass of the fuel divided by the mean height and depth of the vegetation; higher densities slow down the spreading rate of fire. The algorithm for determining the moisture conditions accounts for current rainfall, soil moisture, and surface ponding; moisture can either prevent fire ignition, modify the rate of fire spread, or extinguish a present fire.

Currently, fire is assumed to burn all organic biomass within its areal extent; a "slow" fire will cover less area within the cell per time, similar to a fire of low heat intensity. The linear rate of fire spread is then converted to a specific rate of biomass burning (1/d):

$$fire\_mass\_burn = fire\_spread\_rate * \frac{fuel\_bulk\_dens}{fuel\_loading} \quad \textbf{(31)}$$

where the terms are defined above. This specific rate is then used to calculate the loss of organic biomass in the appropriate sectors.

The spatial movement of fire is different from that of water flow. Fire starts at one point and propagates horizontally within the system (or cell), as opposed to a mass balance flux of water based on differences in head height between sites. Because of this difference, accumulation of fire across the cell is tracked in the state variables FIRE_TO_WEST and FIRE_TO_EAST, which maintain an account of the linear extent of propagation in two directions. (As with the water horizontal fluxes in the Hydrology Sector, we provide examples of these flows in only two of four directions). Depending on the fire's origin (i.e., the midpoint of the system with a lightning hit or one cell edge due to across-cell propagation), the fire has a variable distance to travel before reaching the cell boundary(ies). Wind direction and speed modify the direction and areal extent of the fire spread; in the spatially articulated ELM these parameters will be a factor in propagating fire between cells.

### Unit model translation

In developing the final unit model in STELLA®, the user calibrates it to the different habitats (after thorough debugging if changes were made), and verifies that the model output meets acceptable levels of precision compared to historical data. The equations are then exported from the STELLA® unit model, and software from MIIEE translates them into C code that runs as a simulation in conjunction with hardware drivers. These steps are described fully in the Translating STELLA Models, Spatial Modeling Package Section below.

## SPATIAL MODEL

### Boundary establishment

In Task 1, we established a consensus on the objectives of the current version of the ELM and the general boundaries to be included (Costanza et al., 1992c). In direct consultation with the District and using their aerial photography and other data, we more recently fixed the model boundaries in a precise manner. In doing so, we made some changes to the previous boundaries for the northwest area. Instead of the boundary continuing in a line west from the southern levee of the western portion of the EAA (with no physical basis for that line), the boundary follows L-28 south until reaching Alligator Alley (Figure 1). At this point, the boundary cells follow that highway to the west. The rationale here was to use existing structures that form a "natural" boundary and to reduce the hydrologic complexity of the

omitted region (that can be seen in SFWMD maps of hydrography of the region). Upon reaching Highway 29, the boundary turns south as previously determined. However, the boundary then continues in a straight line to the Gulf waters instead of including a "dogleg" west that would have encompassed a small remaining portion of the ENP. This was done because it is very beneficial to avoid small pockets and acute angles in the boundaries when developing a model of spatial fluxes, and thus we did not include the small portion of the ENP. The alternative of moving the whole western boundary further west was unacceptable due to that creating a thin strip of open area between an arbitrary (non-physical) boundary and the structure of Highway 29. The new boundaries do not change the intent of the consensus and provide a better physical/mathematical rationale for the areal extent of the model.

## Spatial dynamics

Ecological systems are inherently complex, encompassing the physical environment, the biotic response to that environment, and the various interactions and feedbacks among the components. Ecological models have historically been constrained to the assumption that the modeled system was homogeneous throughout its bounds. However, such an assumption is not valid when considering systems on relatively large scales; the Everglades landscape is a complex mosaic of a large variety of land uses/habitats. It is critical to quantify the influence of landscape pattern on the ecological processes in the system, and conversely how changes in the processes may shape the landscape itself.

We have established a spatial modeling system for analyzing such landscape-scale issues for the Everglades. As indicated in the feasibility assessment report (Costanza et al., 1992c), the concept of this development utilizes a modular framework and user friendly software so that future development is relatively unconstrained by the computer code itself. Changes in spatial scales, management components, and simulated ecological processes will be possible without extensive changes to the model code.

The principal components to the spatial articulation of the ELM are: 1) the basic Spatial Modeling Package which forms the core of the grid-based spatial model; 2) the canal routing algorithms, the interaction of canals with model cells, and control structure simulation; and 3) the temporal habitat transitions within the landscape. Each of these topics are discussed below in separate report sections, although the Spatial Modeling Package ultimately coordinates/generates all of the code associated with these sections to run the ELM in space and time.

## Spatial Modeling Package (SMP)

The Spatial Modeling Package (SMP) is the central integrator of all of the components of the ELM. Although the code performs an extremely large number of tasks in implementing a spatial model, most are generic to the ELM and other grid based models developed for our spatial modeling system and are transparent to the user. With the aid of a user interface, the SMP links the unit model, habitat-specific data, spatial data, and canal algorithms to run in space and time. The software has been developed for a variety of platforms and for a variety of modeling objectives, including the ELM. Appendix A contains the preliminary documentation[4] provided to run the Spatial Modeling Package for general spatial modeling and will be modified for the final ELM product. The following provide an overview of the functions that the user observes or undertakes.

### STELLA Translator

This program runs on Macintosh computers, translating the unit model that has been debugged in STELLA into C code. Using several naming conventions for variables, the equations from STELLA are read by the translator and converted into code for running in a parallel processing architecture. Variables of flux between cells (in/out of the unit model

[4] All code of the SMP, and the documentation of the Spatial Modeling Package Section, was written by Tom Maxwell of MIIEE. (410) 326-7248; Internet maxwell@cbl.umd.edu

bounds) are linked to predefined intercellular flows in the model configuration process. The executable program has help files and should be self-explanatory.

### Variable configuration

After translation of the STELLA model, configuration steps are (optionally) needed. One can reconfigure variables to be specific types (serial time series, flux function, habitat dependent parameter, etc.) if needed, define the model time step, define the output variables and their output frequency, and several other such model and parameter attributes. Editing is done with the assistance of the interface (see Model Interface section) that provides explanatory text concerning the choice of attributes. Most of the model variables that are presented do not need alteration from their default configuration.

### Driver code generation

At this step, the code is automatically generated based on the STELLA equations and configuration files generated/modified above. All of the datafiles have been identified, the variable types configured, the output configurations established. Using the development environment of Macintosh Programmer's Workshop (MPW, assuming the favored platform of transputers in a Macintosh computer), the various modules of C code are compiled and linked using software components[5] that generate an executable model in the MPW environment. Analogous steps are taken to build the model driver in other hardware/software environments (see Appendix A).

## Water management

### Overview

The South Florida Water Management Model (SFWMM) is a modeling tool for simulating water routing in the region that has been well accepted by researchers in the south Florida community, as shown by the consensus from our previous workshops (Costanza et al., 1992c). For the initial phase of the Everglades Landscape Model (ELM) development, we are using many of the algorithms developed for the SFWMM to convey water through the canals and control structures in the model area. We report here on the use of algorithms translated (partly) from the SFWMM FORTRAN code to C code that runs on standard serial computer platforms[6] , along with their modification for ELM objectives and implementation in a parallel processing computing environment.

The principal mechanism of water flow in the model is on a cell to cell basis via overland flow routines using Manning's equation. Canals are another major water transport mechanism in the ELM, moving water greater distances within a time step than the comparatively slow sheet flow through vegetation. Compared to the extensive canal network simulated in the SFWMM, however, the ELM (during this phase) incorporates significantly fewer canals (see Figure 8), and instead focuses on water and vegetation processes within the more natural areas of the landscape.

For this version of ELM, we are using most of the algorithms for water conveyance along canal reaches that are used in the SFWMM. The principle changes are associated with implementation in a parallel processing environment and the details of the interaction between the canals. Thus, we will not reiterate the rationale of the hydrologic algorithms, but will focus on: 1) communication between processors for instances when more than one processor in the array of processors shares a common canal; 2) the mechanisms associated with canals' interaction with adjacent cells; and 3) the ecological processes that are simulated within a canal water column. Whereas the final report for Task 2 will include results of working simulation runs and the actual code as it is implemented, here we formalize the algorithms for developing the canal routing code.

The canals in the ELM are divided into a set of canal "reaches" that are linked at upstream and downstream control structures through which water flow is controlled. A canal

---

[5] Libraries of Logical System Tools from Pacific Parallel Research, Inc.

[6] R. Van Zee of the SFWMD ESRD translated the FORTRAN code to C code.

may cross any number of cells along its reach, and the canals and cells may exchange water and dissolved or suspended constituents. Within each canal reach, the canal is assumed to have constant depth and width. Cells that have any intersection with a canal will have a special "canal-containing" designation, with a reduced area (<1 $km^2$) determined by subtracting the surface area of the canal within it. (Although the area of a canal crossing a 1 $km^2$ cell is very small compared the cell area, accounting for mass balance of water dictates the necessity of calculating the areas involved. The canals may be carrying a large proportion of available water within a 1 $km^2$ cell). Figure 9 shows the general schematic of the canal routing, wherein a canal crosses several cells within its reach. Each canal-containing cell has a defined area of interaction with the canal, across which water and material may flow.

The direction of the canal flow within the landscape is determined not by the cell to cell connections in a raster format, but by the vector imposed by the upstream and downstream control structures. This line and its associated width determines the cells that have interaction with canals (see below). There are several instances where canals do not form straight lines between control structures. In these special cases we will define the canal by the cells through which it passes as determined from data sets described below. The determination of the canal direction and cell area interaction is accomplished via the development of a function to compute the areal intersection of the canals with the cells. We are planning on coordinating this development with the District. This function will be useful if the ELM is to be implemented later using different cell sizes, as the information is calculated from coordinates and will thus alleviate the need from another complex input data set of cell-by-cell attributes. Moreover, incorporation of new canals will be made somewhat more easily than a cell-by-cell description of the presence of a canal.

As indicated below, the ELM does not calculate cell to cell flow through canals, but rather iteratively distributes the water stage height along a canal reach, with the control structures responding to the stage as determined by management rules. These control structures are the determinants of flow within the canal network, with management rules that dictate flow through the structures as a function of water stage in particular basins. Whereas the SFWMM relies to a large extent on historical stage discharge relationships to determine flow, we are making an effort to incorporate theoretical weir/culvert flow equations so that realistic scenarios, based on managed response to stage height, can be simulated.

There are several combinations of canals with levees within the ELM boundaries. One configuration is of canals that have a levee on both sides of the canal (Figure 10), such as the North New River Canal section on the southwest side of Water Conservation Area (WCA) 2A. There are canals with a levee on one side only, such as the canals on the east side of WCA 2A. The modeled interactions of cells and the canal reaches varies depending on the presence/absence of levees in the zone of interaction.

Additionally, borrow trenches exist along the inside perimeter of WCAs, adjacent to the levees. These have no control structures or definite boundaries and are not canals as defined and modeled in the ELM. Because they are relatively open channels compared to the shallower adjacent portion of the WCAs, they allow water to flow faster than strictly overland flow through vegetation in the middle of the WCAs. This can be inferred from the distribution of cattails in WCA 2A, which generally follows the contours of these borrow trenches[7] . Nutrients introduced with water from structures appear to be conveyed along the borrow trenches of the perimeter more rapidly than into the interior of the WCA, with cattails predominating in the waters that have elevated nutrient levels along the perimeter[8] . The scale of the SFWMM is large enough that it does not explicitly incorporate the influence of these borrow trenches. However, the ELM is designed to simulate the response of plant communities to factors such as hydroperiod and nutrient regime. Thus, we will incorporate the potential for faster flow along the borrow trenches by using a weighting factor to increase the

[7]SFWMD SWIM Plan for the Everglades, Supporting Information Document, March 1992 p. 134.
[8]Ibid p. 133

depth of the trench-containing cells by an appropriate amount. Note that data estimating the depths associated with these trenches and rates of flow will be required to accomplish this accurately.

**Canal definition data**

The following variables for each canal reach will be stored in external files for use in ELM. The following data are required for each canal reach within the ELM boundaries, including the border cells.

- Canal reach ID
- State plane coordinates of upstream and downstream control structures
- Change in canal water surface elevation between upstream and downstream control structures (m)
- Width and depth of canal (m)
- Crest elevation and crest length of weir at downstream cell (m)
- Levee height (m of height relative to base datum; 0 if no levee)
- Levee location relative to canal (integer attribute: 1 if levee is bearing between 1-90˚ from the edge of canal; 2 if levee is bearing between 91-180˚ from the edge of canal; 3 if levee is bearing between 181-270˚ from the edge of canal; 4 if levee is bearing between 271-365˚ from the edge of canal; 5 if levees are on both sides of the canal)
- Virtual weir flag (0 if downstream end is an actual control structure, 1 if it is a virtual weir).

We assume that a levee is of negligible width; with much smaller cell sizes, the levee area would become significant and a levee presence in a cell with a fixed volume of water would raise the water stage in the cell. In that case, a levee width attribute would be associated with a given canal reach.

The mixing of raster based cell attributes with vectorized canal/levee attributes requires the following algorithm to determine which cells will interact with the canals via overland flow and which cells will interact with the canals via seepage under levees. For a cell at location [x,y] that contains a canal and has a known habitat type and levee location attribute, the following example (Figure 11) shows the routine for determining the cells that interact directly with the canal via overland flow. A similar procedure, (but in an opposite direction from the levee), is used to determine the cells that interact with the canals via seepage under levees. The basin designation indicates which hydrologic basin in which each cell belongs and is delimited by elevation differences, principally levees.

As indicated above, this allocation procedure may involve either cells that physically contain a portion of a canal reach within its boundaries or cells that are immediately adjacent to such cells. Figure 12 provides examples of “interactive” cells that are separate from canals in the horizontal (or vertical, but not shown) direction and some interacting cells that are diagonally opposite a canal-containing cell. The need for cells on the diagonal to receive water is a result of the nature of the canal reach interacting with more than two cells in a given direction at a time. Details of an example are shown in Figure 13. Cell E in Figure 13 would interact with cells F and I via normal overland flow in the southeast direction *if* a canal/levee was not present in the cell. Cell E has the majority of its area on the levee side of the canal and is therefore defined as being in the basin with impounded water. Thus, that cell does not interact directly with cells F and I via overland flow of water. However, the canal section shown to be physically within the cell itself does have overland flow connection to the southeast. Moreover, the canal reach is considered in the ELM to be one long cell and will interact via overland flow with a large number of cells in the southeast direction. The section of canal that is shown within cell E will be hydraulically connected to cell J for overland flow. The alternative of dividing the flow from the canal section within cell E among cells F and I has similar algorithm complexity (if not more complex due to division?) to the current choice. However, that alternative appears likely to produce an artifact in distributing the flows among cells because it would artificially distribute the volume associated with more than one canal

section to each cell, i.e., several sections of canal, as opposed to just one, would be interacting with one cell.

**Iterative stage solution**

The unit model operates dynamically in the cells and in the canal. Hydrologic processes such as evapotranspiration, seepage, overland flow and rainfall all occur within the unit model of the canal and the model cell. Normal spatial fluxes of overland and groundwater flow among cells occur from one cell into at most four neighbor cells. However, a canal reach has a larger number of interactions via overland flow and groundwater seepage from all of the cells along the reach. A quantity of water (determined from management rules) is introduced into a reach via a weir/culvert flow equation from an upstream canal reach. Gains and losses due to canal-cell interaction are calculated along the reach, and an iterated solution is sought among the various inputs and outputs of the canal for water stage height on a daily basis. This iterative relaxation process for estimating the daily stages in the canals is described in a SFWMD memorandum[9]. Within a time step to determine the canal stage along the entire reach, the model undergoes a series of iterations until the difference in stage height (error) estimates converges to a sufficiently small value.

**Parallel processing**

Parallel architecture divides the model cells among the available processors (24 in our hardware setup), with each processor taking care of the calculations of the unit model and spatial fluxes for the cells in its domain (see Figure 8). Inter-processor communication occurs in the instances where surface and groundwater spatial fluxes occur between cells handled by separate processors. Because of the computational complexity of the unit model, most of the processor tasks in the layout of the ELM are not dealing with processor communication but are involved with parallel simulations of the unit model within the thousands of cells within the landscape. For canal routing, we introduce another instance of interprocessor communication, and that is when iterating a solution to the canal stage along a reach and the reach crosses a processor domain boundary. In connecting processors in a parallel environment, hardwired links are often used in establishing a physical connection. However, virtual (code-driven) connections are also incorporated in instances where the physical links are impractical. In an analogous fashion, we introduce the concept of a virtual weir for the linkage of a canal reach across a processor boundary. Whereas the flow from one reach to another is controlled by weir flow equations at the structure separating the two reaches, a virtual weir may be embedded within a canal reach if it crosses processor boundaries. In the processor topology indicated in Figure 8, no canal reach is split into more than two sections. Thus two sections are created within a physical canal reach, with the virtual weir providing a communication link between processors that share a canal. Unlike an actual weir, however, the virtual weir has zero impedance to water crossing it and is thus a heuristic device that effectively "removes" the discontinuity of the canal at such processor boundaries. The "flow" across the virtual weir is passed from one processor to the other, providing the information for the determining the stage height along the entire canal reach. This continues as the iterative relaxation proceeds, with both sub-reaches being involved in the iterative process. In terms of coding, it is the simpler and easier of the two options that we are considering for implementing canal flows in the transputer-based parallel processing environment.

**Canal - cell interaction**

The unit model simulates a variety of hydrologic processes, including the following that are pertinent to canal-cell interactions. 1) Overland flow is calculated using Manning's equation, with a roughness coefficient that depends on dynamic simulation of plant biomass, numeric density, and plant morphology. 2) The unit model calculates seepage of water (termed

---

[9] SFWMD memorandum from Ray Santee, Water resources Engineer, WRD, RPD to Kent Loftin, Supervising Professional Engineer, WRD, RPD. Subject was Changes and Improvements Made in the South Florida Water Management Model. Date: January 22, 1987.

percolation for the general case) from that stored above the sediment/soil surface into that stored in sediment pore space (either in unsaturated or saturated storage). 3) Transpiration associated with plant growth and maintenance is simulated. It is based on relative humidity and uses plant efficiency estimates of mass of water used to mass of carbon fixed, which in turn depends on plant physiology. Evaporation is simulated using pan evaporation estimates and pan coefficients. The unit model thus explicitly incorporates the hydrologic processes that occur in both the canal and grid cells. Water (and associated nutrients and sediments) is transported between cells and canals by the standard inter-cellular spatial fluxes of water as described in the assessment report.

Canal-cell interactions are thus driven by the same mechanisms as the rest of the cell-cell interactions. The unit model is configured to operate at variable scales, with cell size as a variable input. Thus, the changes in the unit model that are associated with canal reaches are minimal. The principal change is the use of an area of exchange across cell-canal boundaries determined by the cell of interaction, a value which the unit model within the canal obtains from the Spatial Model Package links, as opposed to having it stored in the unit model code itself. It should be noted that the variable cell sizing induced by overlaying canals within the grid cell landscape is not equivalent to changing the grid cell size; the grid network is fixed, whereas canals merely reduce the habitat area within a 1 $km^2$ cell.

## Habitat determination

### Transition algorithm

An important aspect of the ELM structure is the dynamic nature of the habitats within the cells of the landscape. As environmental conditions change with time, the habitat type of the cells may change in response. There are a number of landscape models that simulate the ecological or physical processes within a heterogeneous landscape, but they do not incorporate mechanisms for the landscape to change in response to modeled processes. We have developed the conceptual structure, and associated logical pathways, for implementing a HAbitat Transition (HAT) algorithm within the ELM simulation. Due to the somewhat uncertain nature of the research data available on plant competition in response to the three environmental variables, we will incorporate modifications during the spatial model calibration phase of Task 3.

For initial simplicity, our algorithm currently assumes that a model cell is homogenous with respect to vegetation cover, and thus its habitat type. Each habitat has an identified optimum range of historical attributes associated with 1) fire, 2) hydrology, and 3) nutrients. The transition from one habitat to another depends on both the current habitat type and the historical environmental attributes listed above. Because of the assumption of homogeneity of vegetation within a cell (for this preliminary version), the habitat type of a cell changes in a binary fashion from one type to another. However, before this transition occurs, conditions for growth have become less favorable for the current habitat, and growth rates would usually be reduced due to nutrient and water limitations. The transition between different habitats is not accompanied by a large switch in biomass, merely in species composition.

The planned algorithm to allow more gradual transitions from one mixture of plant species to another assemblage in a heterogeneous cell will incorporate a 4-dimensional response surface (Figure 14), where habitat type is the dependent variable, with fire, nutrients and hydrology being the independent variables. For each cell, we maintain track of a historical fire attribute based on its intensity and the elapsed time since that classification. Similarly, we maintain track of a proxy for eutrophication depending on a four classification of nutrient concentrations and the elapsed time of the classification level. For hydrology, we monitor hydrologic attributes that classify inundation level and the elapsed time of that classification. These attributes will place a cell within the response surface at a unique point indicating the probable habitat depending on the attributes. Potential succession from one habitat type to another then depends on the current habitat state of the cell. A lookup table provides the

possible transitions among habitats, which are implemented if the new conditions warrant a succession from the current habitat type.

### Hardware

As indicated in the Spatial Modeling Package Section, we have drivers to support a variety of computer platforms, with 24 transputers installed into a Macintosh computer being the primary choice for most runs. The advantage of a parallel processing architecture such as transputers lies in the distribution of computation among many processors. For grid-based spatial models such as the ELM, the advantages are enormous compared to running the simulation on a single processor. Because the same unit model needs to be solved in each of thousands of grid cells in a single time step, significant increases in computational speed can be achieved by distributing the grid over multiple processors versus a single serial processor for the whole grid (Figure 15).

For sensitivity analyses and some of the repetitive debugging runs, we anticipate using the massively parallel CM-5 supercomputer. Accessing the CM-5 at the National Center for Superconducting Applications via the Internet, we will be able to more rapidly debug and analyze the spatial components of the ELM with this computer.

## DATA ORGANIZATION

### Unit model process data

#### Linked habitat databases

A vital component of any model is the data used in its parameterization. There are 130 required inputs for the unit model, including variables, rates and initial conditions. With a model of this areal extent and process complexity, the efficient compilation and organization of the data is critical. We have designed a set of linked databases[10] for the process-oriented data that change among the ELM habitats (habitat-specific data) in order to automate the transfer of the parameters to the Spatial Modeling Package. The databases are organized to match the sectors of the unit model, with a separate database for each sector such as Macrophytes, Hydrology, Dissolved Inorganic Nitrogen, etc. (Figure 16). Within each database are separate records for each ELM habitat; a record contains the fields containing the data for each model parameter. Each database has the rate parameters, initial conditions, threshold parameters, and other data that are used in the unit model and that vary from one habitat type to another. These parameters may be static (invariant with time) data, time series data, or data dependent upon another parameter (enter X and Y pairs).

Within each sector's database, we provide the user with three different perspectives on viewing information about the data. In the initial view, one sees only the parameter name as it is used in the STELLA unit model and the field containing the numeric data. The parameters are all seen on one screen, with different "pages" or screens (=records) for each habitat type. In the second viewing mode, another field provides parameter documentation with a definition and the required units. In the third viewing mode, the documentation and units fields are replaced with a field for the user to provide (unlimited) comments, including the literature/researcher source and any other pertinent information. Moreover, this view provides a separate field for a numeric (1-5) grade attribute, whereby the subjective quality of the data can be evaluated. For example, the nitrogen:carbon ratio of sawgrass that was measured in the Everglades during four seasons may be considered high quality information ranked 1; conversely, plant growth data obtained from the literature for a plant in a different geographic/climatic region would be ranked intermediate to poor in grade depending on the evaluation of the assumptions involved in the conversion related to the species, temperature or

---

[10] We used FileMaker Pro for the Macintosh, a pseudo-relational database program. This is an easy to use program that merely does not have the dynamic (automatic) linkages among linked databases. Whereas the linkages are established only once when the system is designed, the user needs to invoke a simple update command to obtain new data in the central database from a daughter database.

other factors specific to the data. This grade allows a rapid evaluation of the overall quality of data for different habitats and/or model sectors.

These separate databases are linked into the Central Database. This database file again contains separate records for each habitat, and has fields for all of the parameters in all of the model sectors that arranged in a defined (array-based) order. The only purpose of this database (which can be viewed if desired) is to provide a central linkage of all of the habitat-specific parameters and which are exported as an ASCII (text) file. The export file is read directly into the SMP for running the spatial ELM model. When new data are found for any habitat-specific parameter, the user opens the pertinent sector's database, enters the data in the appropriate habitat's record, and documents the new information. The Central Database is then opened and updated by retyping the habitat (record) name that needs updating with new data.

This system provides users with full access to the critical data of the ELM in a format that allows one to easily focus on and evaluate particular areas of interest. Importantly, anyone can view the numeric data, its source, and its perceived quality, and subsequently further evaluate that aspect of the ELM. Although we designed this custom format specifically for increasing the ease of parameterizing the ELM and therefore recommend its use, standard tab-delimited (or DBF) import/export capabilities are available for exchanging data with other database programs such as Oracle.

## Spatial data maps

### Habitat type maps

One of the principal data sets that we are using for developing the ELM is that of habitat classification analyses for the years 1900, 1953, and 1973 that was developed at the Center for Wetland Resources at the University of Florida in the 1970's. The (original) habitat type data were compiled by Costanza (1975) into a the form of handrawn, color map hardcopies. The 1900 map of the "primitive" state was prepared "primarily from 1953 Agricultural Stabilization and Conservation Service photoindex mosaics and ASCS general and detailed soils maps". While in most cases the natural areas in the 1953 photographs were assumed to be essentially unchanged from their primitive state, land use in areas that were developed in 1953 were extrapolated from soils information. "Vegetation maps prepared by other investigators were also used, especially the 'Vegetation Map of Southern Florida' by John H. Davis (1943)", along with miscellaneous other lesser sources (Costanza, 1975). The ASCS photo index mosaics (1:250,000 scale) for the years 1948 to 1955 (mean 1953) were used in compiling the 1953 land use map. For the 1973 map, Costanza (1975) used a 1973 False Color Infrared Mosaic by the National Aeronautics and Space Administration. Subsystems were cut out of mylar prints of the maps using a heated nicrome wire, with the pieces then weighed to determine their relative coverage.

The following descriptions[11] are the key to the habitat classification system used in these maps. We are currently determining the best means by which to reconcile this classification set with the very similar set called for in the ELM from prior workshops (Costanza et al., 1992c). For example, melaleuca and some other exotics are not defined in the present maps, but have become recognized as important in the Everglades community composition since the early 1970's when the maps' data were compiled.

*Grassy Scrub Systems*

Treeless systems composed of grasses and shrubs which occur on seldom flooded dry areas with frequent fires. Dominant species are *Seronoa repens* (saw palmetto) and *Aristida stricta* (wiregrass). Soil and drainage characteristics are similar to pine Flatwoods but increased frequency of fire prevents the growth of pines. Activities of a man in harvesting pine trees, lowering water tables, and increasing frequency of fires have maintained many former pineland areas in this classification. Also known as dry prairie and unimproved pasture.

---

[11]Land Use Subsystem Classifications: from pp. 12-16 in Costanza (1975).

*Pineland systems*

Three types of pine dominated woodlands: 1) Pine flatwoods - occurring on old marine terraces (sea bottoms) characterized by low nutrient soils, poor drainage and occasional fires (4-10 yr. frequency). Dominant overstory species are *Pinus elliotti* (slash pine), *Pinus palustrus* (longleaf pine) or *Pinus serotina* (pond pine) with *Seronia repens* (saw palmetto) as the dominant understory species. Some areas have became commercial pine plantations and many areas are used as rangeland. 2) Sandhill - these occur on old dunes characterized by excessively well drained sandy soils with very low nutrients and frequent fires (1-3 yr. frequency). Dominant overstory species are *Pinus palustrus* (longleaf pine) and *Quercus laevi* (turkey oak) with *Aristida stricta* (wire grass) as the dominant ground cover. Many former sandhill areas south of the frost line have been converted to citrus production. 3) Sand pine scrub: these occur on old dunes characterized by excessively well-drained, sterile, sandy soil (slightly less water and nutrients than sandhills with infrequent fires ( 20-50 yr. frequency). These forests are generally even-aged and have even-height since the infrequent fires usually destroy the entire forest with system adaptation for subsequent reproduction (*serotinous cones*). Dominant overstory species is *Pinus clausa* (sand pine) with *Seronoa repens* (saw palmetto) as the dominant understory.

*Hardwood systems*

This classification is an aggregation of three forest types, all of which are characterized by a diverse mixture of broadleaf species, moderate soil nutrient levels and high leaf area index. Differences in hydroperiod produce: 1) xeric hammocks on drier, never flooded sites with *Quercus virginianna* (live oak) dominating; 2) mesic and hydric hammocks on moist but seldom flooded sites with *Quercus nigra* (water oak), *Percea borbonia* (red bay), *Magnolia virginiana* (sweet bay), *Magnolia grandiflora* (magnolia) *Liquidamber styraciflora* (sweet gum), *Acer rubrum* (red maple) and *Quercus laurifolia* (laurel oak) variably dominant; 3) mixed hardwood swamp forest in seasonally flooded areas with many of the same tree species as in the hammocks but with more variable dominance (stands dominated by bay trees with standing water for extended periods are called bay heads). The hardwood classification actually covers the spectrum from upland to wetland systems but is aggregated here because of similar productivity levels and the difficulty of making the distribution at this level of detail. Relatively rare larger stands of the exotic species *Melaleuca leucadeudra* (melaleuca) and *Casuarina equisettifolia* (Australian pine) are also included in this classification.

*Lakes and ponds*

Freshwater ecosystems characterized by open water with slow exchange and seasonal stratification. In lakes the limnetic and profundal zones are large compared to the littoral zone and are main production areas while the opposite is generally true for ponds. Lakes in the region vary from oligiotrophic to eutrophic, but the large percentage (by area [but outside of ELM]) are the latter.

*Cypress Domes and Strands*

Ecosystems adapted to prolonged seasonal inundation in shallow depression or along sloughs, rivers and large lakes. Those occurring in shallow depressions receive water and nutrients from surrounding areas with sluggish water circulation. The canopy assumes the characteristic dome-like shape with smaller trees on the periphery and larger trees toward the center. Dominant species is *Taxodium distichum var nutans* (pond cypress). Areas receiving flowing water and higher nutrient levels along rivers and sloughs are dominated by *Taxodium distichum* (baldcypress) and are known as cypress strands.

*Wet prairie*

Grassy systems adapted to seasonal inundation and dry periods with fire. Water levels are generally only a few inches in the wet season and fires occur annually to triannually. Dominant

species are *Eleocharis cellulosa* (Spikerush), *Rhynochospora tracyi* (bulrushes) and various other sedges and grasses.

*Scrub cypress*

System composed of widely spaced dwarf cypress trees with a wet prairie understory. Water levels in the wet season are slightly higher than wet prairie and the dry down is not quite as severe. This leads to frequent but light fires. Dwarfed *Taxodium distichum var nutans* (pondcypress) is the dominant woody species with many species of grasses, sedges and rushes in the understory.

*Fresh water marshes and sloughs*

Grassy systems which are seasonally to continually inundated. Water levels are higher than wet prairies (1 to 1.5 ft) and fire is less frequent. Characteristic vegetation includes *Pontederia lanceolata* (pickerel weed), *Thalia geniculata* (fire flag),*Typha spp*. (cattail) and many other species of sedges, rushes, grasses and reeds.

*Sawgrass marshes*

System dominated by dense growth of *Mariscus jamaicensis* (sawgrass) to the exclusion of almost all other species. This system is adapted to occasional fires when the surface of the soil is moist so that only the accumulated dead grass is burned off and thus requires almost continual inundation. When fires burns off the upper peat layer, the sawgrass rhizomes are destroyed and the species is slow to reestablish. Sawgrass deposit peat rapidly if deep burning fires do not occur, and most of the present agricultural production in the everglades is built on this peat.

*Beach and dune*

Sand dunes and beaches and associated vegetation are formed by the interaction of a suitable sand source and wave and wind action. Vegetation consist of sparse salt-tolerant grassy and herbaceous species such as *Uniola* spp (sea oats), *Ipomoea pes caprae* (railroad vine) and *Coccologa urifera* (sea grape). Beaches with adjoining urban development are classified as urban [outside of ELM].

*Scrub mangrove*

Areas of stunted or dwarfed mangroves occurring in the transition zone between the well-flushed coastal mangroves and fresh water systems. The small size of the trees is thought to be due to the somewhat hypersaline conditions, low nutrients flows and poor soils. Dominant species is dwarfed *Rhizophora mangle* (red mangrove).

*Salt marsh*

Occurs in the broad intertidal flats where there are low waves and good tidal flushing. They are capable of surviving frost stress unlike mangroves; some areas of periodic frost alternate between salt marsh and mangrove. They are floristically simple, containing generally two species of grass: *Spartina alterniflora* and *Juncus roemerianus*..

*Mangrove*

Marine based forest adapted to grow in salt water and anaerobic muds. Freshwater inputs from land and their associated nutrients seem to be important to their survival, however. they are not frost tolerant and therefore grow only below the frost line. Dominant species are *Rhizophora mangle* (red mangrove), *Avicennia nitida* (black mangrove), *Laguncularia recemosa* (white mangroves) and *Conocarpus erectus* (button-wood)

This data set has undergone a number of transformations from the original, hand-drawn maps to digital information in a GIS. These maps were digitized (Costanza, 1979) into a format used by mainframe lineprinters. Because of limitations imposed by the printer, the data

cells had rectangular dimensions with 40 lines in the vertical dimension and 32 spaces (a 1.250 ratio) in the horizontal dimension. The actual dimensions of each cell was 0.6437km by 0.8046 km, for a cell area of 0.5180 $km^2$ (original measure = 128 acres).

This digital data set was then transferred into the MAP II GIS on the Macintosh, which uses rasterized information of square (not rectangular) cells[12]. The vertically compressed map image was then expanded using the "warp" operation in MAP II. Warp produces an output map that is based on the informational content of the original, but which is rectified to a different set of coordinates. Two maps were used in this operation to rectify each habitat map: a copy of the targeted habitat map (Copy_Habitat_map) and a null map (Null_map) that had the coordinate dimensions desired for the rectified habitat map. The Null_map was created by creating a map of (null) cells with 1.25 times the number of rows in the Copy_Habitat_map and the same number of columns. Tie points were identified in the four corner cells in both the Null_map and the Copy_Habitat_map. We then used the warp operation, employing nearest neighbor interpolation, to produce a rectified Habitat_map. The resultant map had the same informational content as the Copy_Habitat_map, but with a realistic aspect ratio of the map. The resulting cells have true resolution of 0.6437 km per side of the square cell.

This fine-scaled data set then needed rescaling to match the 1 $km^2$ data set of the ELM grid. For this operation, the operation of "respace" in MAP II created an output map based on the informational content of the input map, but with a lower cell resolution (larger cells). A (different from above) null map with 1.0 km resolution was created as the map containing the targeted resolution. The respace operation created a map whose cell values were computed as the most frequently occurring value of the corresponding cells of the input map, weighted by area. (Ties in frequency were broken by taking the largest of the values).

Because the original habitat data files did not contain georeference points, we needed to reconcile those habitat maps with some existing map for which there were geographic reference points. This was necessary to both provide a standard reference for creating compatible overlays and to ensure that the various transformations on the original data resulted in a habitat map that had appropriate physical dimensions (with no distortions). The SFWMD[13] provided us with the exact model boundary cells that were identified by state plane coordinates. This data, which was reformatted and read into MAP II, provided a map of model cells that defined the ELM boundaries (see below). To determine the exact location of a particular land feature within a model cell, we used a hardcopy of the hydrography (vector) lines superimposed on the ELM boundary cells overlay. Using the 1973 habitat map, we used the outline of the WCA's and the south and west coast of Florida to provide approximate tie points for superimposing the model grid on the habitat map, with the hardcopy of hydrography providing guidance in placement. The overlay of the two maps did not provide a perfect match, and four tie points were selected to fine-tune the habitat map to the model cells overlay. These tie points included the northern tip of WCA 1, the southeast corner of WCA 2B, a distinctive point of land in the mid-Everglades in Florida Bay, and another distinctive point of land on the western-most point of Cape Sable. These tie points were used as the linkage for a warp operation on the 1973 habitat map. With this map accurately reconciled to the grid, it was used to provide the tie point coordinates for the 1900 and 1953 habitat maps (which were all based on the same grid coordinate system)[14]. Figure 17 a-c show the ELM habitats at 1 $km^2$ resolution for the years 1900, 1953 and 1973.

---

[12] In this (untransformed) format the rectangular cells were distorted into a vertically flattened image if viewed in their original form (with a cell measuring a distorted average value 0.7197 km on a side).

[13] Marie Pietrucha, Ken Rutchy, and Les Vilcheck of the SFWMD ERD provided the maps and associated data files from Arc/Info and ERDAS data bases.

[14] The 1900 map had an origin that was 1 cell different from the other maps, and which was compensated for in the operation.

## SFWMM data sets

The bulk of the spatial data that we are using are from the SFWMD. Although we have not found access to all of the data, much of the data are in computer databases within the District.

**Structure presence map.**

This map (corresponding to the "on_map" variable in the unit model) contains information on the presence of some structural attributes for each cell. The "on_map" is a special map in the SMP used primarily to identify non-void cells that are included in the boundaries along with other attributes. The integer attributes for each cell in the map are the following, with reallocation depending on the information the District provides us on the structures:

0 = void, out of model boundaries
1-99 = control structure ID number if present anywhere in cell
100-199 = canal reach ID number if canal is present anywhere in cell
200-254 = reserved for future use
255 = cell in model bounds, without any structural attributes

**Monitoring stations map.**

This map ("monitor_map") contains the presence/absence of monitoring stations for surface water stage, groundwater stage, rainfall, and evaporation time series data. The map is linked to the files of time series data (that may also include temperature, windspeed, etc) that are collected at the sites.

0 = void, out of model boundaries
1-49 = rainfall monitoring stations
50-59 = evaporation monitoring stations
60-174 = surface water monitoring stations, *including* those that are defined as control structures (not all control structures monitor level).
175-254 = ground water monitoring stations
255 = cell in model bounds, without any monitoring station

**Levee seepage map.**

This map indicates the cells that have potential interaction with canal segments via seepage across levees. This seepage is defined as a "spatial flux" in the ELM. It adds another class of flux variable (see Spatial Modeling Package section) to the set of spatial fluxes of overland flow and groundwater flow. The integer value of the cell is the Canal reach ID of the interacting canal. In the instance where several canals will have such interactions with a cell, an exception table value is given, which points to the lookup data table containing the canal reach ID's associated with seepage interaction with that cell. Note that this attribute of cell-canal seepage includes cells that do not have a canal within their boundaries on a mixed vector/raster diagram (Water Management section).

0 = void, out of model boundaries
1-49 = exception codes for that have interaction with more than one canal
50-99 = reserved for future use
100-199 = canal reach ID

**Canal-cell interaction map.**

This map indicates the cells that have potential interaction with canal segments via overland flow or (vertical) percolation (as opposed to horizontal flux of water via levee seepage). The vertical flow of water occurs as a non-spatial movement of water within a canal unit model. The integer value of the cell is the canal reach ID of the interacting canal. In the instance where several canals will have such interactions with a cell, an exception table value is given, which points to the lookup data table containing the canal reach ID's associated with

interaction with that cell. Note that this attribute of cell-canal interaction includes cells that do not have a canal within their boundaries on a mixed vector/raster diagram.

0 = void, out of model boundaries
1-49 = exception codes for that have interaction with more than one canal
50-99 = reserved for future use
100-199 = canal reach ID

**STATDTA data file**

We are using the latest static data (STATDTA) file from the SFWMD as the primary source of information on spatial distribution of several variables. Because those data are based on a ~10.25 mile$^2$ grid, we interpolated the data given in that file to provide a smoother transition among the 1 km$^2$ cells in ELM[15]. We are currently seeking to update some of these data from other sources. In particular, we lack much of the spatial data within the mangrove zone of the ENP that was not included in the SFWMM. For the preliminary model runs, we have made assumptions, stated in each category, on the changes in data from the mangrove fringe to the coast.

**Elevation map**

All of our elevation data currently are from the STATDTA file. We assume a linear decrease in elevation from the measurements used in the SFWMM at the edge of the mangrove zone to the (zero elevation) land bordering the Gulf of Mexico. Figure 18 indicates the spatial distribution of land surface elevation.

**Initial groundwater stage**

All of our initial stage data currently are from the STATDTA file. We assume a linear change in stage from the measurements used in the SFWMM at the edge of the mangrove zone to the land bordering the Gulf of Mexico, with the latter estimates taken from the southern tip of Florida.

**Initial surface water depth**

All of our initial stage data currently are from the STATDTA file. We assume a linear change in stage from the measurements used in the SFWMM at the edge of the mangrove zone to the land bordering the Gulf of Mexico, with the latter estimates assumed to be zero.

**Rainfall basins**

We are currently using the rainfall basins identified in the SFWMM for distributing rainfall with the ELM boundaries.

**Aquifer depth and permeability**

All of these data currently are from the STATDTA file. We assume a linear change in depth and permeability from the measurements used in the SFWMM at the edge of the mangrove zone to the land bordering the Gulf of Mexico.

## Spatial data lookup tables

For data collected at monitoring stations, all possible monitoring stations are included in the fields for each data file (for consistency). Thus, there will appear to be a large amount of missing data.

---

[15] A computer program converts spatial (row-column) data from 80 columns per line (with multiple lines per record) to as many columns as there are cells in a particular record (row ID). To prepare the data for interplation of the ~10 km$^2$ data to a finer 1 km$^2$ grid, the program then (optionally) creates a window around each SFWMM data value with void cells. This effectively creates a ~10 km$^2$ window of 9 ~1 km$^2$ cells, with the central cell containing the non-void data. Either the original coarse scale data without voids or the modifed data file are provided a header and for direct input in the GIS. The FORTRAN source code and executable file are available from CEES. For data to be used in the ELM, the map with void cells is interpolated in MAP II based on the nearest neighbor, non-void cells in the surrounding quadrant.

1) "interaction.tbl" = length of canal within interacting cell. Each record contains the following fields. The mode of interaction is Seep/Other, referring to a) either seepage under a levee into a different basin (=attribute 1), b) overland flow or percolation into the same basin as the canal (=attribute 2), or c) in the case of a levee on both sides of a canal, seepage area *2 (=attribute 3)

| Cell_ID | CanalReachID | AreaInteract | Seep/Other |
|---|---|---|---|
| T[142,207] | T[50] | $m^2$ (float pt.) | 1,2, or 3 |

2) "rain.tbl" = rainfall data collected at monitoring stations. One record per day, with different field for each collection site.
3) "evap.tbl" = evaporation data collected at monitoring stations. One record per day, with different field for each collection site.
4) "sf_wat.tbl" = surface water stage data collected at monitoring stations, including control structures. One record per day, with different field for each collection site.
5) "gd_wat.tbl" = ground water stage data collected at monitoring stations, including control structures. One record per day, with different field for each collection site.
6) "levee.excpt" = Holds attributes of IDs of cells that have interaction with more than one levee/canal.
7) "wind.tbl" = wind speed and direction data collected at monitoring stations, including control structures. One record per day, with different field for each collection site.
8) "rel_hum.tbl" = relative humidity data collected at monitoring stations, including control structures. One record per day, with different field for each collection site.
9) "cloud.tbl" = Cloudiness data (in tenths) collected at monitoring stations, including control structures. One record per day, with different field for each collection site. (not currently needed, but useful for calibration)

## Model boundary conditions.

### SFWMM output

Historically, Lake Okeechobee overflowed its banks during rainy periods and flooded into the Everglades to the south, with overland sheet flow of water generally moving to the southwest into Florida Bay over long time periods. The timing of and magnitude of water flow from the lake, and fire propagation during dry periods, created the historical pattern of vegetated landscape in the Everglades (Davis, 1943). The region below the lake is now the managed Everglades Agricultural Area, altering both the timing of water flow and its nutrient content. The urban areas to the east of the Everglades are a general draw on the water resources of the Everglades hydrologic system. In order to reduce the complexity of this version of the model, the ELM's boundaries exclude the agricultural and urban areas (see Boundary Establishment Section). However, time series data on these source/sink regions are needed to drive parts of the ELM.

Until the boundaries of ELM are expanded (in a second phase of the modeling effort after Task 3), we will be taking output files from the SFWMM and linking those time series data to the ELM. Many of the ELM boundaries are defined by levees, such as the conservation areas, and therefore do not have complex boundary flows.

Most data will come from SFWMM, and thus depend somewhat on that format.

1) Surface water time series for each boundary cell; associated nutrients and particulates
2) Saturated water time series for each boundary cell; associated nutrients and particulates
3) Canal flows (or heads) series for each boundary cell; associated nutrients and particulates

**ELM-SFWMM linkage table**

This data file provides the cell-cell linkages between the SFWMM grid and the ELM grid. One record for each boundary cell of ELM in following format: ELM bound cell ID; WMM cell ID; factor; WMM cell ID; factor; WMM cell ID; factor; WMM cell ID; factor. Each factor is the weighting factor determined from the proportion of the total area of the ELM cell that lies within the associated WMM cell (max # WMM cells possible is 4).

## MODEL INTERFACE

### Introduction

Some of the most pressing problems facing wetlands have to do with the management of resources in the face of multiple environmental impacts. There is general agreement that the best management plans are those based on a thorough understanding of fundamental processes. The transfer of the results from research projects to management solutions has not always been straight forward. Many scientists are not adept at putting their results in a format readily usable by managers. Moreover, agency personnel can be overburdened with day-to-day management activities and may see specific scientific results as too esoteric for their needs. Finally, there have been no widely accepted tools to aid in the transfer of science to managers.

An exciting development in the communication and transfer of scientific results is a new body of knowledge whose aim is to facilitate interaction among diverse disciplines. This new discipline, known as "scientific visualization" has as its foundation the adage "a picture is worth a thousand words." Graphs, maps and figures to convey information had been used by scientists for a long time (Tufte, 1990). Scientific visualization is not just presenting results in a graphic manner, it relates topics as diverse as statistics, mathematical modeling and data base management. It allows the scientist to "step-into" the data, simplifying the use of data-sets and enhancing analytical potential (Wright et al., 1990).

Recently several attempts have been made to create information systems that rely on this relational view. The National Center for Supercomputing Applications at the University of Illinois, Champagne-Urbana is one of the centers in the forefront of visualization theory (e.g., (Dwyer, 1990; Robinson, 1990). Several agencies have started projects for information systems. Examples of these efforts can be found in the products generated by NOAA such as COMPAS for coastal planning and assessment for the State of Texas (NOAA, 1990) and an analysis system for shrimp harvest data (NOAA, 1989). A recent example of a coastal planning and managerial tool has been developed by Reyes (1993). This HyperCard™ driven information system compiles available environmental information for a tropical coastal lagoon in Mexico, combining it with several simulation models that can be used as managerial tools.

Our objective is to design a user-friendly, computer based information system to facilitate the organization and communication of the ELM. This system is being constructed in a manner to facilitate the addition of modules of information as they are developed (Figure 19). This system makes use of recent developments in microcomputer technology and makes it possible to deliver to the desk of the researcher or manager a wide range of capabilities and data that earlier could only be accessed on expensive and user-unfriendly mainframe computers. The development of this interface would allow model runtime changes with no user modifications to the program's code if the need for a potential change, and its range of possible values, are identified a priori. Thus, we worked on the development of a "front-end" user interface to the model using the umbrella of the HyperCard programming language for Macintosh computers.

We are assembling an interactive user-friendly interface that oversees and coordinates the different programs, files and applications needed to run the Spatial Modeling Package (SMP). This front-end interface acts in a modular fashion in which each of the modules is a section of the SMP. The resulting HyperCard graphical interface (Figure 19) could take modules of the C code and allow the user to manipulate parameters in the code by selecting a topic and choosing alternatives from the graphical interface- without the user needing to actually view and manipulate C language code. This interface integrates the various software

modules and runs the spatial model, with the most of the functions being transparent to the user.

At the present we have built several part for this information system which consists of: a) an on-line reference manual for the Everglades Landscape Model that provides the guidelines for use of the ELM unit model and describes its assumptions and logic; b) an interface that explains and integrates the use of the database created for the habitat specific parameters; and c) a manual describing and facilitating the file editing to the STELLA translator (see Translating STELLA Models section) for the SMP and the files created with this program.

### Computer Software

For the interactive data access system, we used computer hardware and software that provides: 1) user transparency, 2) low learning curve 3) existing software capable of generating graphic-oriented presentations. For preparation of the system, we chose the programming language HyperCard™. HyperCard differs from other programming languages because lines or strings of code are integrated to modules. These modules are organized in a hierarchical structure and presented as objects or icons that activate the program or "stack," by positioning the pointer or cursor on the icon. These include color maps with active locations, spatially oriented information on pre-set maps or gradients, and graphical data selected and combined by specific request from the user. The information and results from specific queries are presented as different screens ("cards") that the user can "browse" at leisure, giving the user the flexibility to explore different paths or combinations of objects. HyperCard takes an additional step in the management of relational data compared to traditional systems by allowing the user to view information in an large variety of contexts.

HyperCard™ is a software product for Apple Macintosh computer. With it, the programmer can develop either his/her own application or use one of thousands of "stacks" previously developed by others. Given its graphical approach, the applications (stacks) in HyperCard are extremely easy to use. Each stack consists of a group of screens that are interactive and in which any type of information can be presented. Therefore, the screen can contain maps, figures, graphs, text and/or sound. To gain access to more information the user usually has to click the cursor on specific areas of the screen. In essence a HyperCard stack is a highly interactive, user-friendly database. Often a HyperCard stack is developed to be used as a computerized information brochure. One step beyond this would be to use it as a tutorial, a training manual or catalog of information.

The presentation of scientific data for the ELM in an easy to use appealing format for the environmental manager can be accomplished using HyperCard as a presentation tool. The information produced can be organized, prioritized and presented on a group of stacks that require minimum training and are highly interactive. The information is arranged on different levels, from an introduction to the ELM to results and map scenarios of the various changes of the simulation runs.

The multimedia database has been designed as a system or "shell" in which different scenarios or particular training programs can be incorporated as modules. The shell could continue to grow and be customized to cover requests or needs of special user-groups.

## Results

We have developed a prototype shell and begun compilation of information and programs used by the ELM. An average of thirty minutes of interactive viewing at this point gives the user an opportunity to investigate the initial database, and the conceptual approaches to the unit model along with ecological and mathematical assumptions. The data sets include STELLA diagrams for each of the unit model sectors and required inputs for initial conditions and storage for the model variables as well as editing capabilities for the STELLA-to-C translation program.

Early on this project (Costanza et al., 1992c) it was recognized the need to create an overall program that could organize the simulation package and provide an easy to use interface. Given the numerous variety of formats, storage media and methods of transfer of the

data that ELM required, a coordinating shell was imperative to make it possible to run simulation scenarios by new users. For the purpose of efficiently evaluating environmental aspects of the different management alternatives provided by ELM, both spatial and temporal, it is necessary to gather the data at several levels. As an introductory part of this interface, three stacks were design allowing the user to start the manipulation of inputs and translation to the spatial code.

**Unit model Interface**

The STELLA unit model contains 16 sectors that were aggregated into several sections: a) an introductory one (HyperELM), b) global inputs, c) water, d)primary producers and e) biogeochemical processes (Figure 20). Each of these sections presents information that starts from a general level and leads to the equations involved in the simulation. The user can look at more details of a subject on a card by clicking on the icon or word on the card.

The HyperELM stack starts with an introduction (Figure 20). The next card (screen) describes the objectives of the unit model followed by a card showing the general design including a grid map of the study area. At yet a deeper level is a description of how the spatial modeling package interacts with the unit model and, most importantly, a "model structure" screen which gives access to any of the four sections through a series of buttons on the bottom of the screen.

The rest of the stacks (i.e., global inputs, water, primary producers and biogeochemical processes) were developed following a hierarchical structure in which more detailed information is presented as the user requests it by clicking in each card of the stack. This hierarchy includes: a) an introductory card with the STELLA diagram of the sectors included; b) a card with the theoretical explanation of the physical or biological processes involved in the section; c) a general description of the equations and their interactions, along with assumptions and interconnections; d) a card for each equation with explanation of terminology.

The introductory card allows the user to navigate among the different sections, while the rest of the cards in the stack have return paths to their own first section card. As an example of the general structure of how each section was constructed, Figure 21 depicts this overall view for some of the sectors that are in each section, and the path that the user can follow to view all the available information. It is worth noting that one of the advantages of this interface is that all of the diagrams were copied from the STELLA symbolic representation of unit model. The use of this diagram familiarizes the user with what actually he/she could see if the STELLA file is open. Given the windowing environment of the Macintosh computer, the user's guide can be run concurrently with the browsing and editing of the STELLA unit model. Thus, this interface acts as an on-line help for editing the unit model.

**Database interface**

The linked habitat database was structured around a central database which collects and organizes the parameters incoming from 16 different datasets (see Data Organization section). To facilitate the access and transfer of these parameters using the database, we also developed a HyperCard stack that demonstrates the structure of the database. Additionally, it presents each of the datasets, explains the types of data required by each, allows the user to input data into them, and presents a "dummy" export file that could be input into the SMP. The database stack includes three cards. One is an introductory card which describes the structure of the database; the second card describes the individual data files and provides the user with access to the data files throughout their own application program . The third card shows a schematic of how this relational database collects the individual information for each sector and habitat in ELM.

**Input Files Editor**

The Spatial Modeling Package consists of several folders that contain the C-code to run the simulation, the STELLA-to-C translator and the Data and Models folders. In order to spatially articulate and run the unit model component of ELM it was necessary to create a STELLA-to-C translator program. The use of this translator requires the user to edit several

files customizing the initial conditions, configure the flow variables, and the output file destination for the resulting parameters.

A HyperCard stack was created to demonstrate the different components of the SMP and their interactions. The stack presents an introduction to what we have classified as seven steps required to complete the tasks required by the SMP and explains in detail what and how to achieve each of these tasks. (see Spatial Modeling Package Section). Once the user is familiarized with the different parts of the SMP, the next card describes the translator program provides the user with two additional cards in which the user may edit two files from the translation procedure (model.outlist and model.config files) that specify the different variable types and output choices. As an added feature, a debugger check was put into these editing cards. The different types of variables and their requirements are then cross checked to insure that the editing corresponds with the type of variable declared and all the information needed is in place.

## SENSITIVITY ANALYSES

### Evapotranspiration algorithm

Evaporation and transpiration are known to be critical “loss” components within the hydrologic cycle, particularly in areas such as wetlands where water is generally stored at or near the land surface (Duever, 1988; Ewel and Smith, 1992). Evaporation occurs from water in contact with the atmosphere, whereas transpiration is the similar process of evaporation from plant tissues. While there is a critical difference in that the latter evaporative flux can be controlled by plant physiology, the fluxes are often combined into one term, evapotranspiration (ET), for ease of measuring or modeling the quantity. Depending on the scale of measurement, researchers have come to widely varying views on what controls the transpiration part of this flux: meteorologists and engineers concerned with large scale fluxes of water (over hundreds to thousands of meters distance) emphasize the large amount of energy to evaporate water and thus the heat and radiative flux involved; physiologists generally point out that transpiration can be almost entirely controlled by the stomata of the plant in response to differences in its internal and external environments (i.e., water saturation deficit). The actual answer to quantifying the controls on transpiration depends on the scale with which one is addressing the objectives. (See Jarvis (1986) for an analysis of the scaling issues involved in the different perspectives).

In the ELM, the scale that we address is somewhat intermediate between the two

saturation deficit in the atmosphere above the boundary layer of the canopy (the mixed Planetary Boundary Layer on the order of hundreds of meters in height). This (0-1) decoupling factor is a relatively easily obtained measure that varies with gross canopy morphology, with forests generally being near 0.2 (low decouple = strongly coupled) and grasslands being near 0.8 (strongly decoupled).

The above mechanisms operate when the plants are not stressed due to water limitations. When water does become limiting, the plants' stomata start to reduce the conductance of water via stomatal closure, and transpiration can become tightly controlled by this water limitation. The below equation determines the relative importance of these controls in determining potential transpiration:

$$pot\_transp = mac\_water\_stress\_fb * hyd\_transp\_stoma * (1 - mac\_canop\_decoupl)$$
$$+ (mac\_water\_stress\_fb * hyd\_pot\_evap * mac\_canop\_decoupl)$$

where *mac_water_stress_fb* is the (dimensionless) extent to which water is not limiting, *hyd_transp_stoma* is the conductance ($m \cdot d^{-1}$), *mac_canop_decoupl* is the dimensionless decoupling factor, and *hyd_pot_evap* is the calculated potential evaporation ($m \cdot d^{-1}$).

We present here the sensitivity analyses performed to analyze the influence of transpiration-related coefficients on the water budget calculated in the unit model simulation. The primary parameters of interest are those which influence the extent of control due to the canopy type. Although we will be performing more detailed analyses on these parameters and others, some broad-ranging conclusions may be drawn from this simple example. Depending on the conductance, the decoupling factor can control whether the system is driven by the physically derived controls versus the canopy related control. For a nominal rate of conductance, the decoupling factor may change the total transpiration to a moderate extent Figure 22a-c. However, the decoupling factor has relatively little control over transpiration when the conductance is low (Figure 23a-c). When conductance is high, the system can be dramatically altered by the plant's control over transpiration, with the decoupling factor very influential (Figure 24a-c). Examining this relation further at high conductances, one sees that there is a threshold point where the interaction of water limitation and the canopy decoupling factor determine the on/off point of transpiration loss (Figure 25); in instances where the canopy is strongly coupled to the external saturation deficit, the system can become water limited due to the high plant conductance and drying down the system over prolonged periods, and the macrophyte community (not shown in figure) reduces biomass dramatically.

## SCALING ISSUES

Scale is a fundamental aspect of developing the Everglades Landscape Model (ELM), and indeed is important to most objectives in ecological research. As such, the tools for analysis of scale dependence are critical. Inferential statistics based on assumed distributions and independent observations are most widely known and used by researchers (ANOVA, *t* tests, etc.). Spatial statistical methods, which incorporate dependence among sampling units, are reasonably well developed for analysis of ecological data (Cressie, 1991; Rossi et al., 1992), and are increasingly used in a variety of studies to determine pattern and the influence of scale on ecological research. Moreover, fractal geometry (Mandelbrot, 1983; Milne, 1992) provides a useful tool to describe the complexity of spatial and temporal patterns in ecology. We are using a variety of methods that have been developed, and are working with novel statistics, to analyze some of the fundamental properties of spatial and temporal patterns in spatial modeling. Basing a number of our experiments on fractal characteristics, we are exploring the changes of spatial and temporal properties as the scale (defined below) of the model and analysis changes. This Scaling Issues section (reproduced from our Task 2.7 Report) describes a) the manner in which we plan to develop means by which to quantify the extent of scale dependency in the development of the ELM; and b) results to date, some of which are in press (Costanza and Maxwell, *in press*).

We are analyzing two aspects of scaling, temporal and spatial. Here we consider spatial scale to be described by both the grain (cell size) and extent (total area considered), and have focused on changing the grain aspect of scale. Similarly, temporal scale refers to the sampling frequency and the total duration under consideration. Although the combined effects of temporal and spatial scaling will be of significant interest at a later stage of the project, we treat them separately in this report on the initiation of the experiments.

We have initiated the investigation of temporal and spatial scaling issues associated with the ELM. We anticipate that these scaling experiments will continue through the development of the ELM, providing greater levels of sophistication as we progress. The purpose of this summary is to indicate the types of investigations that we are conducting and some results to date.

*Spatial Scaling*

First and foremost, we analyzed the relationship between spatial resolution of landscape data and the predictability of the pattern in that data. We applied the analysis to a simple null "model" of observed landscape change, investigating effects of "model" resolution on predictability of the landscape change. The basis of this thesis is that there are limits to the predictability of natural phenomenon at particular resolutions, and "fractal like" rules determine how both data and model predictability change with resolution. During Task 3 we will proceed to implement these concepts, and others, for analysis of scaling changes.

*Temporal Scaling*

Secondly, we are in the process of investigating methods to describe complex time series of data (such as rainfall or cloudiness) with summary statistics that will allow us to use data that is available on a very fine scale and apply it in the model, on a coarser time scale, to describe complex temporal phenomena. We seek to discern the inherent structure in the phenomena by fractal analysis in sampling windows of varying size to determine the relative complexity of the data. A predictability index, based on deviation from the mean within sample windows, is similarly calculated for the data using the varying window sizes. After using this information to seek the optimal window size for the data set, we propose to use various summary statistics within the window intervals to characterize the data for use in a simulation model. In this case, we are seeking to reduce the computational complexity of a model, more closely matching the potentially coarser time step of a model with data that was originally on a finer scale - while retaining the model behavior associated with the more complex data set. We believe that it may be possible to develop general rules for characterizing time series of varying degrees of complexities and patterns. If we are successful, this characterization may be of utility in reducing some of the computational complexity of the ELM.

*Process Complexity Scaling*

At the interface of these two scaling issues is the consideration of the scale of the processes that are simulated within the unit model, or process complexity. This level of scale parallels that of spatial and temporal scale. When we refer to spatial grain in this report, we refer to the grain of the landscape itself, usually in units of distance such as meters or kilometers. Likewise, temporal scale refers to the sampling frequency of data or output of the model. The scale of the modeled processes encompasses the degree of complexity that is incorporated into the equations, and is directly analogous to the scale due to partitioning biotic and abiotic components that are simulated. For example, this represents the difference between modeling a tree as an entity composed of many fine-scale components such as leaves, twigs, roots, etc., and modeling it on the scale of one "big leaf". Using the unit model parameterized to a sawgrass habitat, we are initiating model experiments to analyze the effects of changing aggregation levels of the processes and variables in the model.

## Plans

We plan a series of experiments to investigate issues ranging from aggregation of parameter estimates to spatial model response to varying cell size. These investigations include the following projects:

**Unit model:**

1) Explore means to summarize complex time series that are recorded at high temporal resolution so that smaller data sets may be used in coarser scale models, more closely matching the sampling frequency with the model time step. We have initiated this process, and anticipate applying it to Everglades data if it is deemed to be beneficial. The use of this process does not appear necessary for ELM data at this time, but may be beneficial with other data at a later phase of the modeling project.

2) Explore the effects of aggregating state variables and process equations in the unit model, determining the influence of simple averaging, other more complex mathematical routines, partitioning, and/or combining these with recalibration. For most of the ecological processes the unit model state variables are already fairly aggregated, perhaps as much as desired for the current model objectives. As with 1) above, the analysis of optimal aggregation may become more critical if/when greater degrees of process complexity are built into the model, as may be desired by field researchers in later phases of the project, or when simplified models are required for other purposes.

**Spatial model:**

3) Explore effects of changing spatial scale on the model output. The use of comparative statistics such as those defined in this report will facilitate comparisons of model results across scales. We would like to set up the spatial model for a region such as Water Conservation Area 2 that has data at a high spatial resolution (small grained), at least compared to many other regions within the ELM boundaries. The influence of heterogeneity in that landscape can be discerned via implementing the model at varying spatial grain sizes. Inherent in this exploratory analysis is the determination of appropriate algorithms that may capture the within cell heterogeneity of land cover or other attributes. Weighted averages of the process variables for a variety of plants represent a combination of the unit model complexity and the behavior of the spatial model output. This scaling issue is probably the most critical to the implementation of the ELM at this point, as we recognize the heterogeneity of vegetation cover within some of the 1 $km^2$ cells.

## Fractals, scaling and predictability

We hypothesized that an important determinant of the predictability of phenomenon is the scale (resolution and extent) of the analysis. By resolution we mean “grain size” or the size of the smallest unit of measure, with increasing resolution corresponding to finer grain. We can distinguish two ways that resolution might affect predictability. One is the increasing difficulty of building predictive models at increasingly finer resolution. For example, the position and velocity of individual molecules in a gas is highly unpredictable, but the temperature of the gas (which is an average of these motions at a much cruder resolution) is highly predictable. Likewise, it is easier to predict general climate patterns than it is to predict the exact geographic location and timing of rainstorms (the weather).

On the other hand, finer resolution allows more detail to be observed and internal patterns in the data to be seen that may not have been observed at cruder resolutions. One example are the warm core gyres that form in the Gulf Stream and were not observed until remote sensing images of sufficiently fine resolution were available. Another example is the quest by the military to obtain high enough resolution satellite images to see the features (such as tanks and airplanes) of interest to them that would not appear on lower resolution images.

Some phenomenon are known to vary in a regular way with resolution. For example, the regular relationship between the measured length of a coastline and the resolution at which it is measured is a fundamental one behind the concept of fractals (Mandelbrot, 1983) and can be summarized in the following equation:

$$L = k\, s^{(1-D)} \qquad (1)$$

where:
L = the length of the coastline or other "fractal" boundary
s = the size of the fundamental unit of measure or the resolution of the measurement
k = a scaling constant
D = the fractal dimension

This convenient "scaling rule" has proved to be a very useful in describing many kinds of complex boundaries and behaviors (Mandelbrot, 1983; Turner, 1987; Milne, 1988; Turner et al., 1989; Olsen and Schaffer, 1990; Sugihara and May, 1990). We hypothesized that this same kind of relationship might exist between resolution and predictability (and possibly other measures as well) and might be useful for developing scaling rules for understanding and modeling. For initiation of the spatial scaling experiments, we tested this hypothesis by calculating both data and model predictability for a landscape at a number of different resolutions.

## Spatial scaling: Methods

Colwell (1974) applied information theoretic concepts to the problem of estimating the degree of predictability of periodic phenomena. The method is similar to autocorrelation analysis, except that it is applicable to both interval and categorical data and may thus be more appropriate, for example, for comparing patterns of land cover. Predictability in this context refers to the reduction in uncertainty about one variable that can be gained by knowledge of another. For example, if the seasonal rainfall pattern in an area is predictable (e.g., there is always a severe dry summer), then knowing the time of year provides information about rainfall (if it's summer, it must be dry). If there is no relationship between rainfall and season, time of year tells us little and the rainfall is relatively unpredictable from a knowledge of time of year.

### Measurement of Predictability: Spatial sets

These techniques can also be applied to spatial data. In this application, one is interested in the degree to which the uncertainty about the category of a particular pixel is reduced from knowledge of other aspects of the same scene, or from knowledge of aspects of other, related, scenes. There are several aspects of a scene that might be used as predictors. We discuss two implementations based on 1) the state of adjacent pixels in the same scene, which we call "auto-predictability" or $P_a$; and 2) the state of corresponding pixels in other, related scenes, which we call the "cross predictability" or $P_c$. Other combinations of these two and higher level analyses (i.e.. adjacent pixel pairs, triplets, etc. or multiple cross comparisons) are also possible and useful for various purposes (Turner et al., 1989).

The method in general can determine if there are regularities in a spatial data set, ranked on a scale from 0 (unpredictable) to 1 (predictable), and the answer can be interpreted as the degree of departure of the scene or comparison between scenes from a random (totally unpredictable) pattern.

To estimate predictability, one first assembles a contingency matrix with states or conditions of the pixels along the left axis, and corresponding states of other pixels along the top. For auto-predictability the categories in a map are listed on the left and along the top of a matrix. The numbers in the matrices represent the frequency of occurrence in the mapped data of the category (or category pair, triplet etc. for higher level analysis) listed along the top of the matrix lying adjacent to the category listed along the left. This yields information about how predictable the patterns of adjacency are in the sample map data.

The contingency matrix can be any set of meaningful spatial relationships in the data. For example, another way of setting up the matrix is to define the predictability of one scene given another scene. For example, we might want to know the predictability of a landscape in

one year given information in some previous year(s), or we might want to know the predictability of a real landscape compared to a landscape model's output. We call this the "cross" predictability, because it provides information on the predictability of a given pixel's category given knowledge of the category of the corresponding pixel in another scene.

Following Colwell (1974), we define $N_{ij}$ to be the elements in the contingency matrix (i.e., the number of times in the data that a pixel of category i was adjacent to one of category j for auto-predictability analysis). Define $X_j$ as the column totals, $Y_i$ as the row totals and Z as the grand total, or:

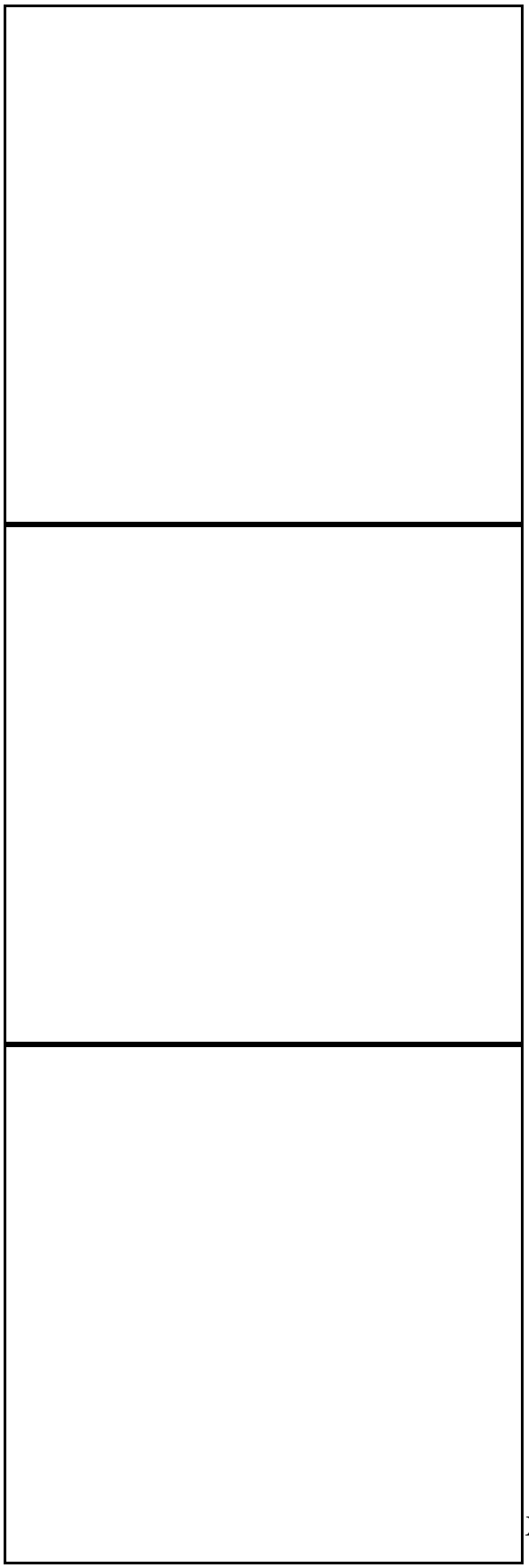

$$X_j = \sum_{i=1}^{s} N_{ij} \qquad (2)$$

$$Y_i = \sum_{j=1}^{t} N_{ij} \quad (3)$$

and

$$Z = \sum_i \sum_j N_{ij} = \sum_j X_j = \sum_i Y_i \quad (4)$$

Then the uncertainty with respect to X is:

$$H(X) = - \sum_{j=1}^{t} \frac{X_j}{Z} \log \frac{X_j}{Z} \quad (5)$$

and the uncertainty with respect to Y is:

$$H(Y) = - \sum_{i=1}^{s} \frac{Y_i}{Z} \log \frac{Y_i}{Z} \quad (6)$$

and the uncertainty with respect to the interaction of X and Y is:

$$H(XY) = - \sum_i \sum_j \frac{N_{ij}}{Z} \log \frac{N_{ij}}{Z} \quad (7)$$

Then define the conditional uncertainty with regard to Y with X given as:

$$H_X(Y) = H(XY) - H(X) \quad (8)$$

Finally, define a measure of predictability (P) with the range (0,1) as:

$$P = 1 - \frac{H_x(Y)}{\log s} = 1 - \frac{H(XY) - H(X)}{\log s} \quad (9)$$

where s is the total number of rows (categories) in the contingency matrix.

This last measure gives an index scaled on the range from 0 (unpredictable or maximum uncertainty) to 1 (totally predictable or minimum uncertainty). Predictability will be minimal when all the elements in the contingency matrix ($N_{ij}$) are equiprobable (i.e. when all entries are the same), and will be maximized when only one entry in each column is non-zero. Most real spatial data will fall between these extremes.

**Application**

The Kissimmee/Everglades drainage basin in south Florida represents one of the most rapidly changing and intensively modified landscapes in the country. A set of three land use maps with 26 land use categories were prepared for the years 1900, 1953 and 1973, in order to analyze the dramatic changes that had occurred in the region during this interval (Costanza, 1975; Costanza, 1979). For the predictability analysis we used versions of the land use maps which had been manually digitized into 128 acre (0.52 $km^2$) rectangular cells (Costanza, 1979). This produced an array with overall dimensions of 576 rows by 400 columns (230,400 total cells) of which about 93,000 were inside the study area. Each cell was assigned one of 26 land use categories ranging from natural to agricultural to urban systems (Costanza, 1979).

**Software and Algorithms**

Land use data was imported into Map II, a simple and easy to use GIS for the

Decreasing the resolution (increasing the grain) of a spatial data set involves the repetitive resampling of a specified number of smaller cells into larger cells. Analytically, this is accomplished by moving a resampling matrix (whose size is the number of rows and columns of the original data needed to make a single cell in the new raster) through the original raster. The cell values falling within the resampling matrix are tabulated and used to determine the value of the appropriate larger cell in the new, coarser resolution raster. We experimented with several methods of resampling or aggregating the spatial data. The first method, which we call *proportional aggregation* assigns the cell values in the coarser-grain raster according to the most dominant category found within the resampling matrix. A second method, termed *random aggregation* assigns new categories by randomly choosing from the categories found within the resampling matrix. The major difference between the two methods is that rare categories are more likely to be preserved when the data is resampled with the random aggregation scheme. While the choice of aggregation scheme can be significant in many spatial analysis, we found that the aggregation scheme made little difference to the results of our particular experiments. We settled on a version of the random aggregation scheme that is both simple and suits our immediate needs. In this version, aggregation takes place in steps. In each step the original map is aggregated using a 2x2 resampling matrix yielding an aggregated map with 1/4 the number of cells of the original. In each 2x2 resampling matrix we choose the category of the northwest cell as the category for the cell in the aggregate map. This process was repeated on the new aggregate map to yield a series of maps each with 1/4 the total number of cells of the one preceding it in the series. Figure 26 shows the results of this process for the South Florida, 1973 data set.

We developed algorithms in a parallel version of the C programming language to calculate auto and cross-predictability for mapped data on Inmos Transputers (a form of RISC based parallel processor) on a Macintosh (Costanza and Maxwell, 1991). Transputers are extremely fast for this sort of calculation. For example, for the South Florida data (a 576 x 400 array), calculation of auto-predictability and printing results to a text file took approximately 2.4 seconds using a Macintosh IIci with 4 transputers[17].

## Spatial scaling: Results

### Auto-Predictability Experiments

We calculated $P_a$ for several different years and at five different resolutions. We started with the maximum resolution of the data and gradually degraded it by aggregating pixels. In each step we halved the resolution by aggregating 2x2 blocks of pixels at the previous resolution into single pixels. Resolution is frequently indicated as the length of a side of a cell (pixel), with higher or finer resolution corresponding to smaller cell (pixel) sizes. For example, LANDSAT satellite data has 30 meter resolution, while SPOT satellite data is finer resolution at 18 meters. In our plots we wanted higher resolution to correspond to higher (not lower) numbers, so we measured resolution as the number of cells per $km^2$. Fifty meter cells would have a resolution of 400 cells/$km^2$, while 200 m cells would have a resolution of 25 cells/$km^2$.

We fit the equation:

$$P = k\, r^{(1-D_P)} \qquad (2)$$

where:
P = the spatial predictability ($P_a$ refers to auto-predictability, $P_c$ refers to cross-predictability)

[17]The algorithms also work on serial machines, only slower. Each tranputer is approximately the speed of a SUN Sparc station so the 4 transputer time is about four times the speed one would expect on a Sparc station. Contact Tom Maxwell for more information about using transputers for spatial analysis.

r = the resolution measured as the number of cells/km$^2$
k = a scaling factor
$D_P$ = the fractal predictability dimension (dimensionless)

by first transforming it into log-log form:

$$ln\ (P_l) = ln\ (k) + (1\text{-}D_P) ln\ (r) \qquad (3)$$

and using standard linear regression analysis to solve for the parameters k and $D_P$

The results are summarized in Table 2,which indicates the high $R^2$ for this relationship for both of the study sites.

Table 2 . Fractal auto-predictability dimension (given as $1\text{-}D_{AP}$), scale constant (k), adjusted $R^2$, and degrees of freedom (df) for auto-predictability ($P_a$) from regression of equation 3. ** indicates significant at the .01 level, * indicates significant at the .05 level.

| Year | k | $(1\text{-}D_{AP})$ | adj $R^2$ | df |
|---|---|---|---|---|
| 1900 | 0.6364 | 0.111 | .999** | 4 |
| 1953 | 0.6383 | 0.085 | .988** | 4 |
| 1973 | 0.6250 | 0.096 | .981** | 4 |
| all years | 0.6332 | 0.097 | .958** | 14 |

**Cross-Predictability Experiments**

We calculated $P_c$ by comparing maps from the 3 different years. This is analogous to a simple "null model" that predicts land use patterns for one time from patterns at some previous time or times. This “model” includes no information on the underlying processes of change, but we were interested in how changing the resolution of the maps affected the predictability and the “null model” of no change is an interesting point of reference. We fit equation 3 to the data and the results are shown in Table 3.

Table 3. Fractal cross-predictability dimension (stated as $1\text{-}D_P$), scale constant (k), adjusted $R^2$, and degrees of freedom (df) from regression of equation 3 for cross-predictability ($P_c$). ** indicates significant at the .01 level, * indicates significant at the .05 level.

| Year | k | $(1\text{-}D_P)$ | adj $R^2$ | df |
|---|---|---|---|---|
| 1900/1953 | 0.5764 | -.011 | .943** | 4 |
| 1953/1973 | 0.4936 | -.017 | .778* | 4 |

Results of both the auto and cross-predictability experiments are plotted together on a log-log scale in Figure 27. The strong linearity of the relationship for all cases is apparent, as

is the fact that auto-predictability ($P_a$) increases with increasing resolution while cross-predictability ($P_c$) decreases slightly with increasing resolution, although with a smaller $D_p$. These results are consistent with our original hypotheses.

In addition, this "null model" is of limited real usefulness since it embodies none of the underlying processes that caused the land use changes. In the more general case of dynamic landscape models, or models in general, we would not expect such high initial values of predictability, and would expect the predictability to fall more quickly with resolution. We are currently building the ELM to be one dynamic spatial to be used in testing this hypothesis, which can be summarized in Figure 28.

## Temporal scaling

Time series of data have varying degrees of complexity and pattern, which results in varying success in using summary statistics to characterize the data. Rainfall, cloudiness, and solar insolation are examples of some of the time series data that may have different underlying processes and pattern. Biological processes such as carbon fixation and nutrient uptake may be measured on a fine scale, but otherwise need to be characterized on a coarser scale. These data may exist on finer scale (higher sampling frequency) than that desired for a coarser scale simulation. There are several approaches to using data from complex time series for simulation or other purposes, ranging from using all of the information to using simple averages over specific time intervals. A problem with the former is the potential for excessive computational complexity associated with using all of the information on a finer scale. With the latter approach, simple averages have the potential to lose significant information and have significant error in aggregation that depends on the degree of nonlinearity, the extent to which patterns are reciprocal, etc. Thus, there is a need to develop rules for scaling time series data of ecological processes from fine scale measurements to the coarser scales that the ELM and other simulation models may use in their basic time step.

We are developing algorithms with which to determine the appropriate sampling scale of a time series. If there is a recurring pattern in the data, a Fourier transform can be used to characterize that pattern. However, a frequency analysis depends on the existence of that periodicity. Such a pattern may often emerge in coarse scale phenomena such as annual cycles, but the aperiodic information at finer temporal scales would be lost. In the case where the information is not periodic, we need other measures to sample and characterize the data.

For this investigation, we want to use a variety of tools in an exploratory analysis. We wrote a program[18] (in C) to read the data and subsample it at user defined intervals, the width of which may range from a minimum of 20 units to the number of points in the data set. The fractal dimensions of the data in the window intervals are determined for the entire data set, along with several summary statistics. A predictability index, based on Colwell (1974) as described above for the spatial cases, was also calculated for the data using the number of time intervals defined by the chosen window size. The predictability index is based on the sampled point $N_k$ being in one of 4 states, the state depending on the normalized distance of the point from the mean $X_i$ of its time interval i:

$$State1:\ 0 \le \frac{|N_k - X_i|}{X_i} \le 0.05$$

$$State2:\ 0.05 < \frac{|N_k - X_i|}{X_i} \le 0.10$$

$$State3:\ 0.10 < \frac{|N_k - X_i|}{X_i} \le 0.15$$

[18] S. Hutchinson of the University of South Carolina wrote the code for determining the fractal dimension. We modified the code for our other purposes.

$$State\,4:\ 0.15 < \frac{|N_k - X_i|}{X_i}$$

where k is the total number of points. Thus, this provides a measure of how consistent, or predictable, the data are within each interval of the entire data set. The size of the windows and total number of points determines the number of time intervals i within the k values of the time series. At a window size equal to the number of points in the series, the predictability is 1.0 by definition in that there is only one "sampled" time period. With the distances defined above, a random data set has a predictability of 0.5, (a value which is dependent on the arbitrary distance values chosen in this development example). The predictability values are plotted against window size, with the (changing) slope of the curve depending on the pattern of the data.

The fractal dimension for each interval width indicates the degree of complexity within the interval, and a mean, standard deviation, and coefficient of variation are available to characterize the interval. At this point, we hope to evaluate the efficacy of using different measures of central tendency and variance for the intervals. These statistics are to be used to develop a set of objective rules for determining the optimal width of a sampling window for individual data sets. The basic objective is to merely reduce the error associated with nonlinearities within sample intervals. A narrow window is needed for data that has a complex, non-random pattern over short intervals; a wide window may be used for data that behaves in a more linear manner. Depending on the data and on the equations in the simulation that utilize the data, this summary can be made in different ways. The simplest is the mean within each window, but measures of dispersion may be needed or desired. We are currently determining if some of these relatively simple summary statistics can be used effectively in aggregating a complex time series of data for a coarser scale of input to a simulation run.

The time series data are analyzed in this manner for the range of windows possible/desired. We used a variety of different data sets for analysis, ranging from random distributions to rainfall data from a station in south Florida. The changing slope of plots of the predictability versus window size provide an indication of pattern of the data (Figure 29). The plots of fractal dimension for each window interval, as they change with varying window size, can be used to evaluate the changing complexity as the sampling interval scale changes (Figure 30). The mean associated with those window sizes are provided for comparison. These plots are very preliminary results, using algorithms that will be examined more thoroughly and likely be modified. However, this is presented to indicate one of the directions that some temporal scaling issues may be addressed regarding the ELM.

## Process complexity

One of the fundamental aspects of model development is recognizing the degree of process complexity needed for the stated objectives. We are establishing a set of model experiments to analyze the effects of aggregation of parameters and mathematical relationships in the equations of the unit model. Rastetter et al. (1992) provided a rigorous examination of different methods in approaching the issue of aggregating fine-scale knowledge to predict coarse scale phenomena in simulation models. After an evaluation of the degree of non-linearity in the process, they indicated that there are two reasonable means to accommodate aggregation of processes that have significant non-linearities which pose potential error in the model estimates. One method is a partial transformation using an expectation operator that is based on knowledge of the probability distribution of the fine scale process. Another is the use of further partitioning of processes. Where adequate data are available, calibration provides a very attractive means by which to capture the aggregate behavior of the fine scale processes on a coarse scale. Rastetter et al. (1992) point out that it may be very beneficial to combine a process of disaggregating some fundamental processes where appropriate in conjunction with a recalibration.

Using a modular framework for the unit model development, we have a modeling tool that is amenable to the changing and analyzing process complexity. The unit model is designed

to be able to be run at varying spatial scales and for widely varying habitat types. The base configuration can be readily disaggregated to incorporate more detail on constraints, feedbacks, or other aspects of the simulation. For habitats as diverse as fresh marshes and upland forests, we can evaluate the degree of sensitivity of the parameter set using sensitivity analysis routine built into the STELLA modeling software. The sensitivity may vary across habitat types, showing which aspects of the unit model may need modification to be truly general for implementation across widely varying systems.

A particular feedback or parameter may largely drive a process and value of a stock in one system, but be comparatively unimportant in another. For example, the unit model's simulation of organic material decomposition and remineralization of nutrients currently is constrained by several factors, including temperature, moisture and substrate quality. We implicitly incorporate the redox potential in the sediments using a simple water depth - aerobic zone relation and generalized rate parameters for aerobic and anaerobic environments. This appears to be adequate for our current objectives concerning the stock of nutrients within a broad zone of sediment, but would require more detailed relationships for finer scale model output concerning the fluctuations in nutrient availability in different layers of the root zone. An evaluation of the plant growth response to changes in nutrient availability would indicate whether such modifications are useful toward increasing the precision of the output. Model components such as this may be important in an intermittent wetland habitat if very fine resolution is important, but comparatively unimportant in an upland forest. Such determination, using standard tools of analysis on a modular modeling framework, will constitute the basic design of the scaling of the unit model complexity.

We anticipate that disaggregation of the unit model will not be necessary for the current objectives of the ELM. However, future simulation needs may necessitate some reformulation of the process complexity of the unit model. At that stage, we want to have the means to evaluate the resulting behavior of the unit model with and without the more complex model structures.

## ACKNOWLEDGMENTS

The expert input and assistance of Fred Sklar (SFWMD) has been an invaluable part of this model development process. We would like to thank Marie Pietrucha, Ken Rutchy, Les Vilcheck, Yegang Wu, Kishore Gopu, Randy Van Zee, and Tom Fontaine at the South Florida Water Management District for their extensive assistance in implementing a variety of aspects of the ELM. We reiterate our appreciation to those from throughout Florida (and other regions) who participated in the past Task 1 model development workshops. Beatrice Castaneda (MIIEE) provided assistance in finding the large amounts of data to parameterize the ELM. Tom Maxwell (MIIEE) developed the critically important spatial modeling program for parallel processing and many of the concepts associated with the spatial modeling.

## LITERATURE CITED

Bowie, G.L., Mills, W.B., Porcella, D.B., Campbell, C.L., Pagenkopf, J.R., Rupp, G.L., Johnson, K.M., Chan, P.W.H., Gherini, S.A. and Chamberlin, C.E., 1985. Rates, constants, and kinetics formulations in surface water quality modeling. U.S. Environmental Protection Agency, Office of Research and Development, Athens, GA, 455 pp.

Browder, J.A., in press. Periphyton in the Everglades: spatial variation, environmental correlates, and ecological implications. In: (Editors), Proceedings of Everglades Symposium. Key Largo, FL.

Christiansen, J.E., 1968. Pan evaporation and evapotranspiration from climatic data. J. of Irrig. and Drain. Div., (94):243-265.

Colwell, R.K., 1974. Predictability, constancy, and contingency of periodic phenomena. Ecology, 55:1148-1153.

Costanza, R., 1975. The Spatial Distribution of Land Use Subsystems, Incoming Energy and Energy Use in South Florida from 1900 to 1973. Master's Research Project, Department of

Jarvis, P.G. and McNaughton, K.G., 1986. Stomatal control of transpiration: scaling up from leaf to region. Advances in ecological research, 15:1-45.

Kessell, S.R., 1977. Gradient modeling: a new approach to fire modeling and resource management. In: (Editors), Ecosystem Modeling in Theory and Practice. John Wiley and Sons, New York, USA, pp. 575-606.

Lassiter, R.P., 1975. Modeling dynamics of biological and chemical components of aquatic ecosystems. Southeast Environmental Research Laboratory, U.S. Environmental Protection Agency, Athens, GA.

Mandelbrot, B., 1983. The fractal geometry of nature. Freeman, New York, 460 pp.

Milne, B., 1992. Spatial aggregation and neutral models in fractal landscapes. The American Naturalist, 139:32-57.

Milne, B.T., 1988. Measuring the fractal dimension of landscapes. Applied Mathematics and Computing, 27:67-79.

Nikolov, N.T. and Zeller, K.F., 1992. A solar radiation algorithm for ecosystem dynamic models. Ecological Modelling, 61:149-168.

NOAA, 1989. Computer Mapping and Analysis System for Analyzing Shrimp Harvest Data (CMAS) - evolving assessment capabilities for fisheries management. Strategic Assessment Branch, Office of Oceanography and Marine Assessment, NOAA.

NOAA, 1990. COMPAS - NOAA's Coastal Ocean Management, Planning, and Assessment System. Strategic Assessment Branch (N/OMA31), Office of Oceanography and Marine Assessment.

Olsen, L.F. and Schaffer, W.M., 1990. Chaos versus noisy periodicity: alternative hypotheses for childhood epidemics. Science, 249:499-504.

Rastetter, E.B., King, A.W., Cosby, B.J., Hornberger, G.M., O'Neill, R.V. and Hobbie, J.E., 1992. Aggregating fine-scale ecological knowledge to model coarser-scale attributes of ecosystems. Ecological Applications, 2:55-70.

Reyes, E., Day, J.W., White, M.L. and Yáñez-Arancibia, A., 1993. Ecological and Resource Management Information Transfer for Laguna de Terminos, Mexico: a computerized interface. Coastal Management, 21:37-51.

Robinson, K., 1990. Fires over Yellowstone. NCSA "Access" newsletter, May-Jun 1990. Univ. of Illinois at Urbana. pp. 1-3.

Rossi, R.E., Mulla, D.J., Journel, A.G. and Franz, E.H.., 1992. Geostatistical tools for modeling and interpreting ecologicl spatial dependence. Ecological Monographs, 62:277-314.

Steele, J.H., 1965. Notes on some theoretical problems in production ecology. In: (Editors), Primary production in aquatic environments. University of California Press, Berkeley, CA, pp. 393-398.

Steward, K.K. and Ornes, W.H., 1975. The autecology of sawgrass in the Florida everglades. Ecology, 56:162-171.

Sugihara, G. and May, R.M., 1990. Nonlinear forecasting as a way of distinguishing chaos from measurement error in time series. Nature, 344:734-741.

Tufte, E.R., 1990. Envisioning Information. Graphics Press, 126 pp.

Turner, M.G., 1987. Spatial simulation of landscape changes in Georgia: a comparison of 3 transition models. Landscape Ecology, 1:29-36.

Turner, M.G., Costanza, R. and Sklar, F.H., 1989. Methods to evaluate the performance of spatial simulation models. Ecological Modeling, 48:1-18.

USACOE, 1984. Shore Protection Manual. U.S. Army Corps of Engineers, Vicksburg, Mississippi, 501 pp.

Wiegert, R.G. and Wetzel, R.L., 1979. Simulation experiments with a fourteen-compartment model of a Spartina salt marsh. In: (Editors), Marsh estuarine system simulation. University of South Carolina Press, pp. 7-39.

Wright, J.R., Benabdallah, S. and Engel, B.A., 1990. A normalized user interface for complex simulation models. AI Applications in Natural Resource Management, 4:11-15.

## FIGURES

List of figures with brief descriptor and page numbers where they are referenced.

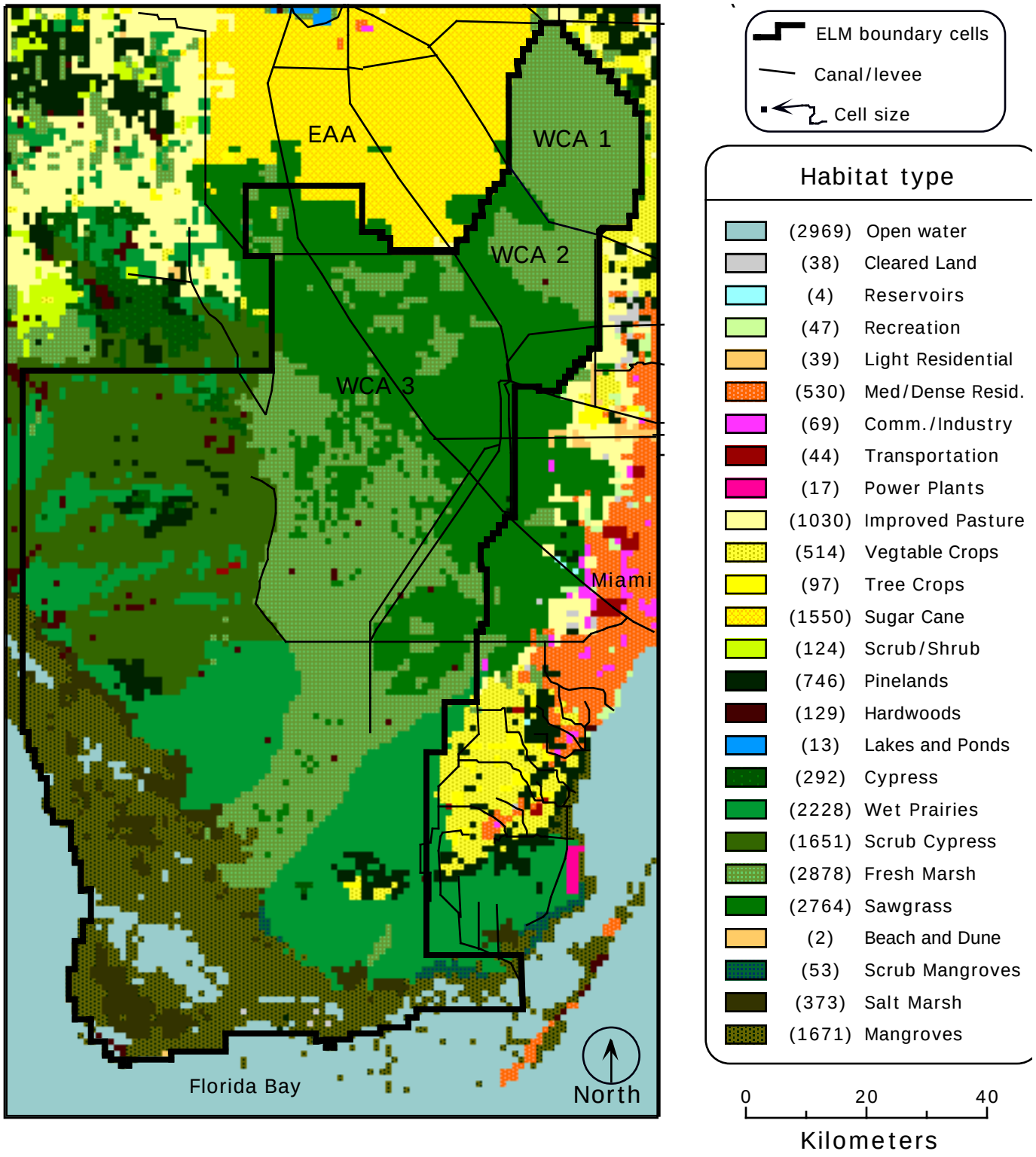


Figure 1. Landscape pattern of habitat types found in south Florida in 1973, the present-day major canal/levee locations, and the cells composing the Everglades Landscape Model (ELM) boundary. The legend shows an example of the 1 $km^2$ cell size used in ELM and the number of cells having each habitat type. The habitat types map layer is a $1km^2$/cell raster representation of the data from Costanza (1979); the ELM uses 14 habitat types, omitting the urban and agricultural regions.

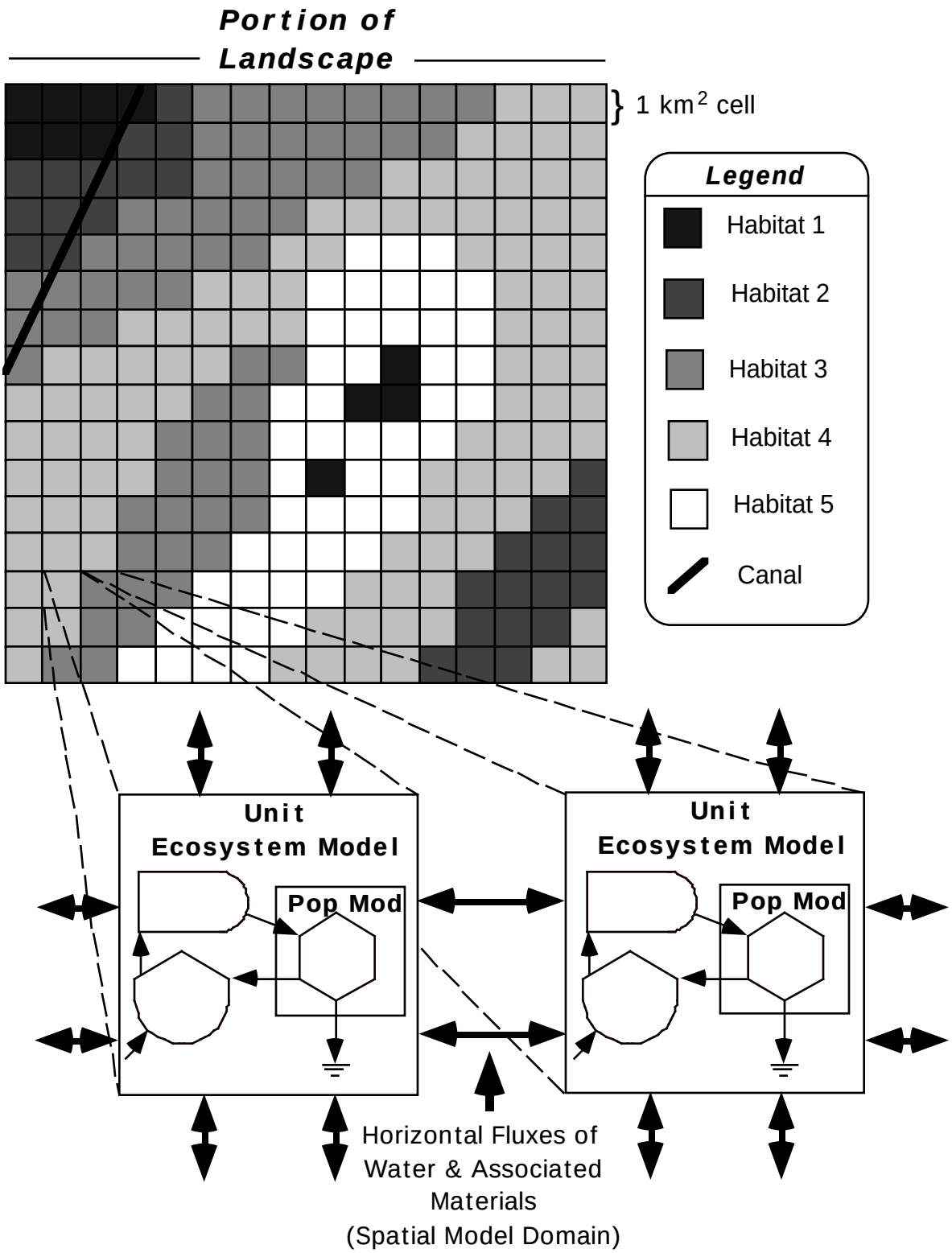


Figure 2. The basic structure of the ELM. Each cell has a (variable) habitat type, which is used to parameterize the unit model for that cell. The unit model simulates ecosystem dynamics via the interactions of biotic and abiotic components. Nutrients and suspended materials in the surface water and saturated sediment water are fluxed between cells in the domain of the spatial model.

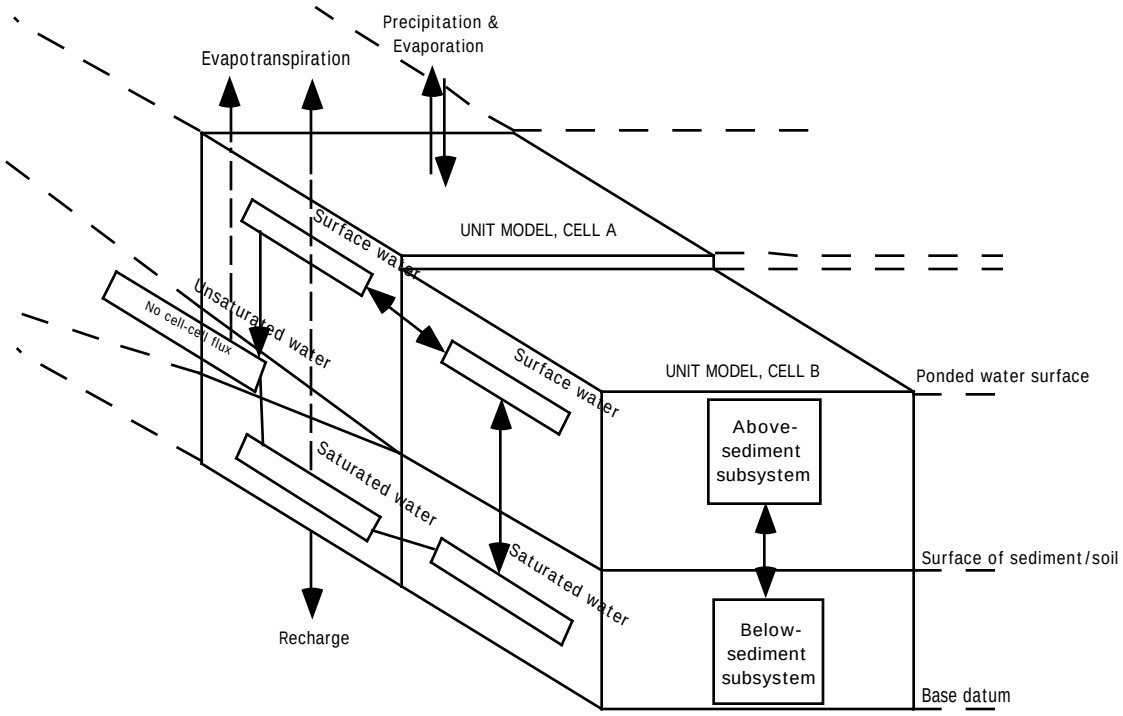


Figure 3. The basic hydrologic variables and flows in the ELM. Within each model cell, vertical flows are simulated by the unit model that is parameterized for the cell's habitat. Horizontal fluxes of water between cells are within the domain of the spatial model, and depend on head differences between cells.

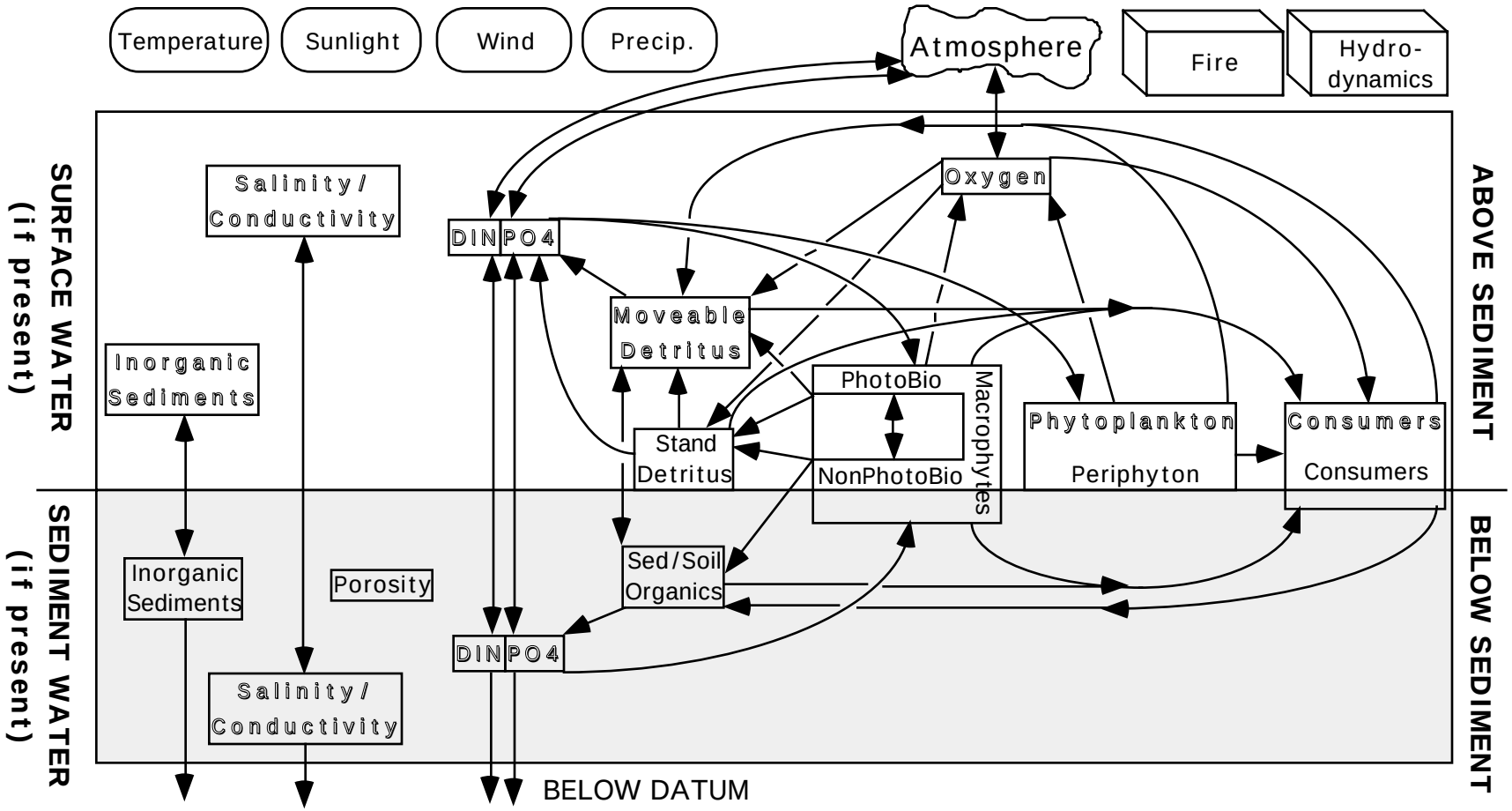


Figure 4. The state variables and mass fluxes of the unit model, excluding hydrology (Figure 3). The model is run within one cell and parameterized for the cell's habitat. Hydrology is important in the vertical fluxes shown and the unshown horizontal fluxes of materials from cell to cell. State variables are enclosed within rectangles, and those that can flux vertically and horizontally with water movement are shown in outline type. Environmental inputs are shown in ⬭ ; fire and hydrodynamics are simulated processes that affect model dynamics. Not shown are a number of indirect, informational flows such as the influence of periphyton on calcite precipitation to the inorganic sediments. Metabolic sinks are not shown. Dissolved Inorganic Nitrogen (DIN) and $PO_4$ are separate state variables with slightly different dynamics. Although not shown, both nutrients are involved in uptake and mineralization processes.

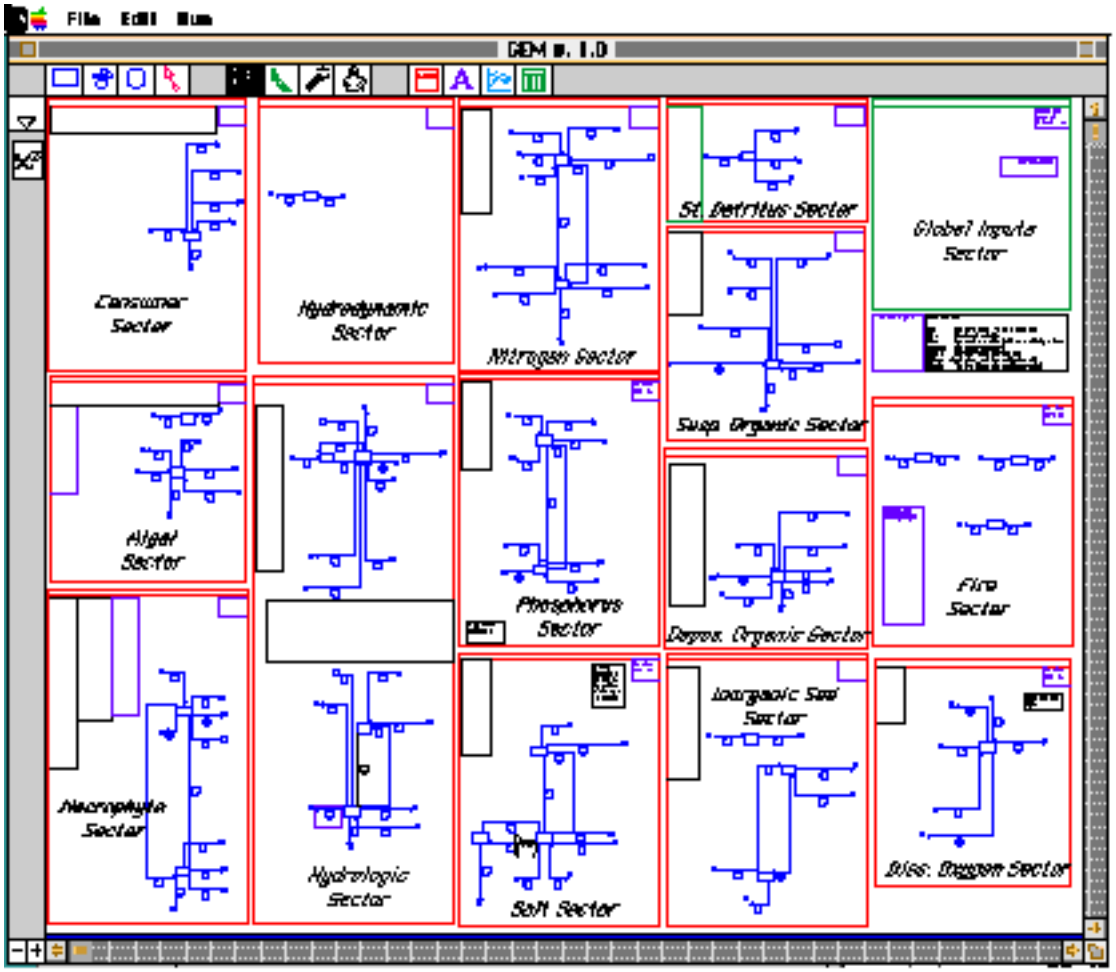


Figure 5. The unit model, GEM, as it appears on the screen of a Macintosh computer. Large, rectangular blocks enclose the 15 sectors, with text labels added in this figure for “navigating”. The model diagram shown above is a simplified map showing only state variables and associated flow pathways. Not shown are the numerous auxiliary variables and information flows.

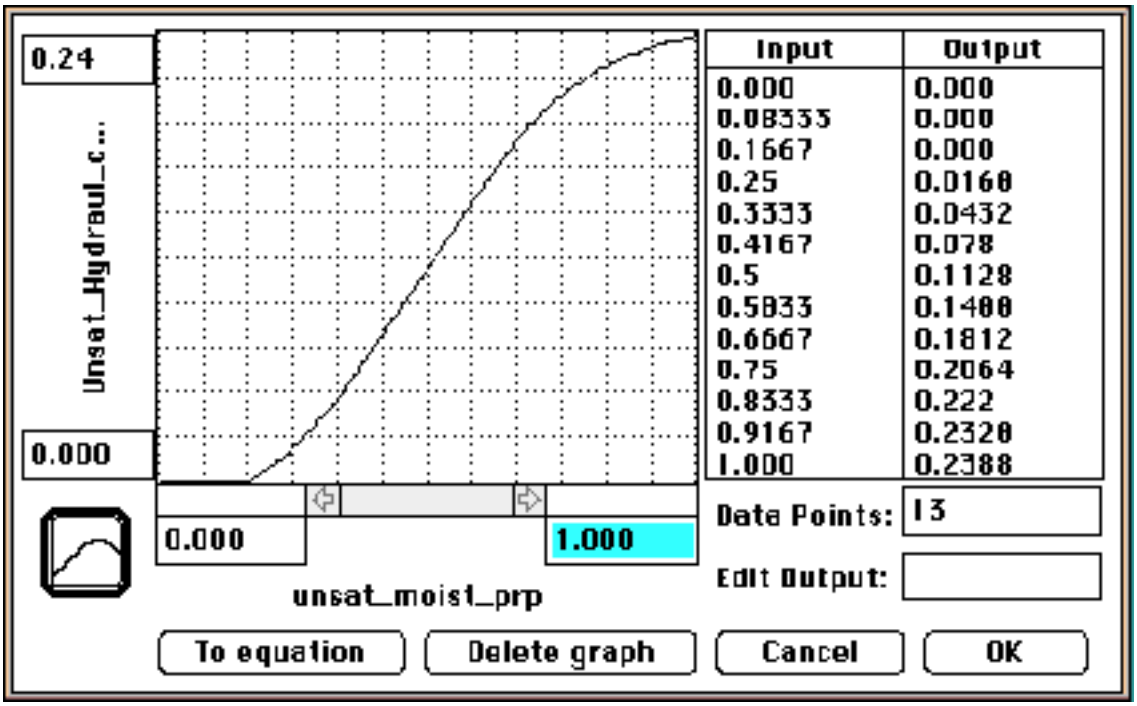


Figure 6. The STELLA® dialog box containing the relationship between the unsaturated moisture proportion (Input, along the X axis) and the hydraulic conductivity (Output, shown on the Y axis).

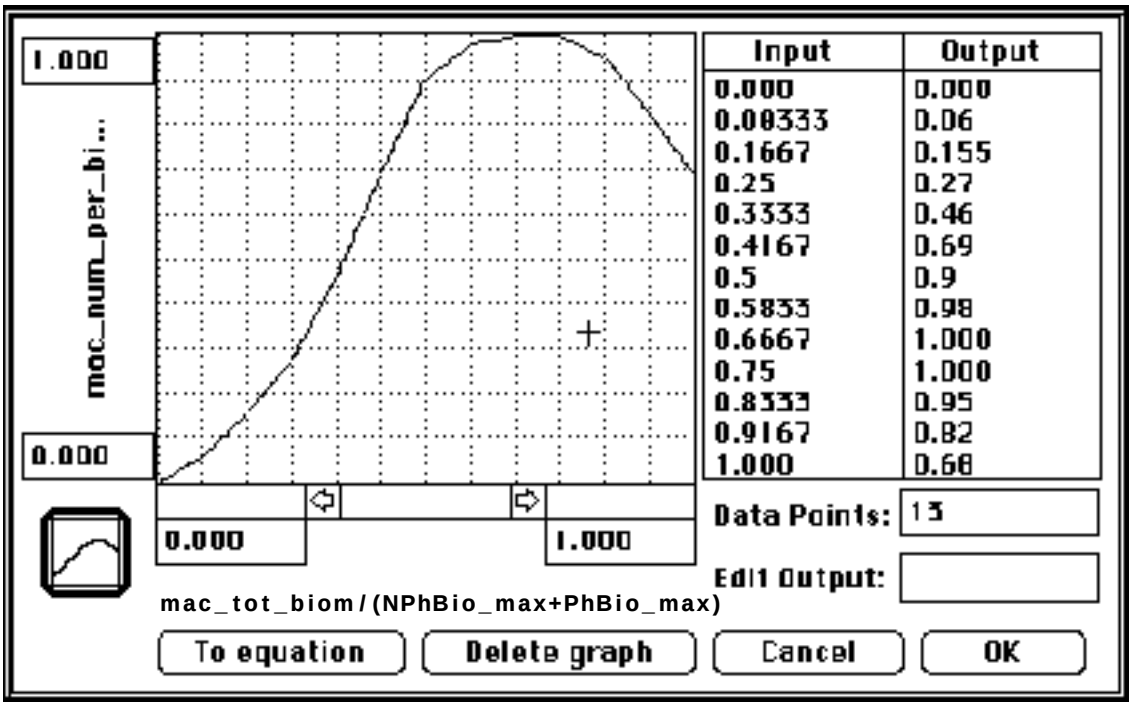


Figure 7. The STELLA® dialog box containing the relationship between the proportion of the maximum biomass that is present (Input, along the X axis) and the number of shoots or trunks per unit biomass (Output, shown on the Y axis).

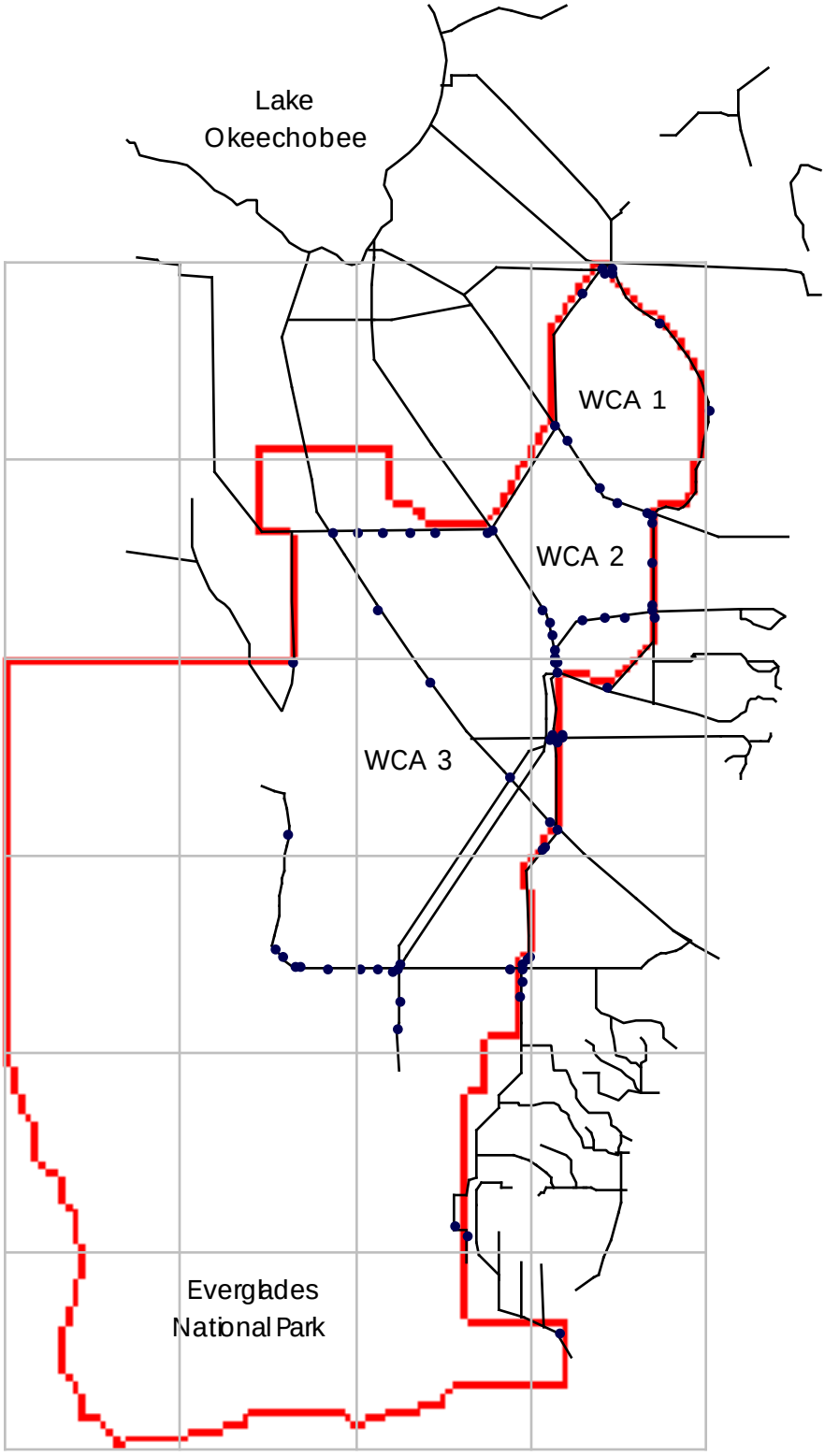


Figure 8. The ELM model boundaries (thicker lines), the control structures (•) included within the boundaries, and the network of major canals and levees in south Florida. The SFWMM simulation includes all of the canals/levees shown. The distribution of 24 transputer processors is shown by the dotted squares. Note that several processors are idle in this preliminary configuration.

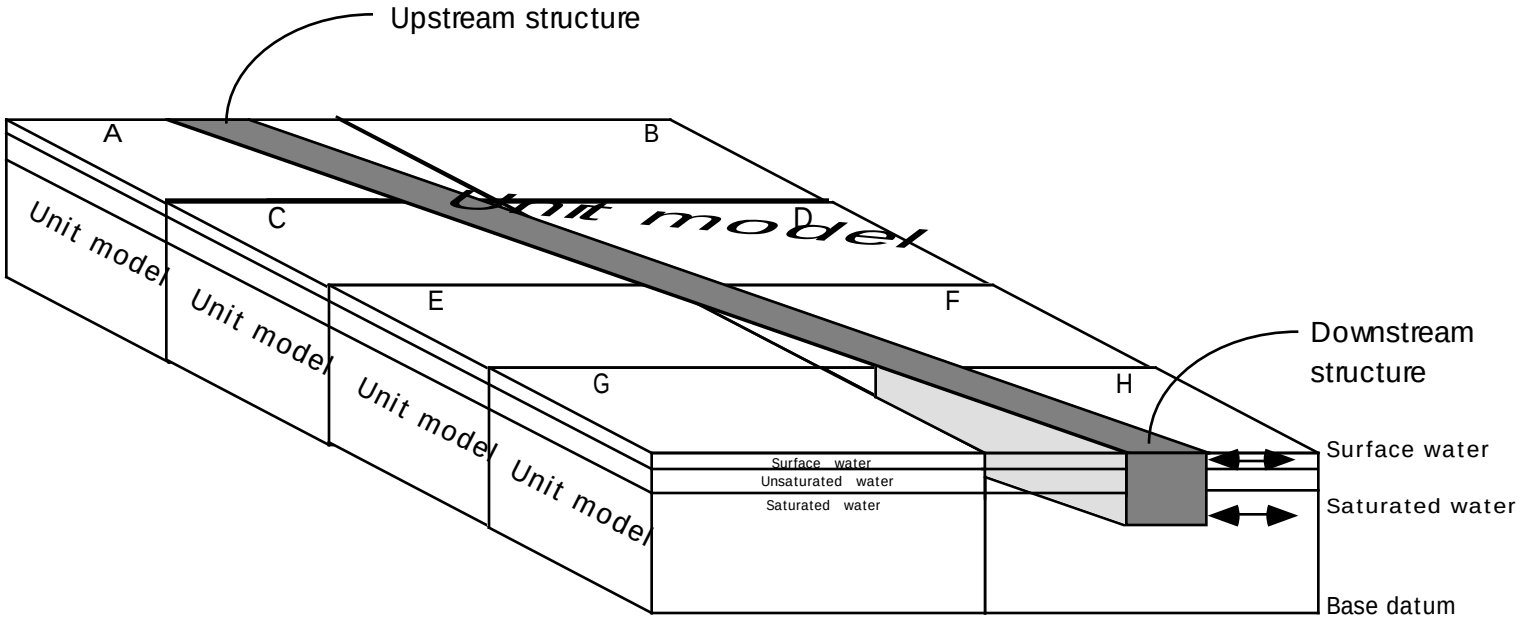


Figure 9 canal;. Spatial articulation of a canal interacting with unit cells. Canal is shown as shaded hypervolume, with the unit model simulating ecological dynamics within the entire volume between upstream and downstream structures of a canal. The areal extent of interaction with unit cells A, C, D, E, F, and H are required for fluxing water and nutrients between the canal and unit cells in the spatial model. Canal depth and width, and height of canal surface water above the sediment are exaggerated in size.

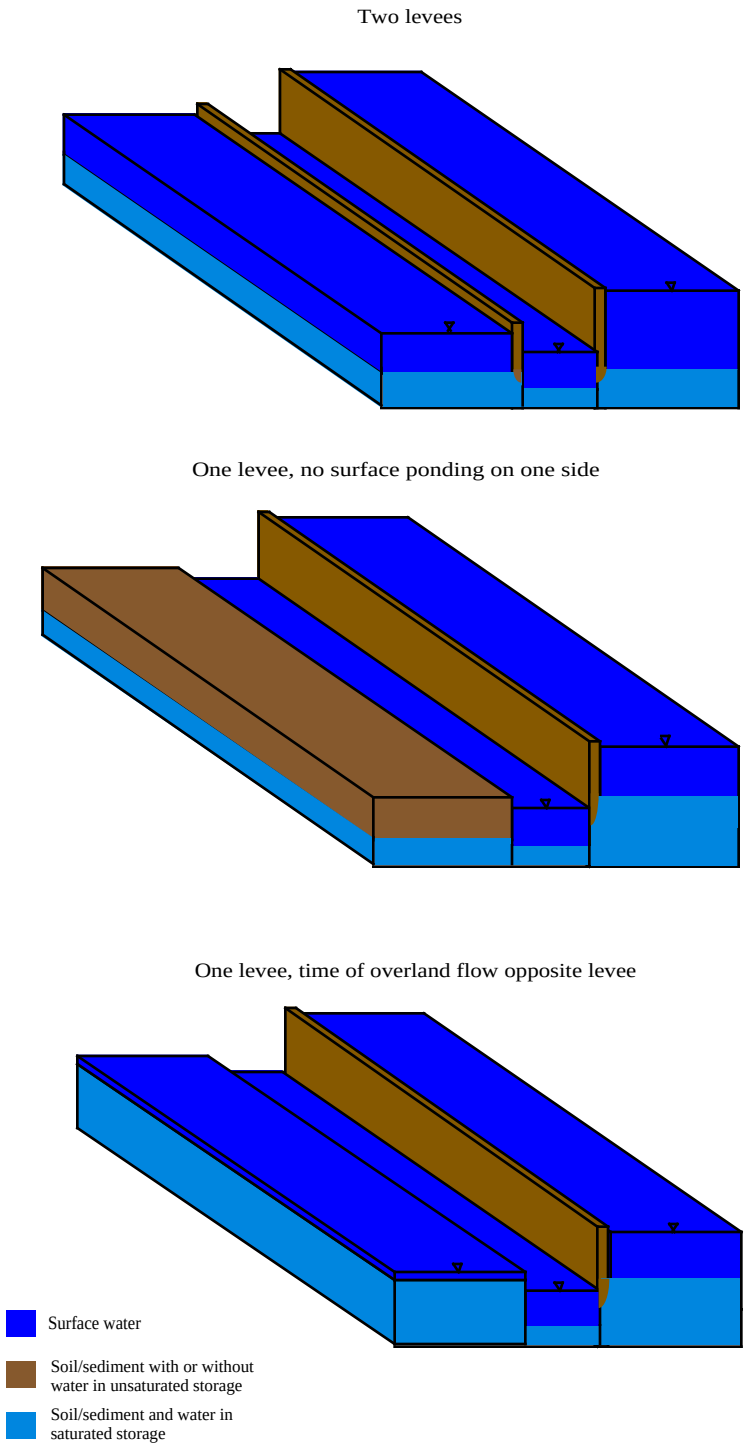


Figure 10. Different combinations of canals and levees that are simulated in the ELM.

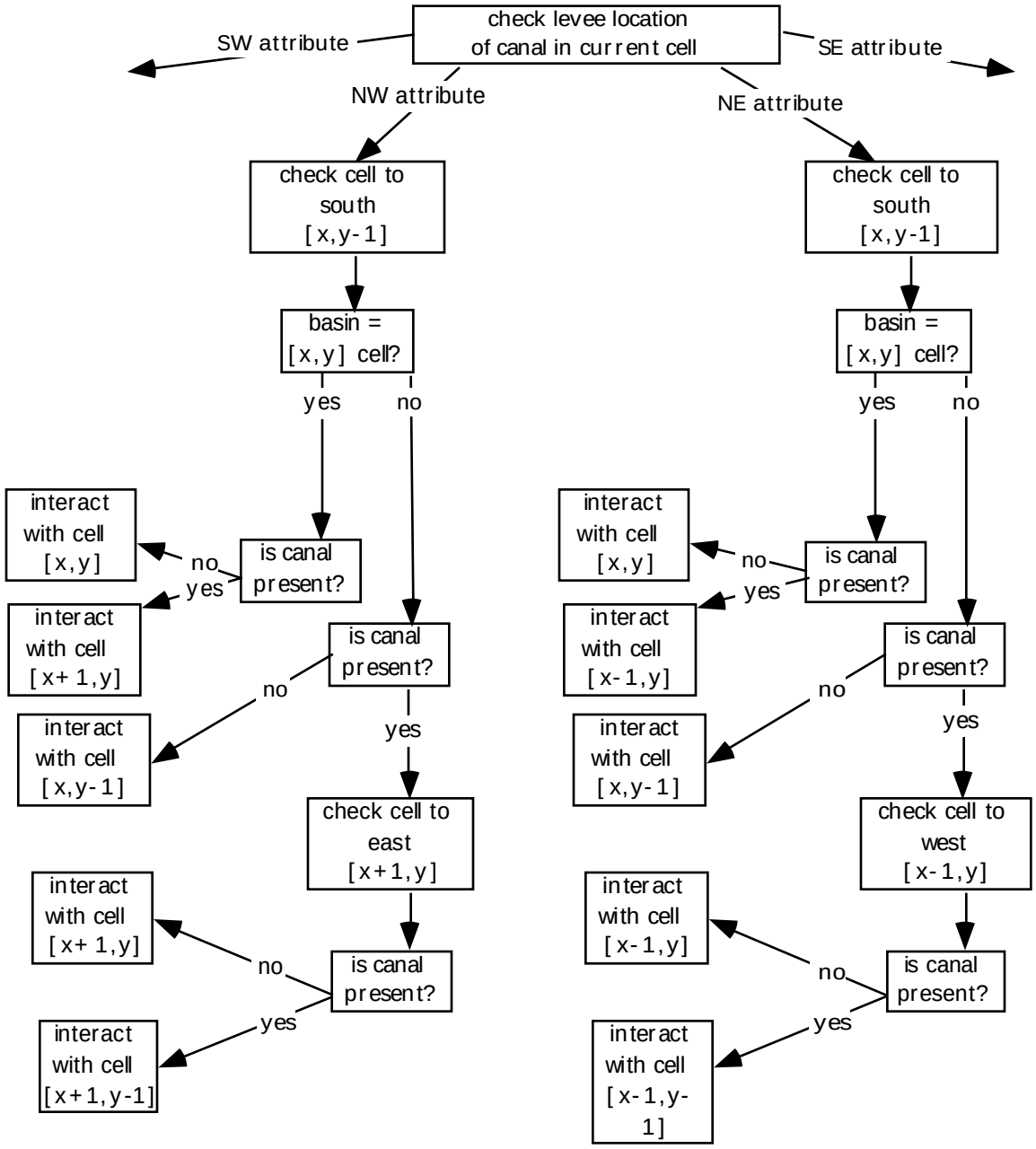


Figure 11. Logic to determine which cells have overland flow interactions with a defined canal. Two of four possible configurations are shown.

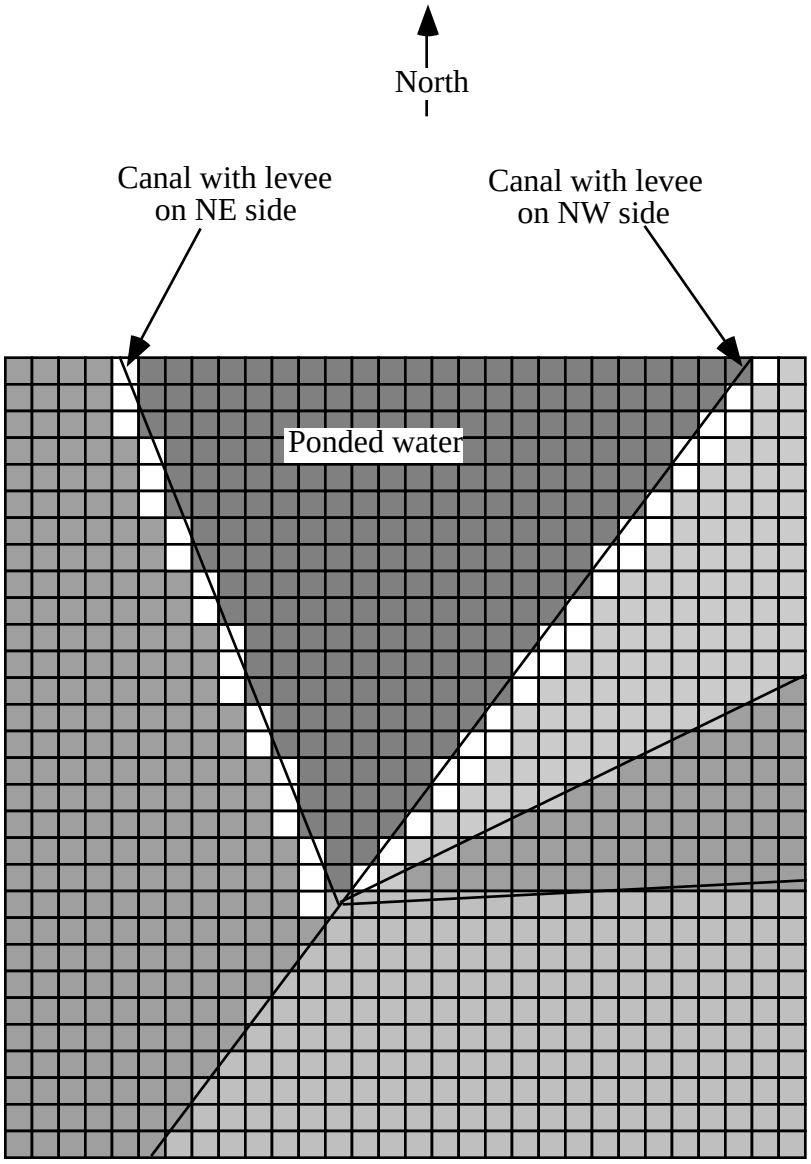


☐ Cells that have overland flow interaction with canal. These cells have basin attributes outside of the ponded water basin.

Figure 12. Configuration of canals, levees and basins. Basins are separated by levees adjacent to canals.

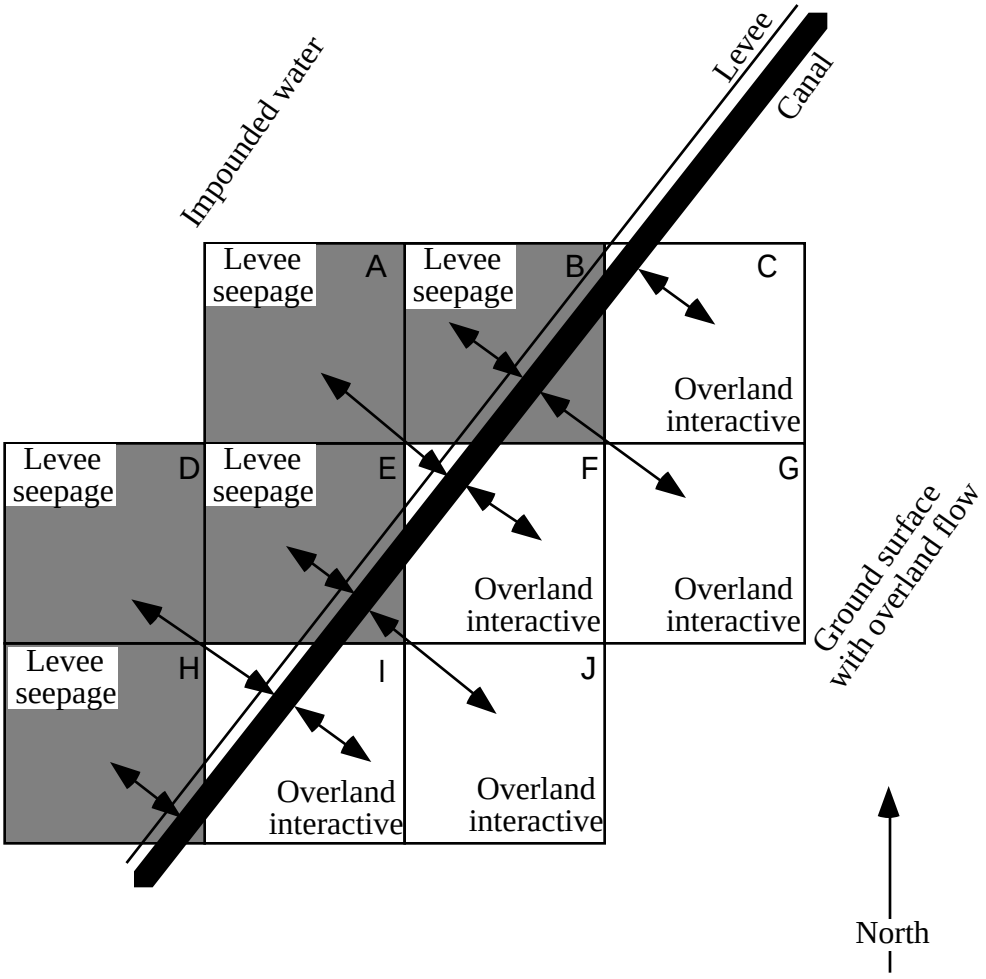


Figure 13. Result of procedure to assign overland flow versus levee seepage attributes to cells near a canal/levee configuration.

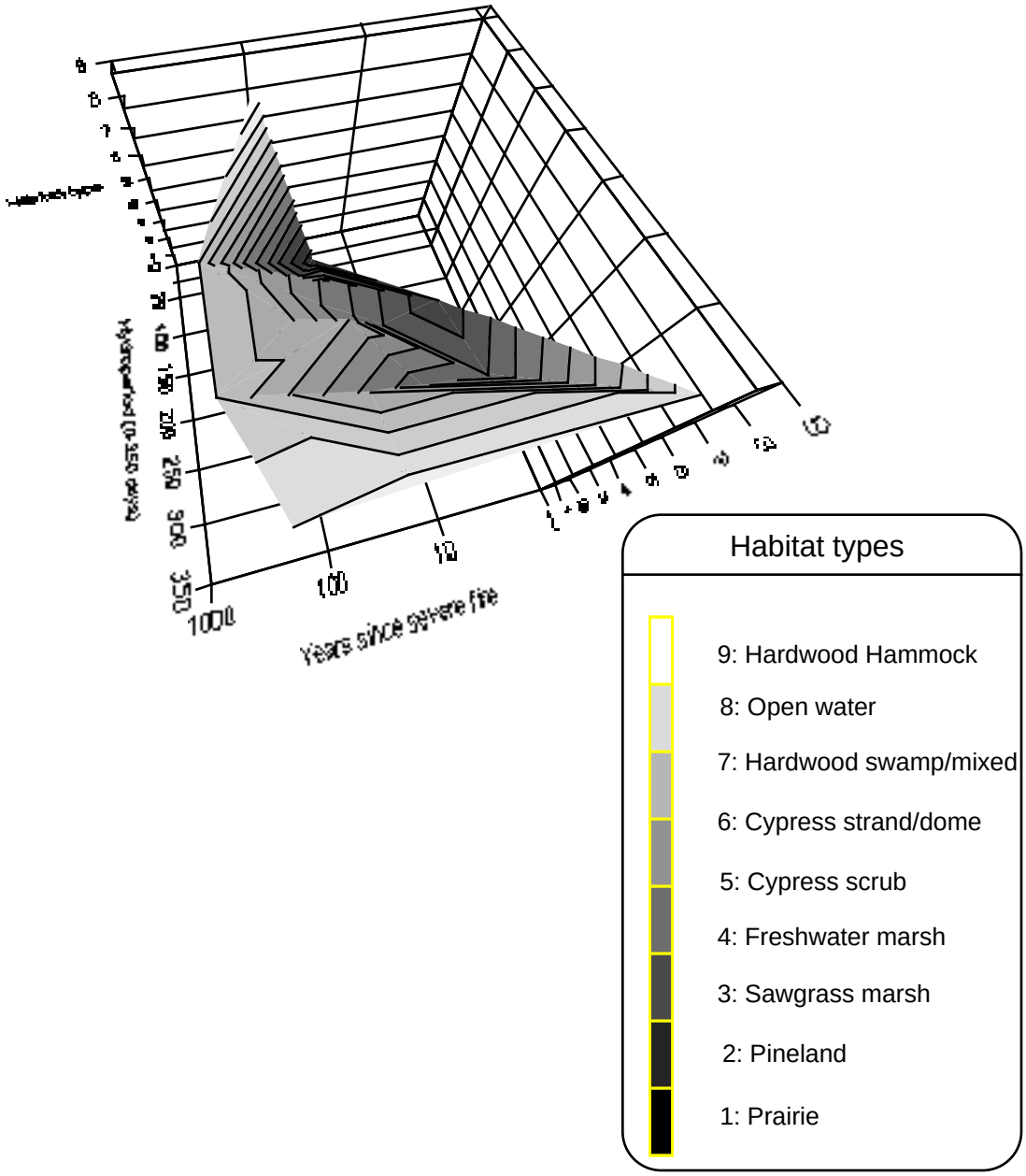


Figure14. Habitat type resulting from varying combinations of hydroperiod and fire frequency, modified from Duever (1984). For the ELM habitat switching algorithm, a fourth dimension of historical nutrient regime is added to this 3-D function.

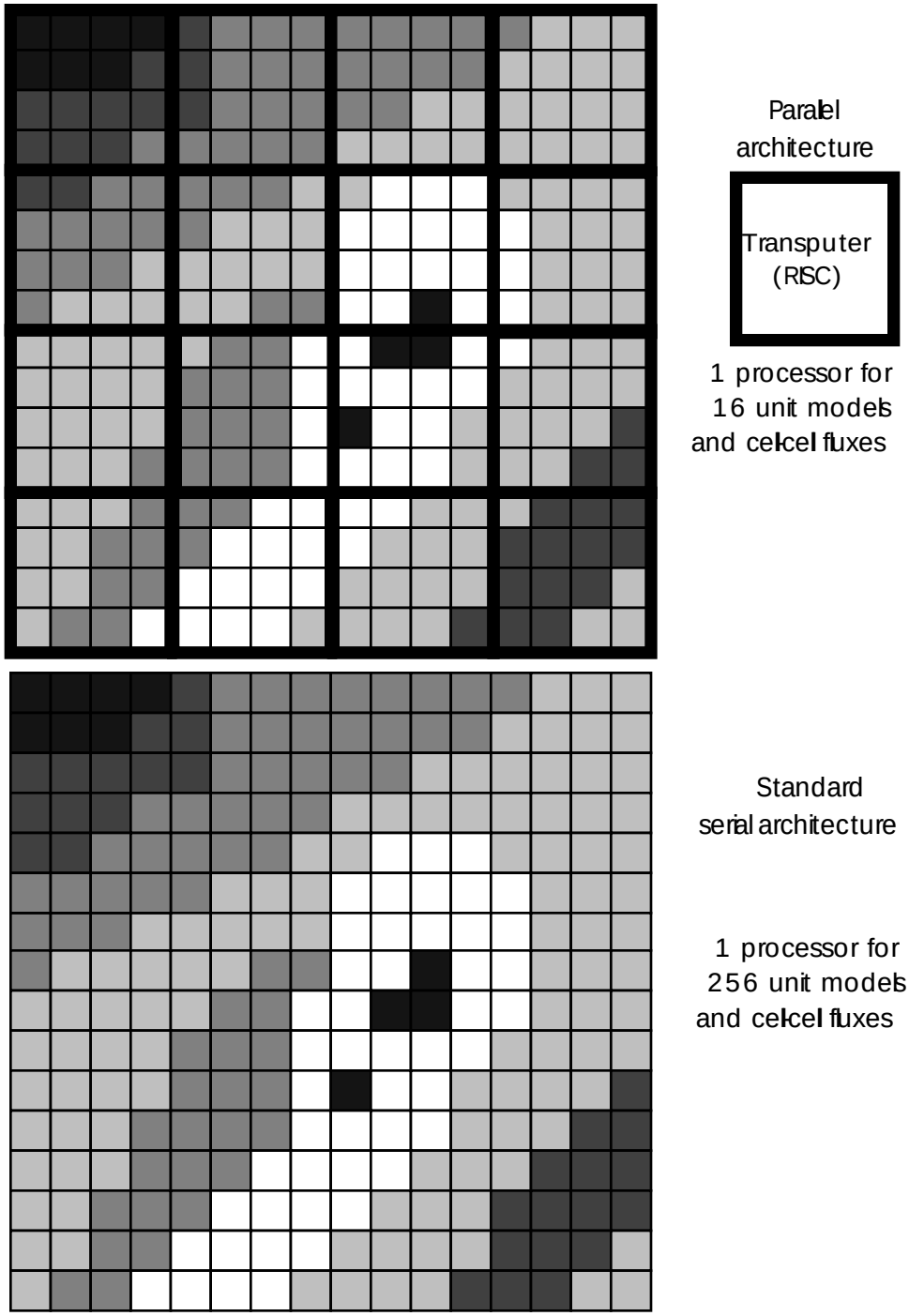


Figure 15. A hypothetical diagram of the distribution of computer processors for a parallel processing architecture versus a standard serial architecture. The computational load of running a unit model in the 256 cells shown is distributed over 16 (24 in ELM) high speed RISC chips in the transputer architecture. In the serial architecture such as a standard workstation, runtimes are longer by a factor close to the extent of load partitioning in parallel.

export as ASCII

| | Unit model Sectors, Daughter Databases | | | | | | | | | | | |
|---|---|---|---|---|---|---|---|---|---|---|---|---|
| | Algae | Depos. Org. Matter | Dissolv. Inorg. Nitrogen | Dissolv. Oxygen | Fire | Global Inputs | Hydro-dynamics | Hydrologic | Inorg. Sediments | Macrophytes | Natural Consumers | Ph |
| Sawgrass | | | | | | | | | | | | |
| Wet Prairie | | | | | | | | | | | | |
| Cypress | | | | | | | | | | | | |
| Mangroves | | | | | | | | | | | | |
| Pinelands | | | | | | | | | | | | |

| | |
|---|---|
| **DIN_dif_coef** | **Diffusion coefficient for Nitrogen** |
| **DIN_K_of_NH4** | **Proportion of NH4 available in pore water for uptake.** |
| **ic_DIN_SED_WT** | **Initial condition, concentration of DIN in sediment water** |
| **ic_DIN_SF_WT** | **Initial condition, concentration of DIN in surface water** |
| **rc_DIN_denit** | **Rate of denitrification; specific rate at reference T=20 C.** |

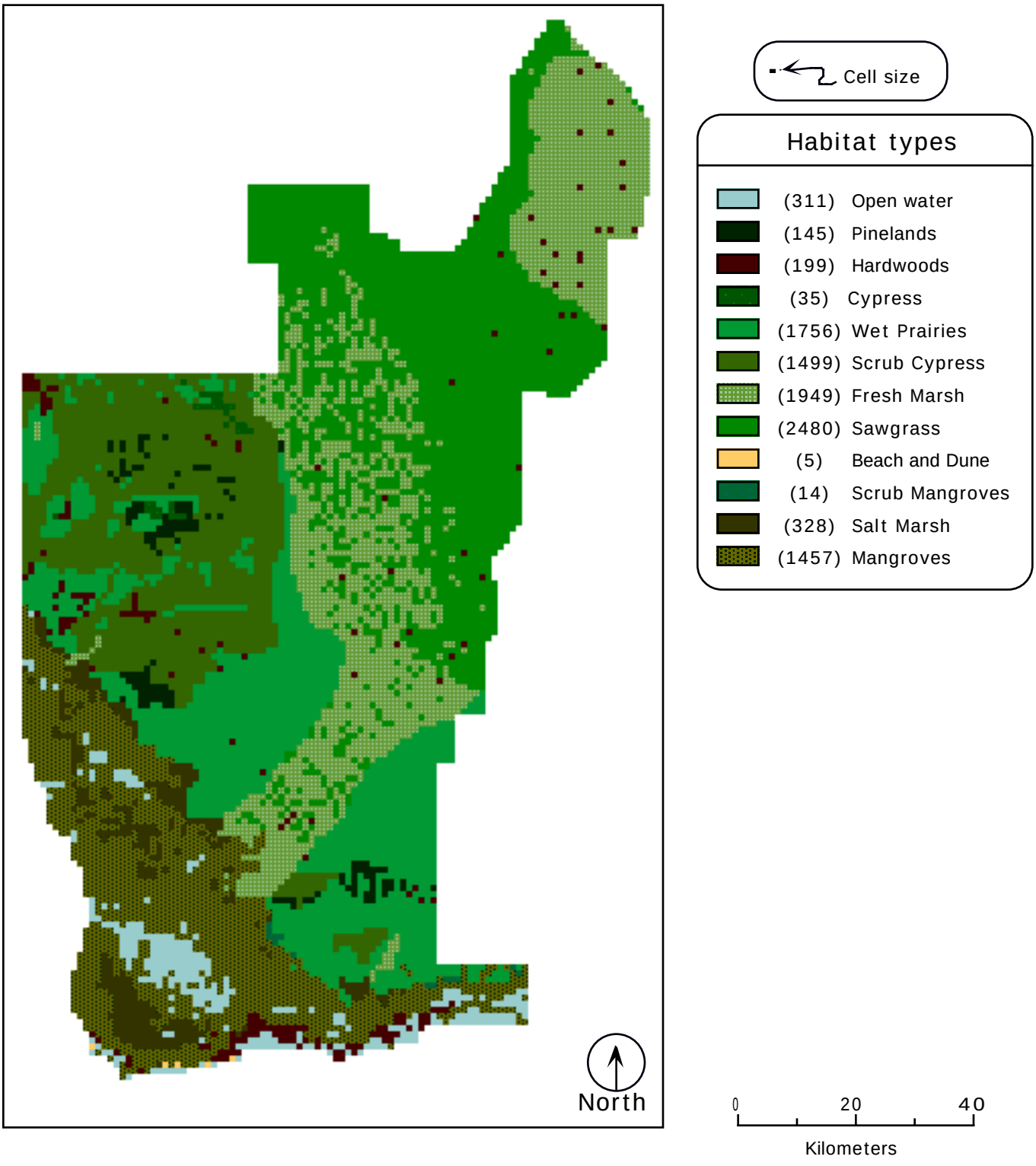


Figure 17a. Habitat types within the ELM boundaries during the period around 1900. Also indicated are the canals present during this time. Numbers in parentheses within the legend box indicate the number of cells that have each attribute.

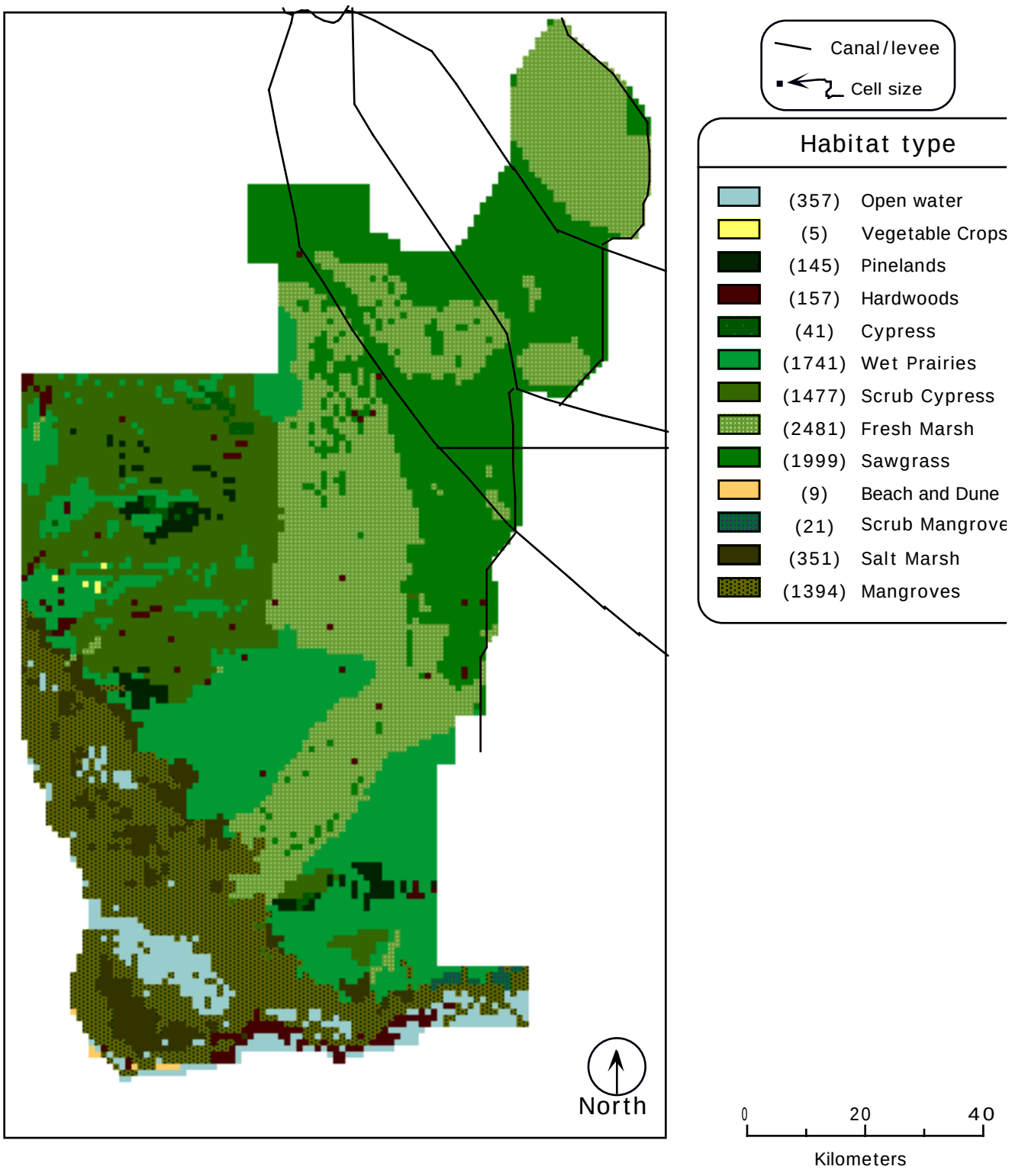


Figure 17b. Habitat types within the ELM boundaries during the period around 1953. Also indicated are the canal/levees present during this time; the levee system along the eastern border was constructed from 1952-1954. Numbers in parentheses within the legend box indicate the number of cells that have each attribute.

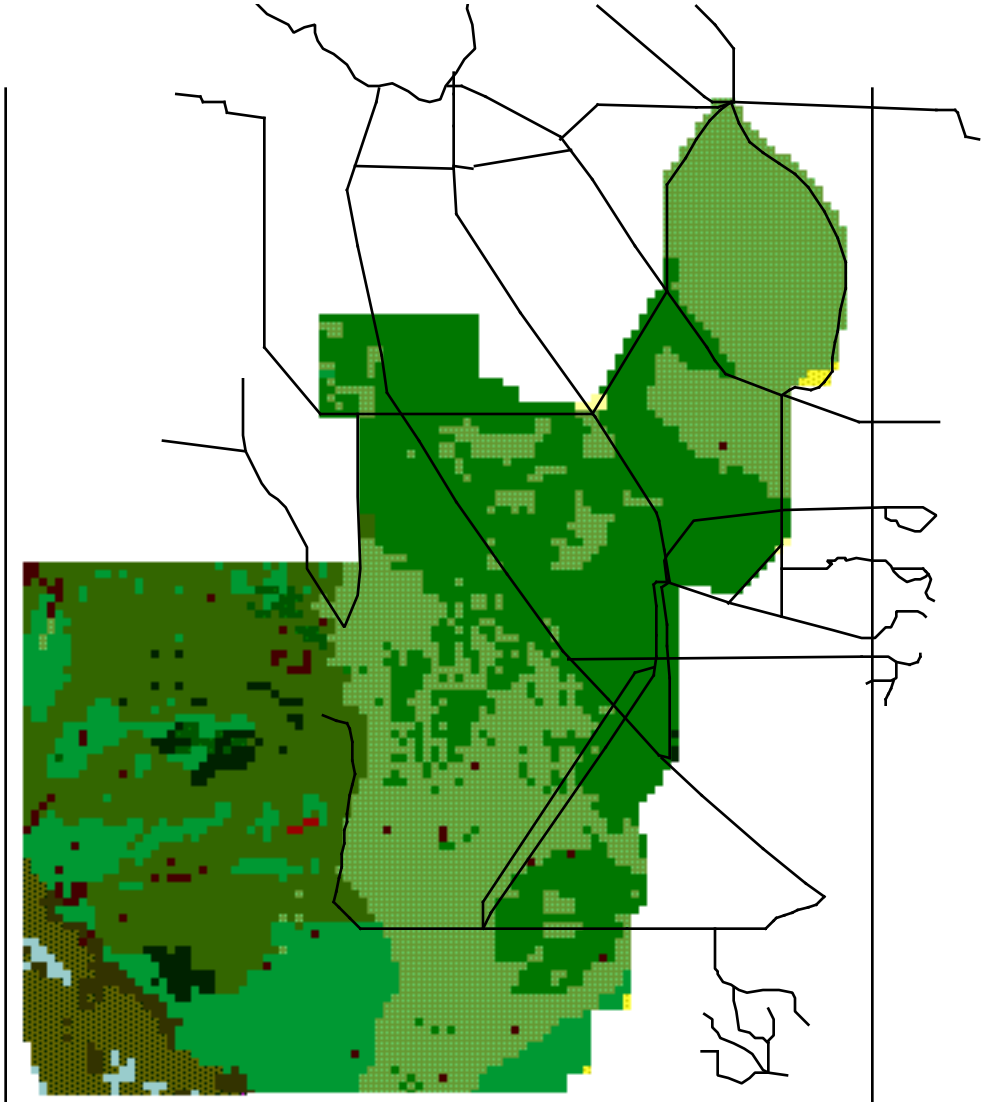

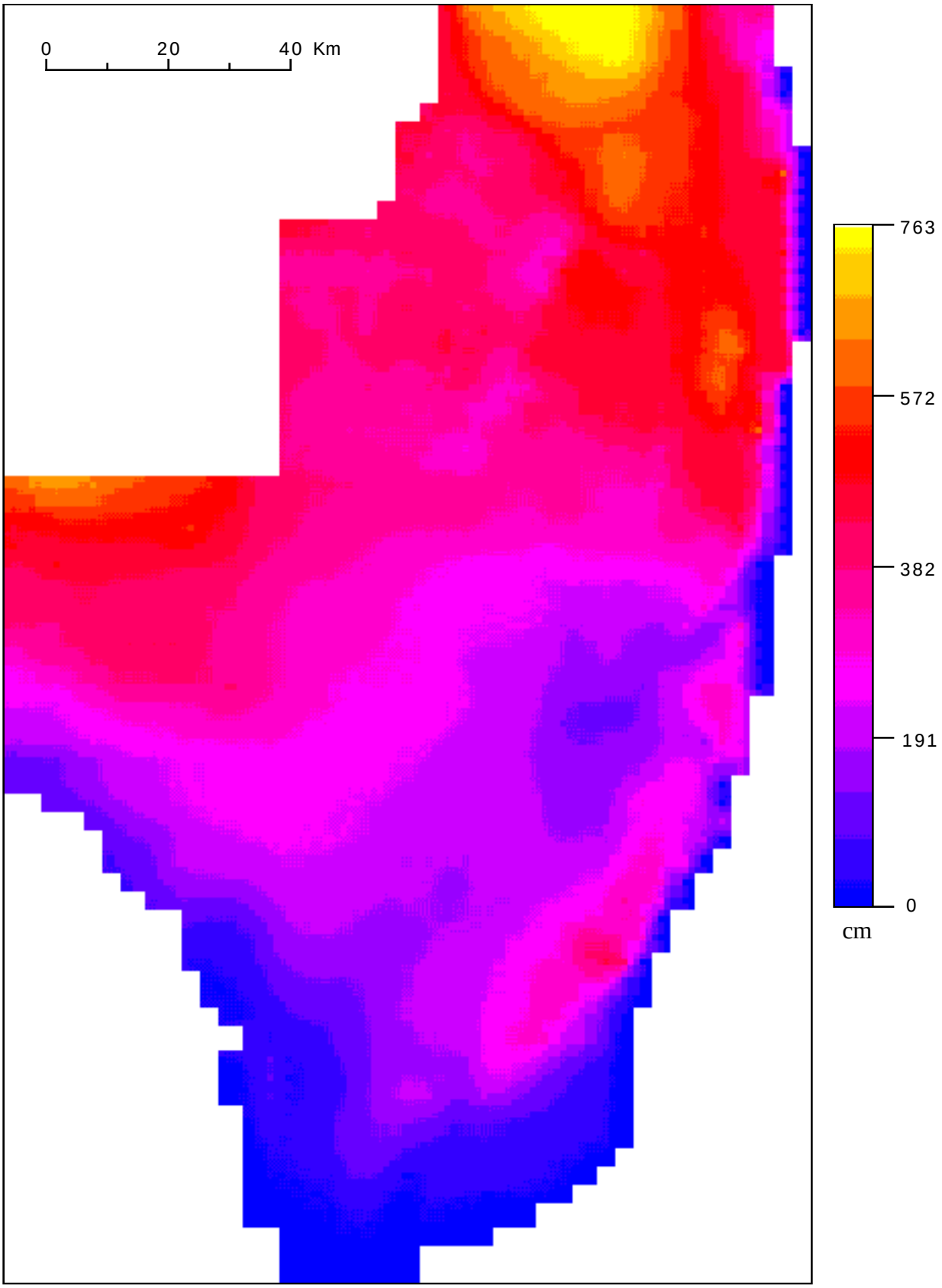


Figure 18. Elevation of land surface within the boundaries of the SFWMM. The 2X2 mile grid data was interpolated to the 1 $km^2$ grid scale shown.

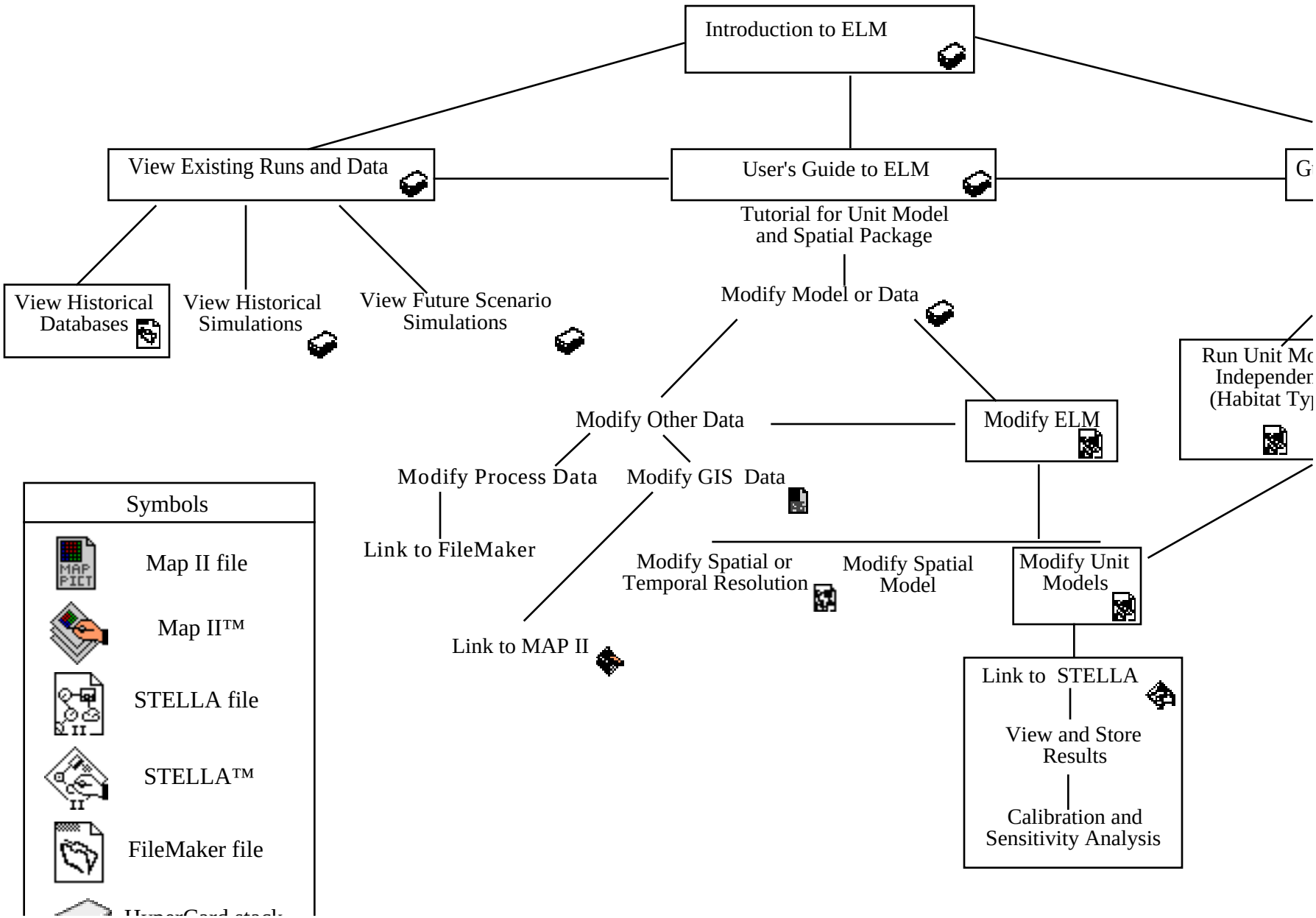
Introduction to ELM
View Existing Runs and Data
User's Guide to ELM
G
Tutorial for Unit Model and Spatial Package
View Historical Databases
View Historical Simulations
View Future Scenario Simulations
Modify Model or Data
Run Unit Mo
Independer
(Habitat Ty
Modify Other Data
Modify ELM
Modify Process Data
Modify GIS Data
Link to FileMaker
Modify Spatial or Temporal Resolution
Modify Spatial Model
Modify Unit Models
Link to MAP II
Link to STELLA
View and Store Results
Calibration and Sensitivity Analysis
Symbols
Map II file
Map II™
STELLA file
STELLA™
FileMaker file

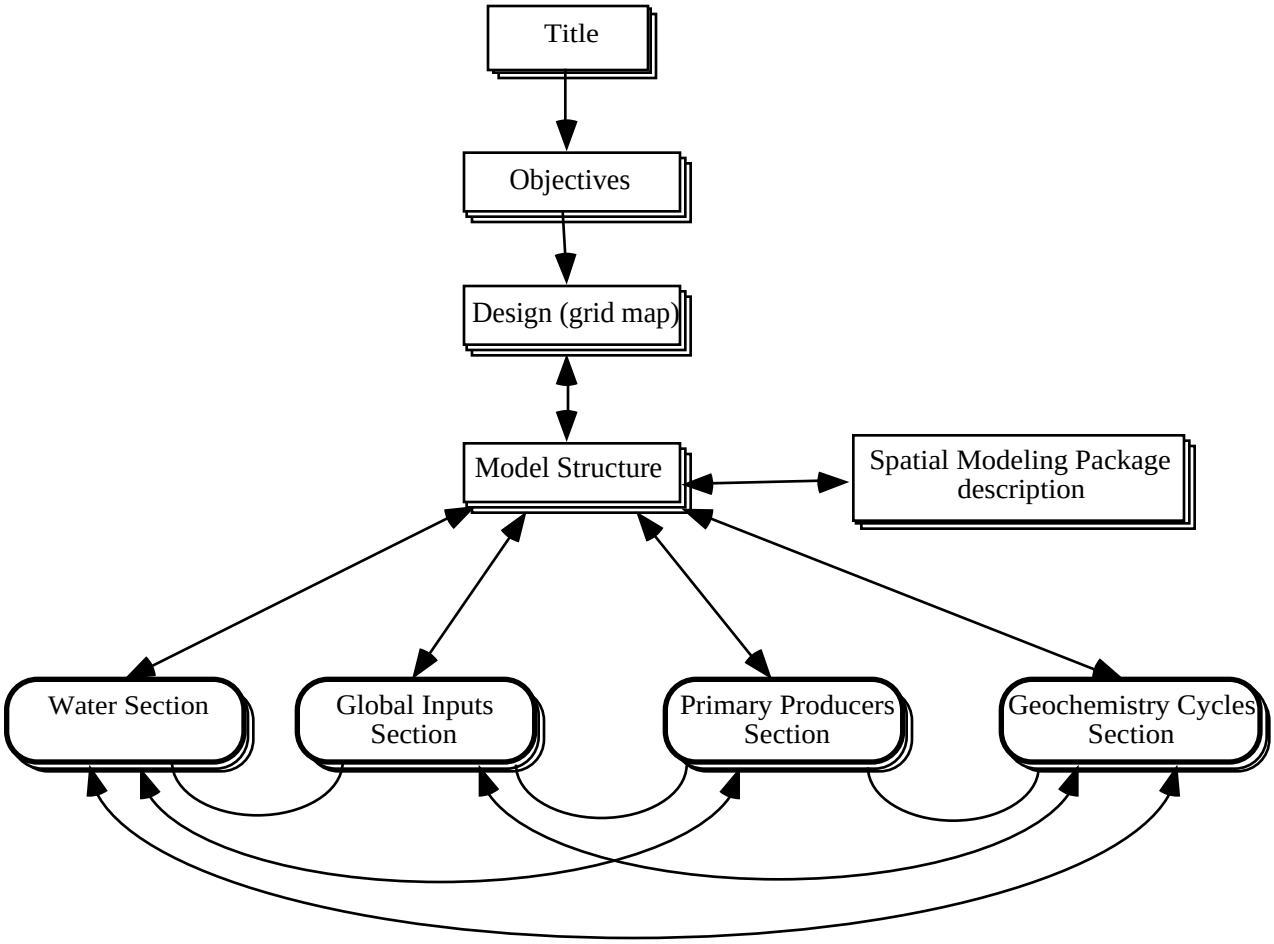


Figure 20. User's Guide Interface. Boxed items are screens/cards. Rounded boxes indicate HyperCard stacks containing the ELM sectors.

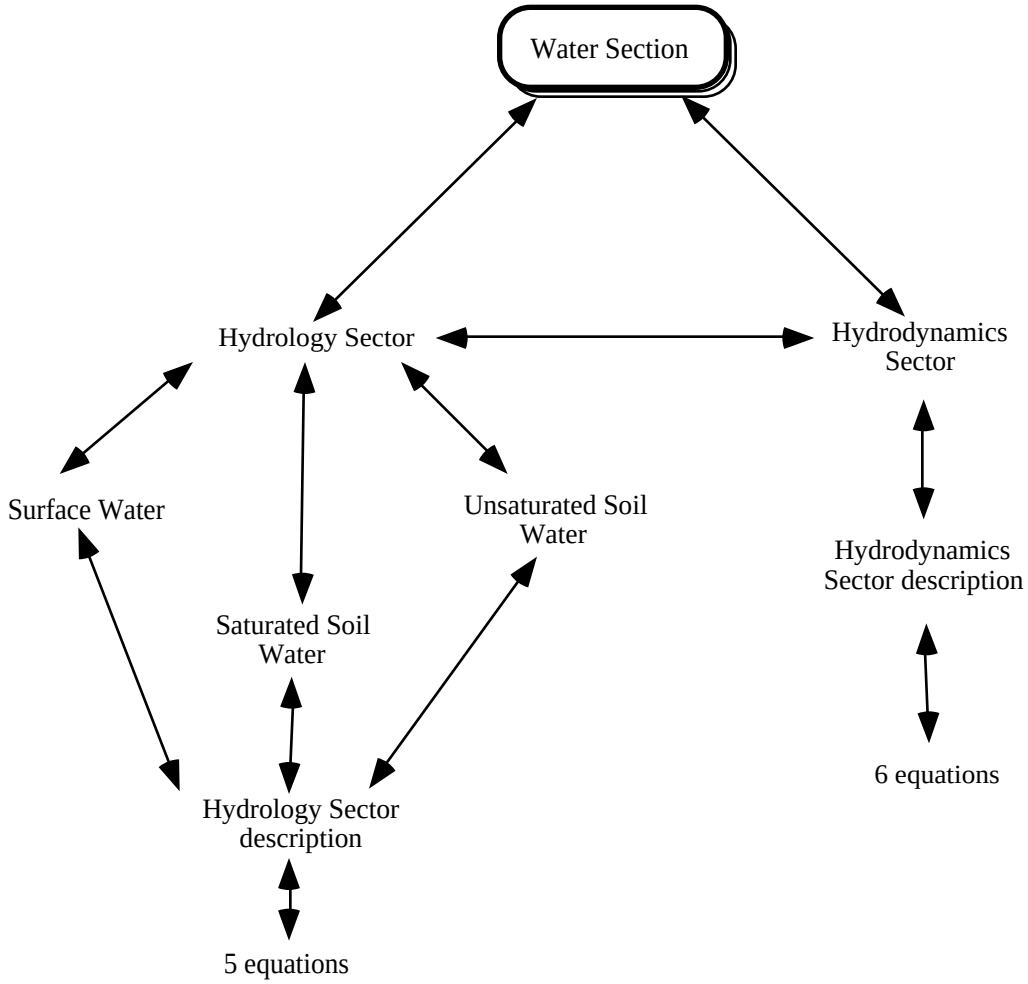


Figure 21. HyperELM stack structure for the Water Section. Items are cards.

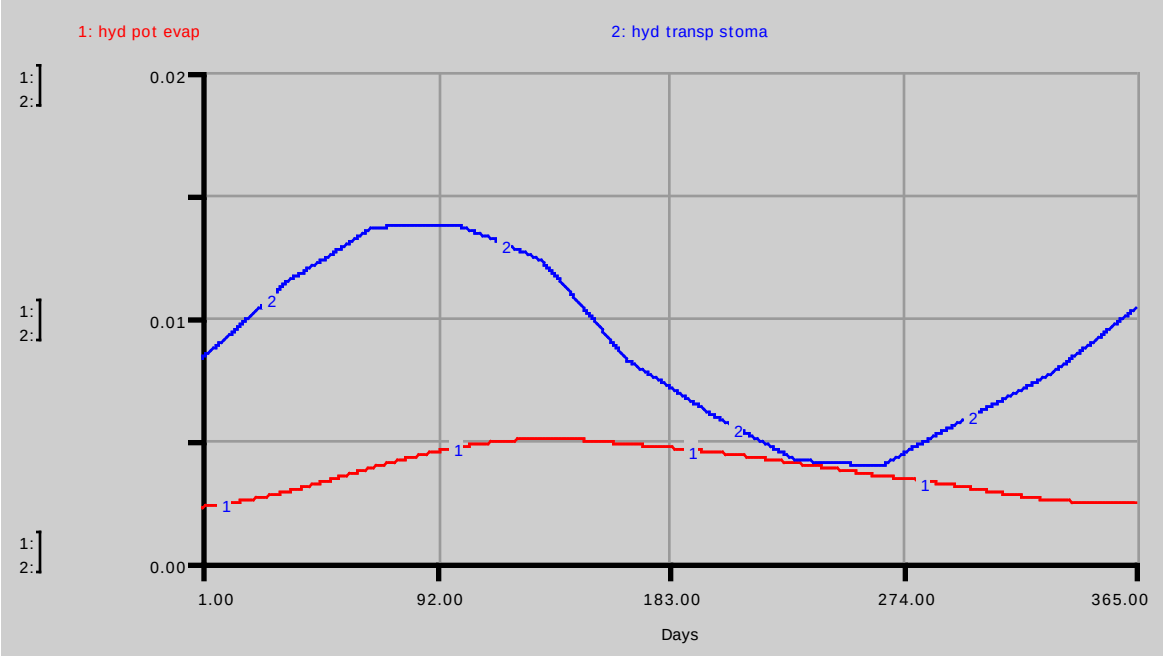


Figure 22a. Nominal canopy conductance=0.1 mol $m^{-2}$ $sec^{-1}$.
Potential evaporation and potential transpiration (m/d) from plants under no water stress when perfectly decoupled (hyd_pot_evap) and perfectly coupled (hyd_transp_stoma) from/to the air outside of boundary layer. (Curve not smooth due to discontinuities in weather data).

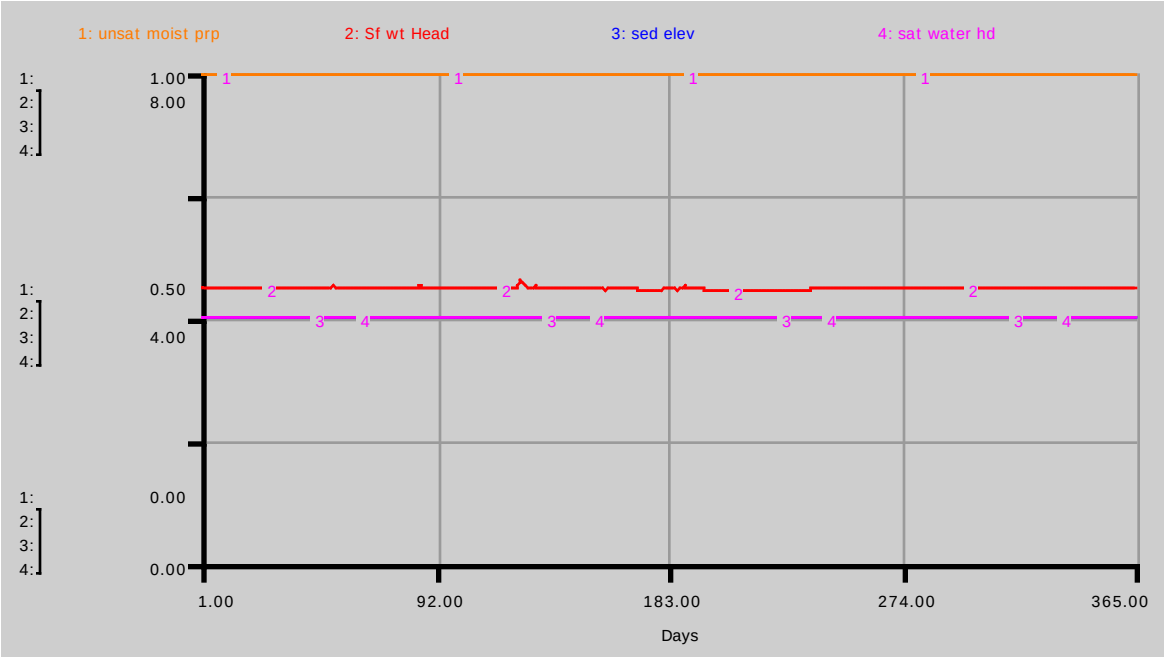


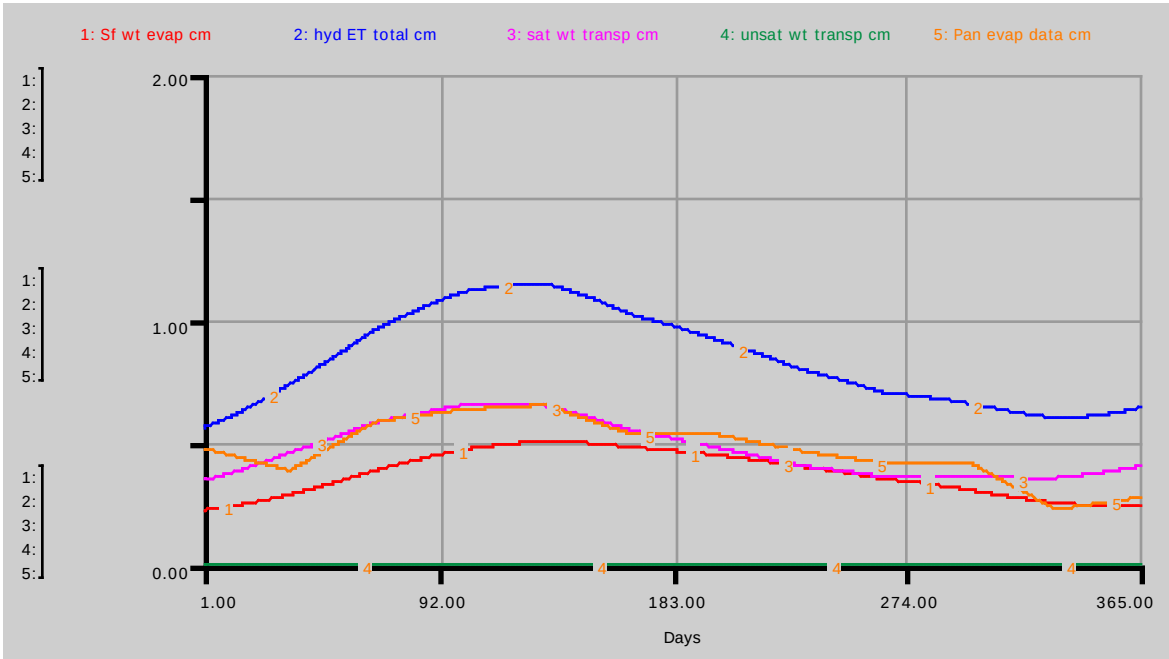


Figure 22b. Nominal canopy conductance=0.1 mol $m^{-2}$ $sec^{-1}$, high mac_canop_decoupl=0.8.
a. Head height (m) of available water in surface storage (Sf_wt_Head) and saturated storage (sat_water_hd) relative to sediment height (sed_elev); the proportion of moisture available in any unsaturated zone is shown by unsat_moist_prp. (No unsaturated zone is present when the saturated storage head is at sediment elevation.)
b. mac_canop_decoupl=0.8 (grassland). Transpiration (sat_wt_transp and unsat_wt_trans), evaporation (Sf_wt_evap_cm), and total ET (hyd_ET_total_cm) in cm/day. Pan evaporation data from Big Cypress station shown relative to simulated evaporation.

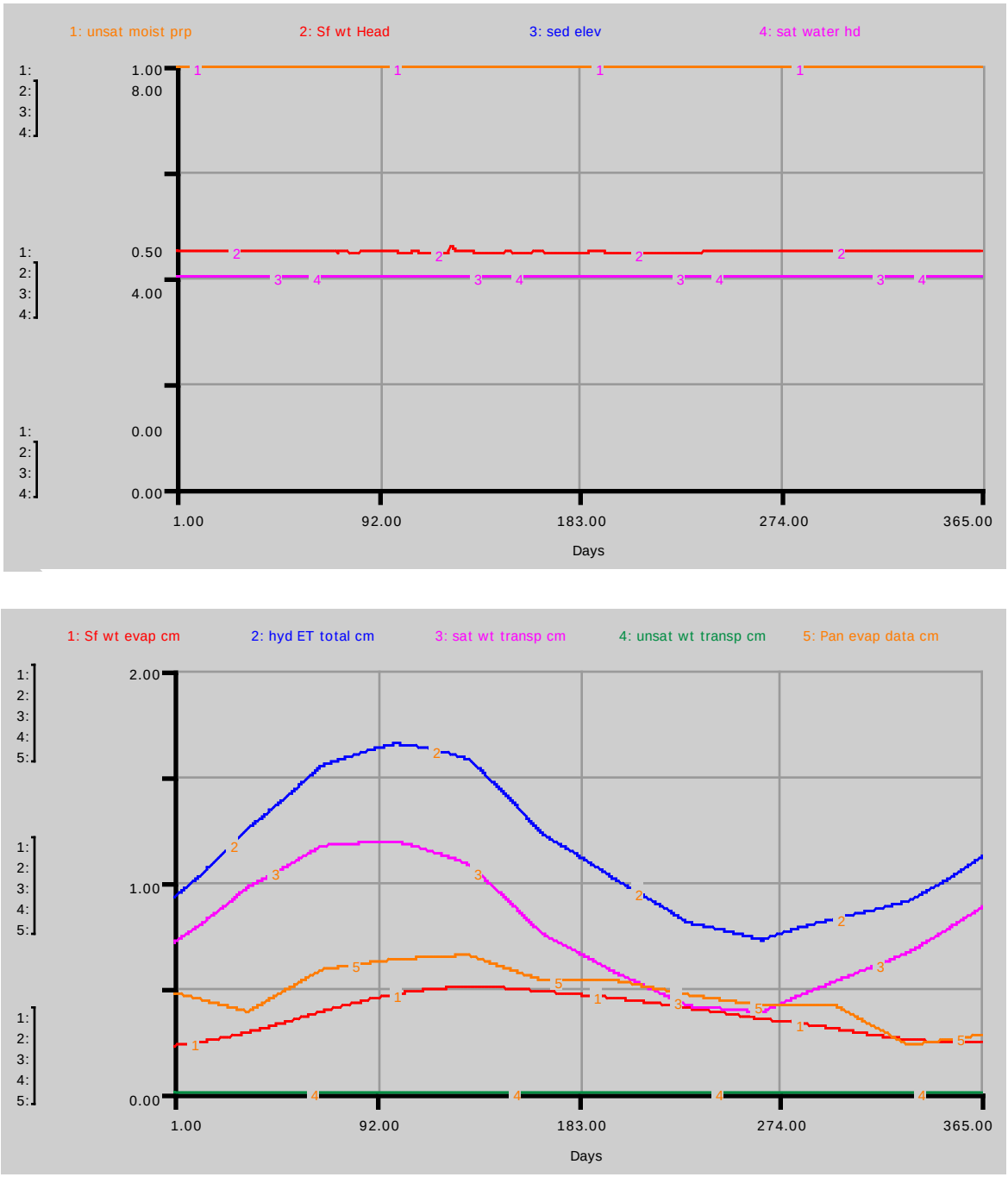


Figure 22c. Nominal canopy conductance=0.1 mol $m^{-2}$ $sec^{-1}$, low mac_canop_decoupl=0.2
a. Head height (m) of available water in surface storage (Sf_wt_Head) and saturated storage (sat_water_hd) relative to sediment height (sed_elev); the proportion of moisture available in any unsaturated zone is shown by unsat_moist_prp. (No unsaturated zone is present when the saturated storage head is at sediment elevation.)
b. Nominal case: mac_canop_decoupl=0.2 (forest). Transpiration (sat_wt_transp and unsat_wt_trans), evaporation (Sf_wt_evap_cm), and total ET (hyd_ET_total_cm) in cm/day. Pan evaporation data from Big Cypress station shown relative to simulated evaporation.

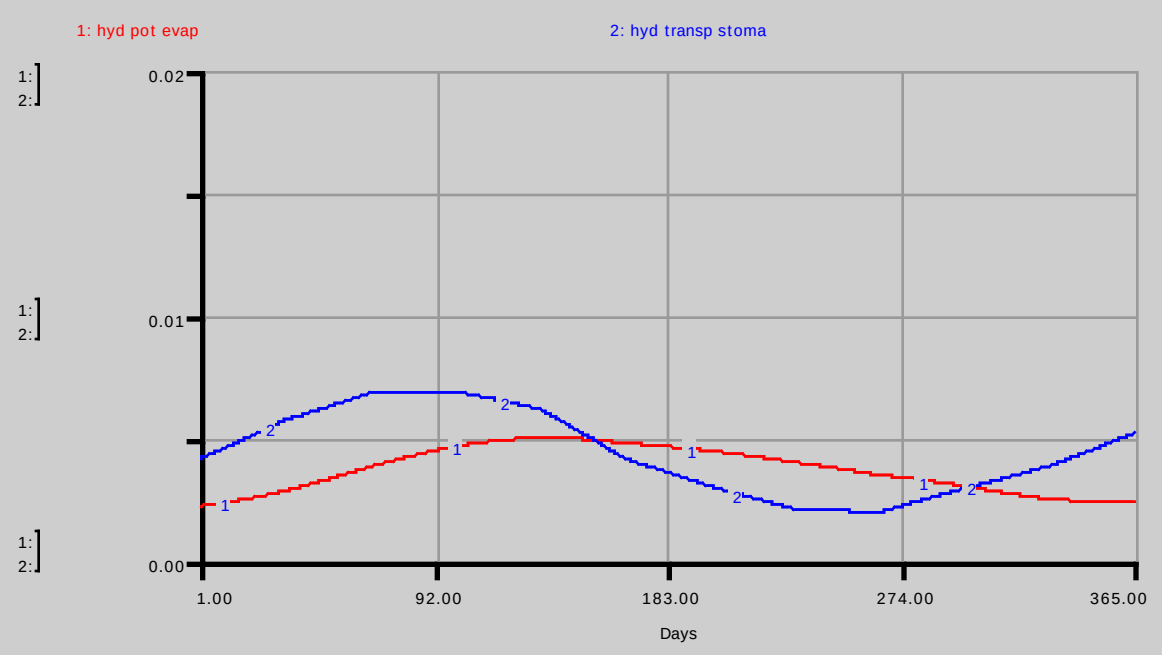


Figure 23a. Low canopy conductance=0.05 mol $m^{-2}$ $sec^{-1}$.
Potential evaporation and potential transpiration (m/d) from plants under no water stress when perfectly decoupled (hyd_pot_evap) and perfectly coupled (hyd_transp_stoma) from/to the air outside of boundary layer. (Curve not smooth due to discontinuities in weather data).

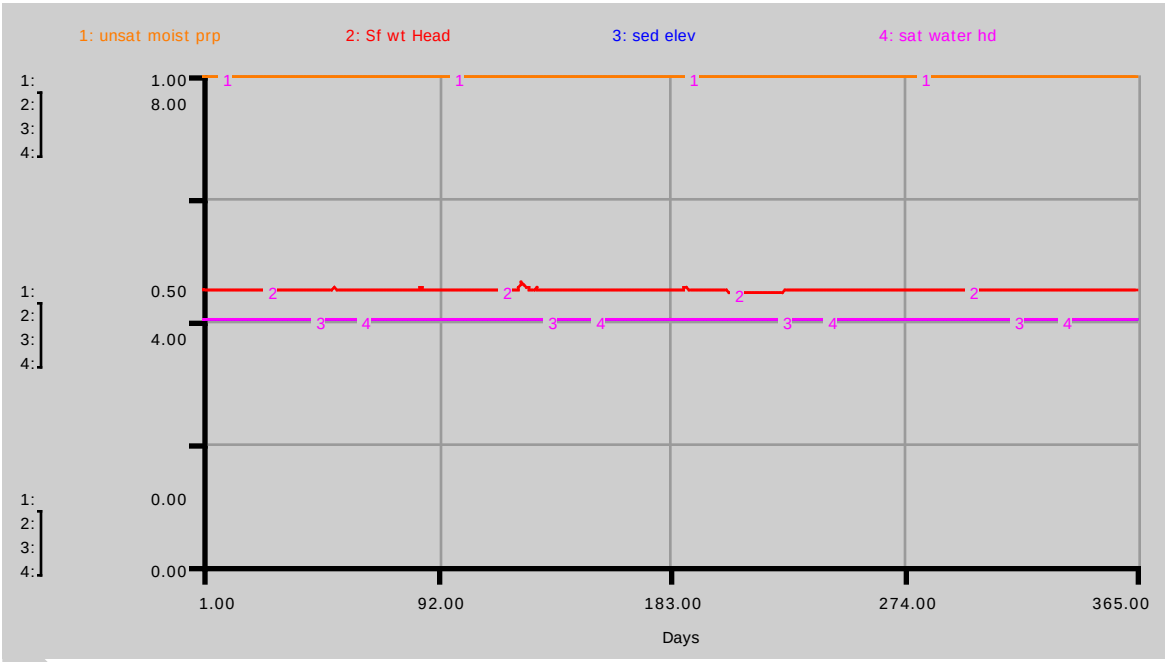


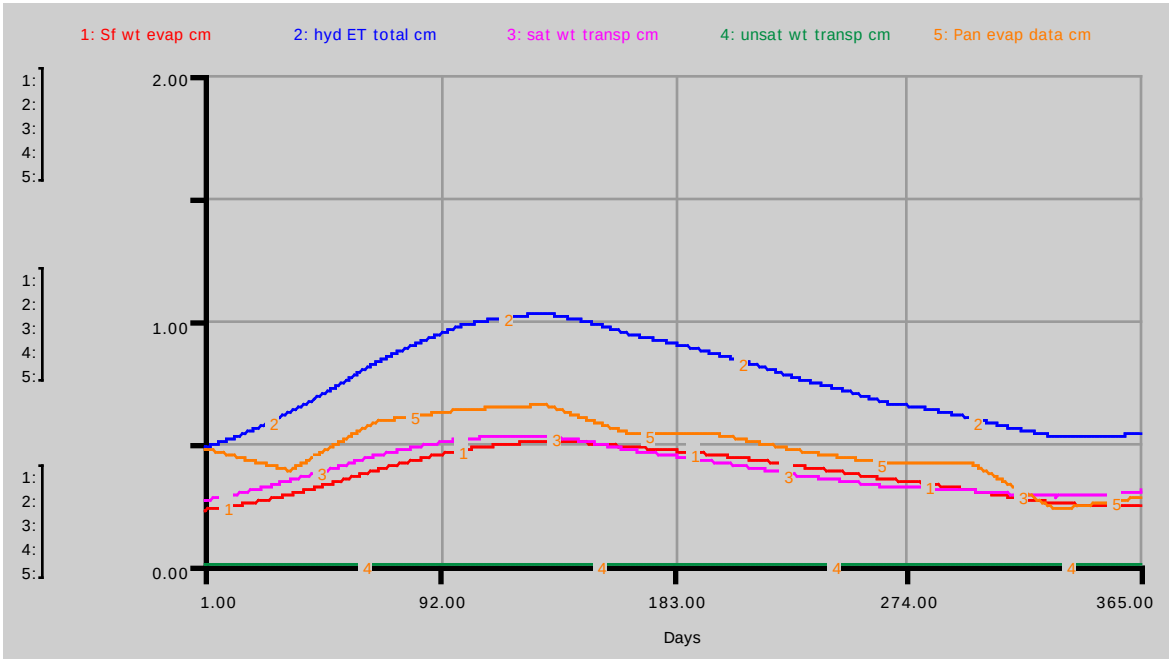


Figure 23b. Low canopy conductance=0.05 mol $m^{-2}$ $sec^{-1}$, high mac_canop_decoupl=0.8.
a. Head height (m) of available water in surface storage (Sf_wt_Head) and saturated storage (sat_water_hd) relative to sediment height (sed_elev); the proportion of moisture available in any unsaturated zone is shown by unsat_moist_prp. (No unsaturated zone is present when the saturated storage head is at sediment elevation.)
b. mac_canop_decoupl=0.8 (grassland). Transpiration (sat_wt_transp and unsat_wt_trans), evaporation (Sf_wt_evap_cm), and total ET (hyd_ET_total_cm) in cm/day. Pan evaporation data from Big Cypress station shown relative to simulated evaporation.

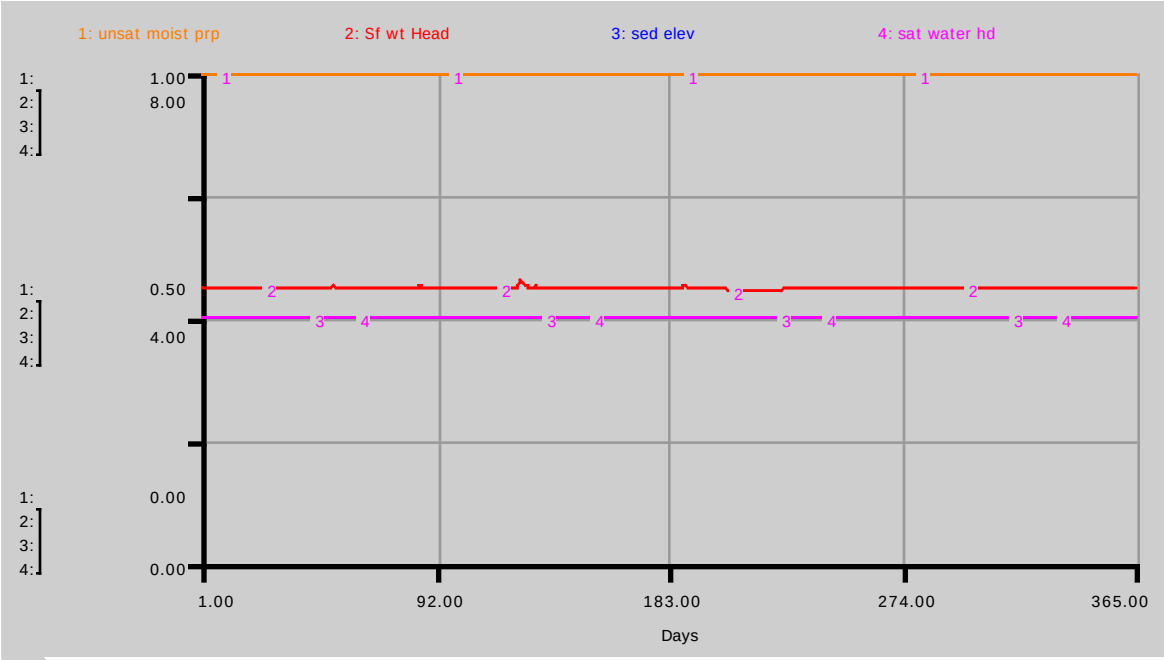


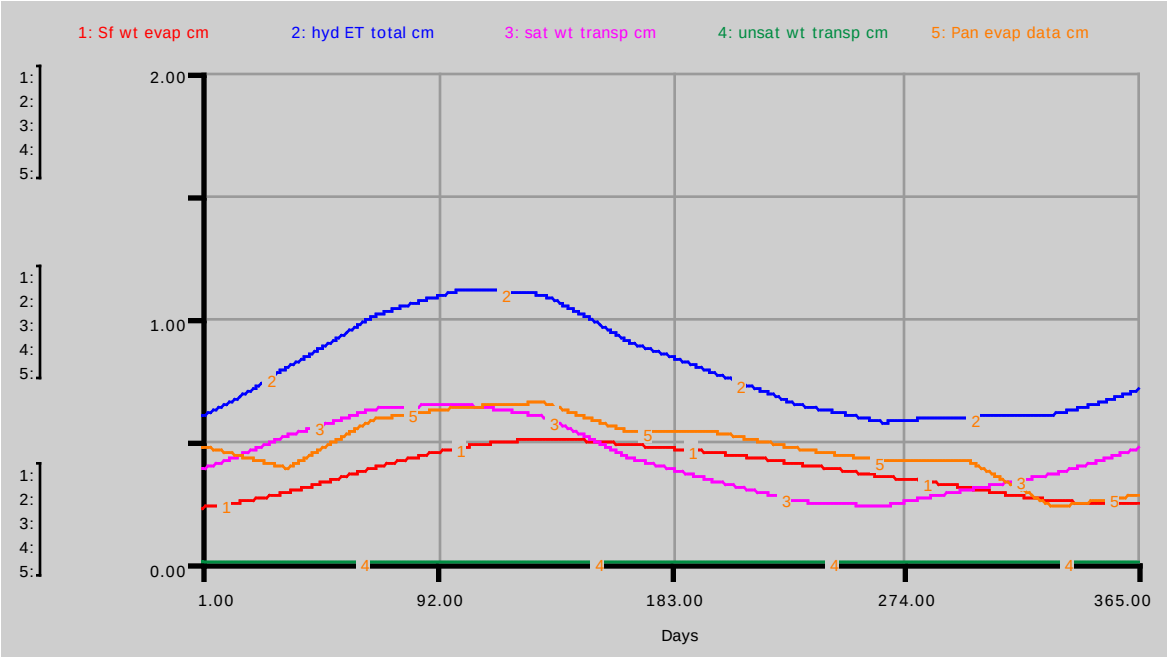


Figure 23c. Low canopy conductance=0.05 mol $m^{-2}$ $sec^{-1}$, low mac_canop_decoupl=0.2.
a. Head height (m) of available water in surface storage (Sf_wt_Head) and saturated storage (sat_water_hd) relative to sediment height (sed_elev); the proportion of moisture available in any unsaturated zone is shown by unsat_moist_prp. (No unsaturated zone is present when the saturated storage head is at sediment elevation.)
b. mac_canop_decoupl=0.2 (forest). Transpiration (sat_wt_transp and unsat_wt_trans), evaporation (Sf_wt_evap_cm), and total ET (hyd_ET_total_cm) in cm/day. Pan evaporation data from Big Cypress station shown relative to simulated evaporation.

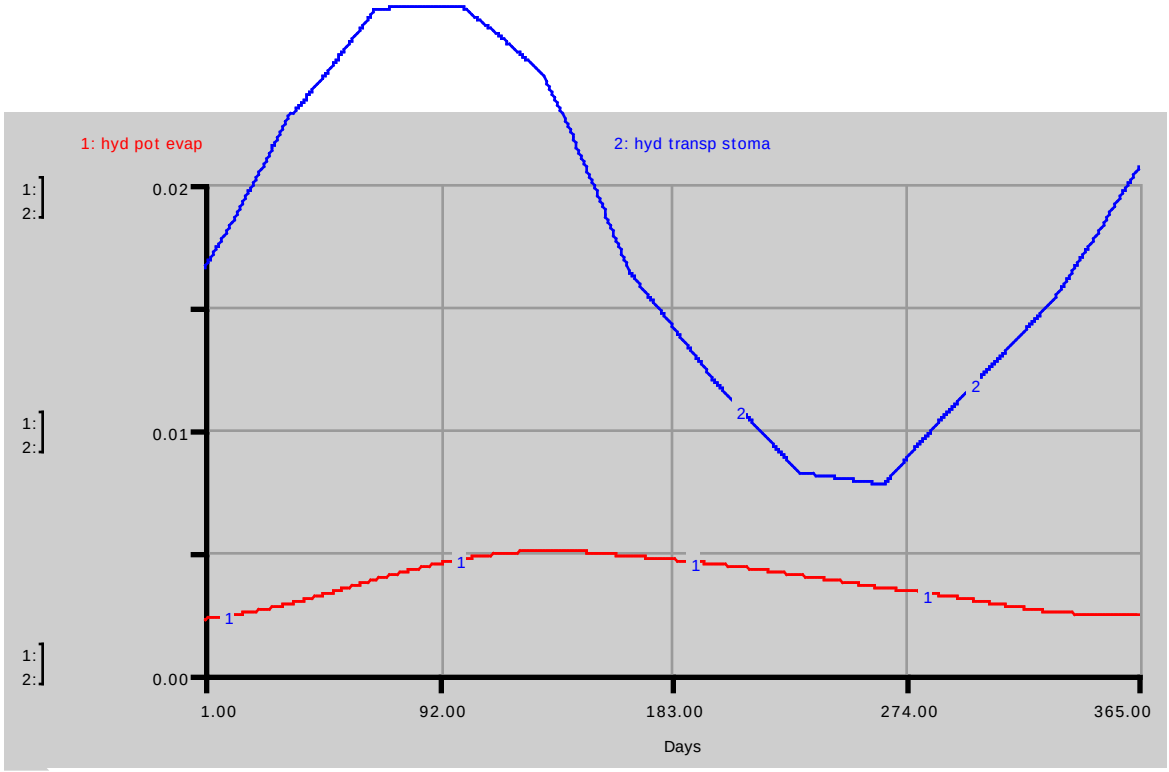


Figure 24a. High canopy conductance=0.2 mol $m^{-2}$ $sec^{-1}$.
Potential evaporation and potential transpiration (m/d) from plants under no water stress when perfectly decoupled (hyd_pot_evap) and perfectly coupled (hyd_transp_stoma) from/to the air outside of boundary layer. (Curve not smooth due to discontinuities in weather data).

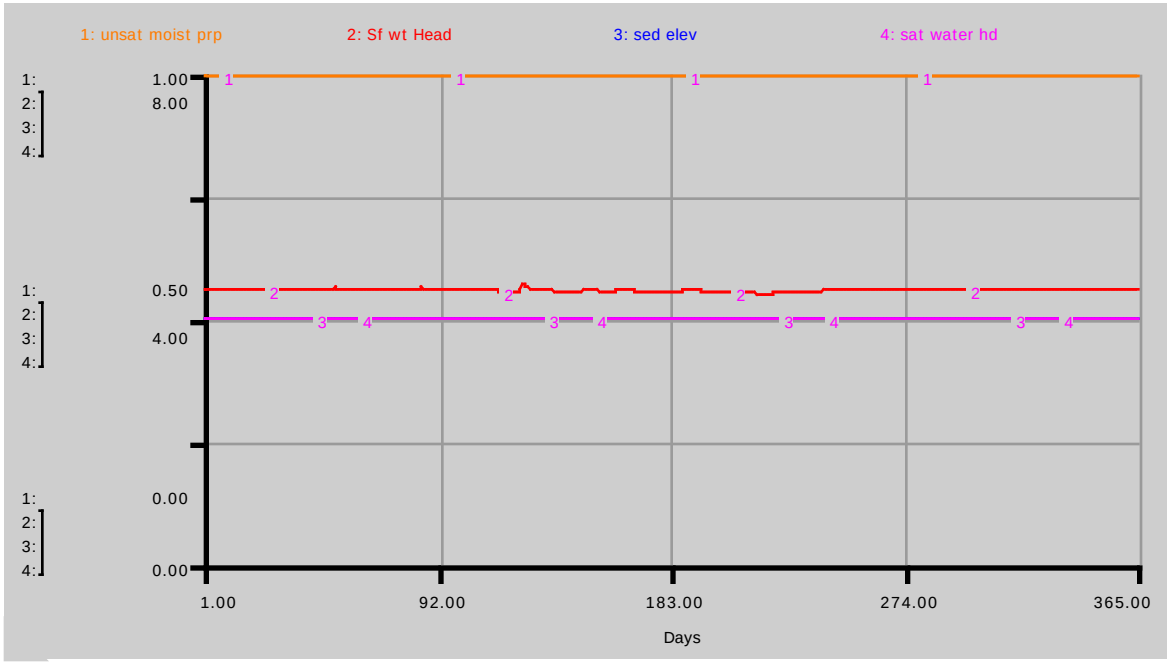


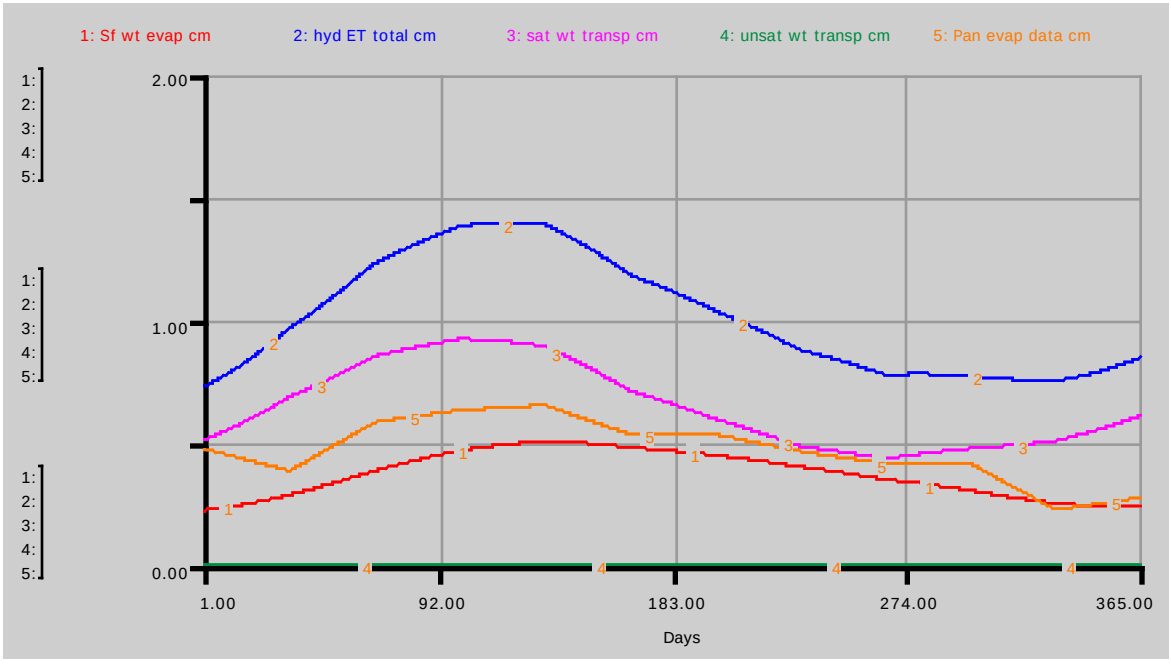


Figure 24b. High canopy conductance=0.2 mol $m^{-2}$ $sec^{-1}$, high mac_canop_decoupl=0.8.
a. Head height (m) of available water in surface storage (Sf_wt_Head) and saturated storage (sat_water_hd) relative to sediment height (sed_elev); the proportion of moisture available in any unsaturated zone is shown by unsat_moist_prp. (No unsaturated zone is present when the saturated storage head is at sediment elevation.)
b. mac_canop_decoupl=0.8 (grassland). Transpiration (sat_wt_transp and unsat_wt_trans), evaporation (Sf_wt_evap_cm), and total ET (hyd_ET_total_cm) in cm/day. Pan evaporation data from Big Cypress station shown relative to simulated evaporation.

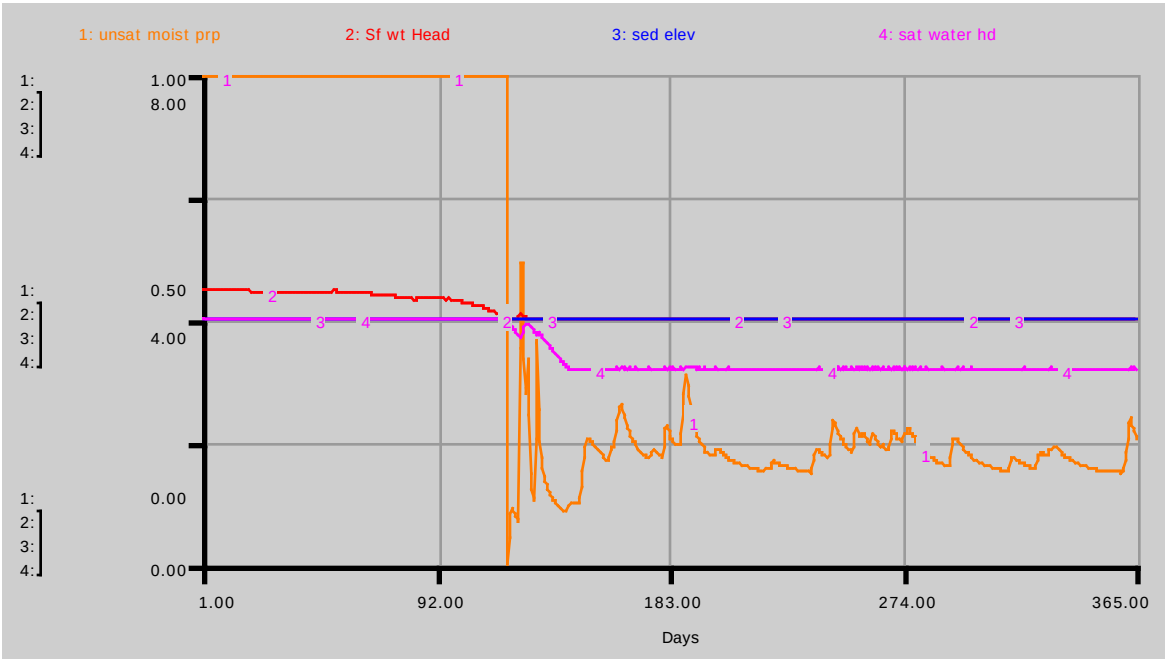


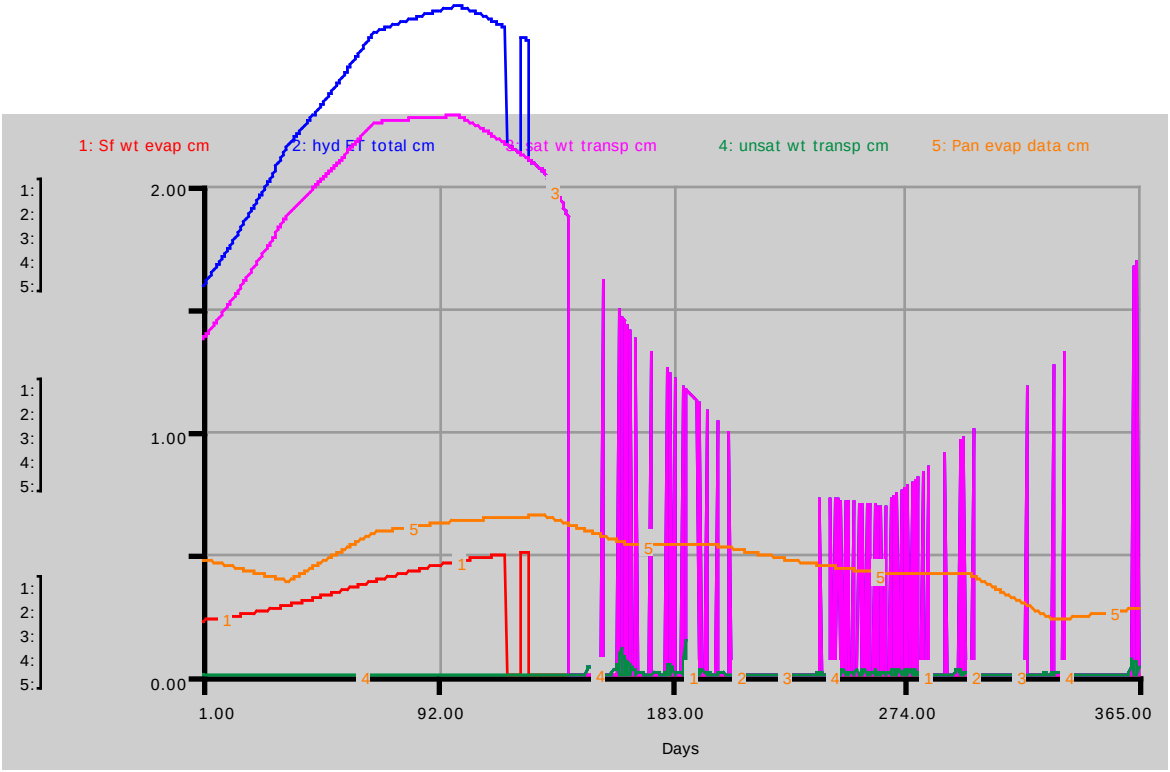


Figure 24c. High canopy conductance=0.2 mol $m^{-2}$ $sec^{-1}$, low mac_canop_decoupl=0.2.
a. Head height (m) of available water in surface storage (Sf_wt_Head) and saturated storage (sat_water_hd) relative to sediment height (sed_elev); the proportion of moisture available in any unsaturated zone is shown by unsat_moist_prp. (No unsaturated zone is present when the saturated storage head is at sediment elevation.)
b. mac_canop_decoupl=0.2 (forest). Transpiration (sat_wt_transp and unsat_wt_trans), evaporation (Sf_wt_evap_cm), and total ET (hyd_ET_total_cm) in cm/day. Pan evaporation data from Big Cypress station shown relative to simulated evaporation.

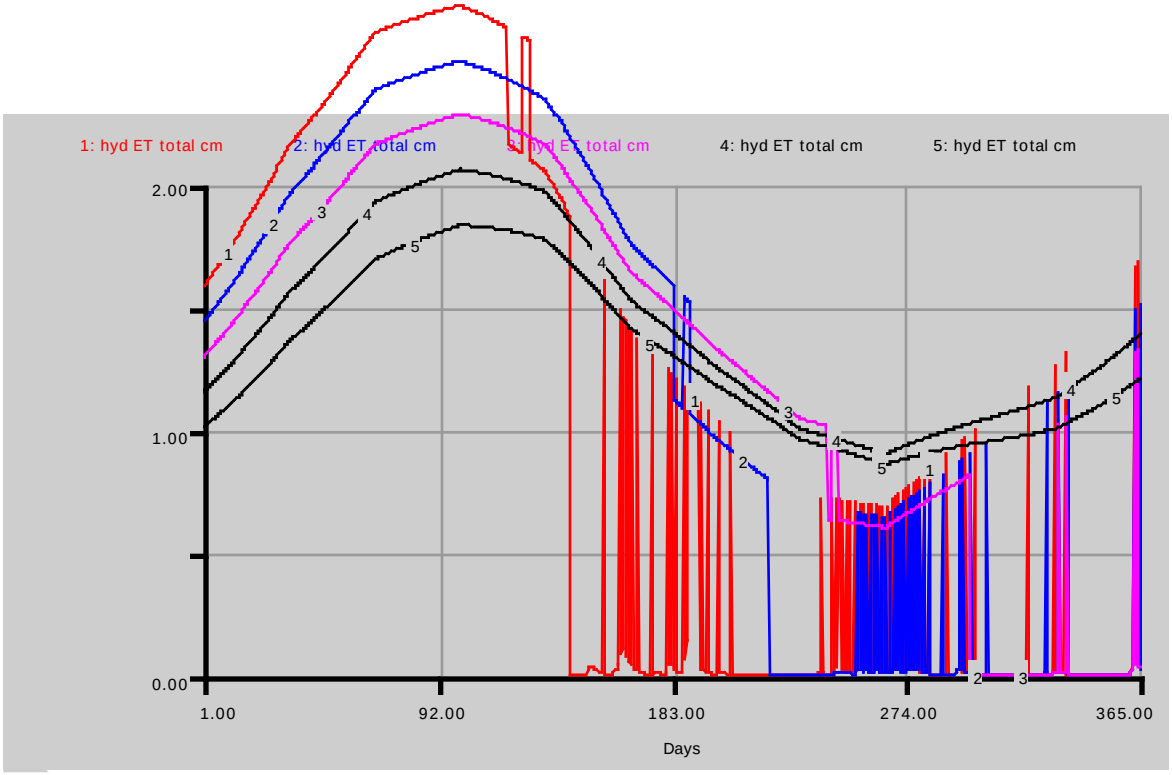


Figure 25. With high canopy conductance of 0.2 mol $m^{-2}$ $sec^{-1}$, total evaporation and transpiration loss under varying canopy decoupling parameters of 0.2, 0.3, 0.4, 0.5, and 0.6 for runs 1 through 6, respectively. Water becomes limiting in the unsaturated zone with decoupling factors of 0.4 and smaller, and transpiration occurs sporadically and rapidly.

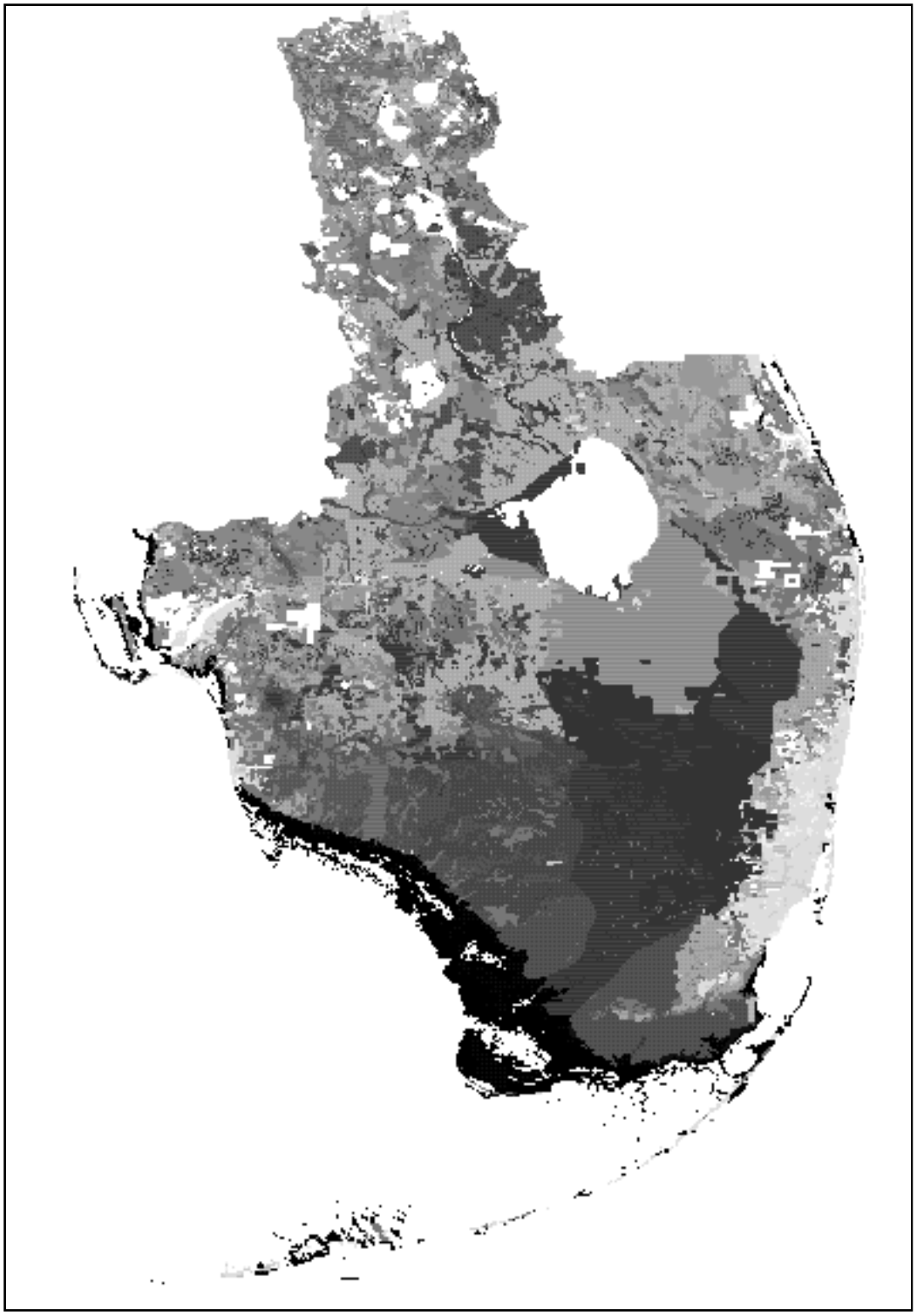

Figure 26a. Example of the random, sequential aggregation scheme applied to the 1973 south Florida data four successive times. These four aggregations, along with the original, make up the five different resolutions used in the analyses. The resolutions used were 1.333 cells/km$^2$ (original data), 0.333 (26b), 0.083 (26c), 0.021 (26d), and 0.005 (26e) cells/km$^2$.

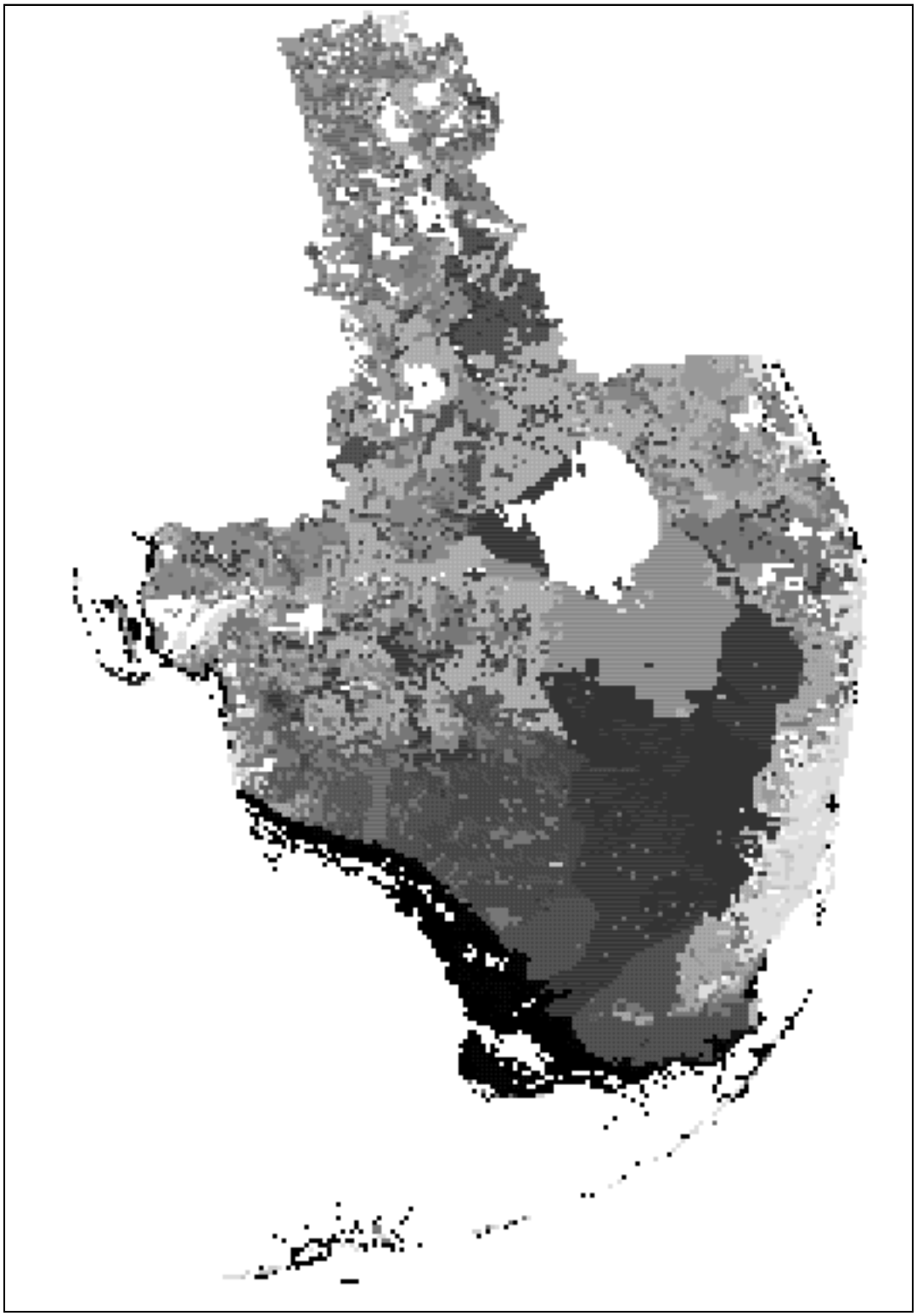

Figure 26b. South Florida at 0.333 cells/km$^2$.

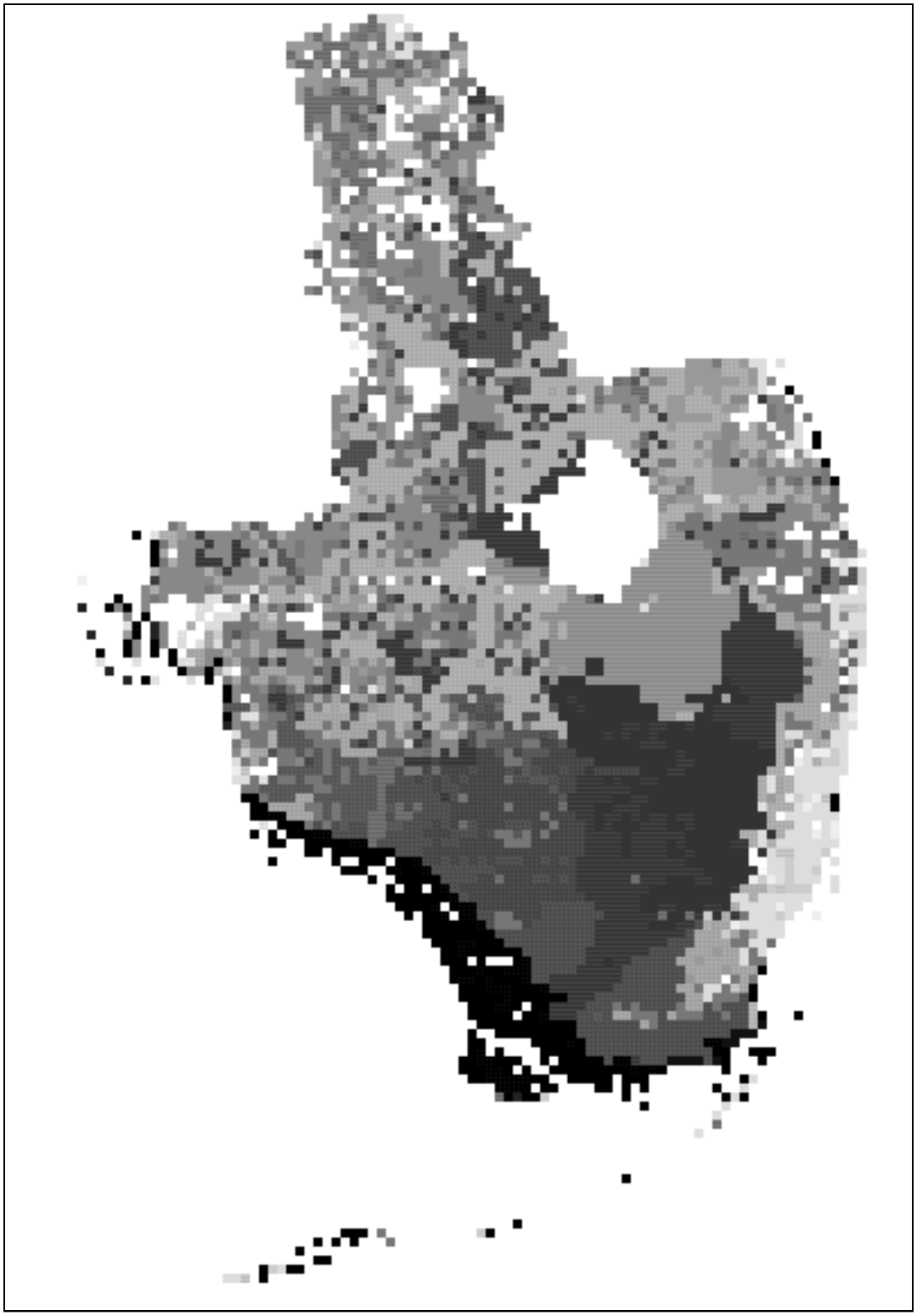

Figure 26c. South Florida at 0.083 cells/km$^2$.

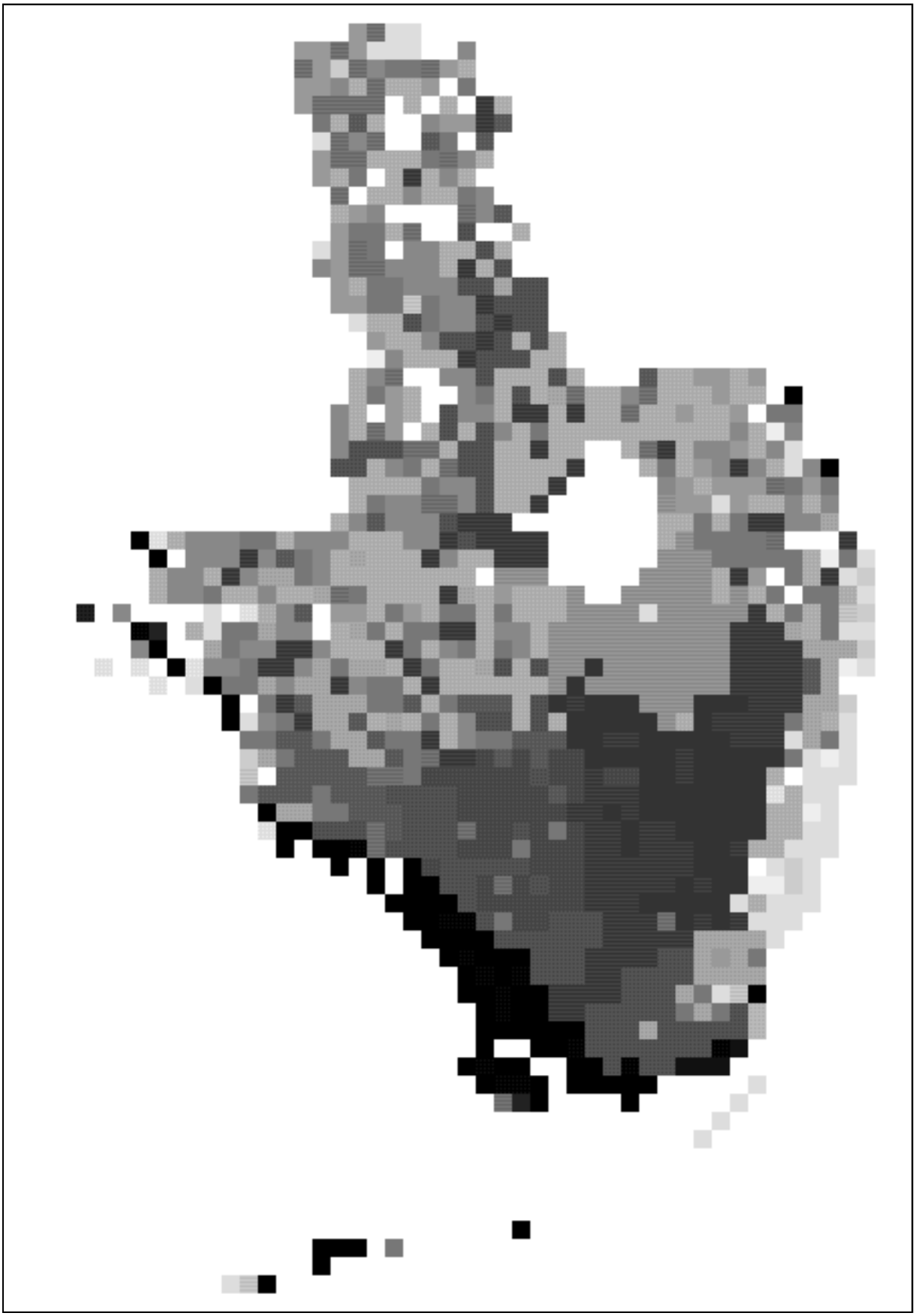

Figure 26d. South Florida at 0.021 cells/km$^2$.

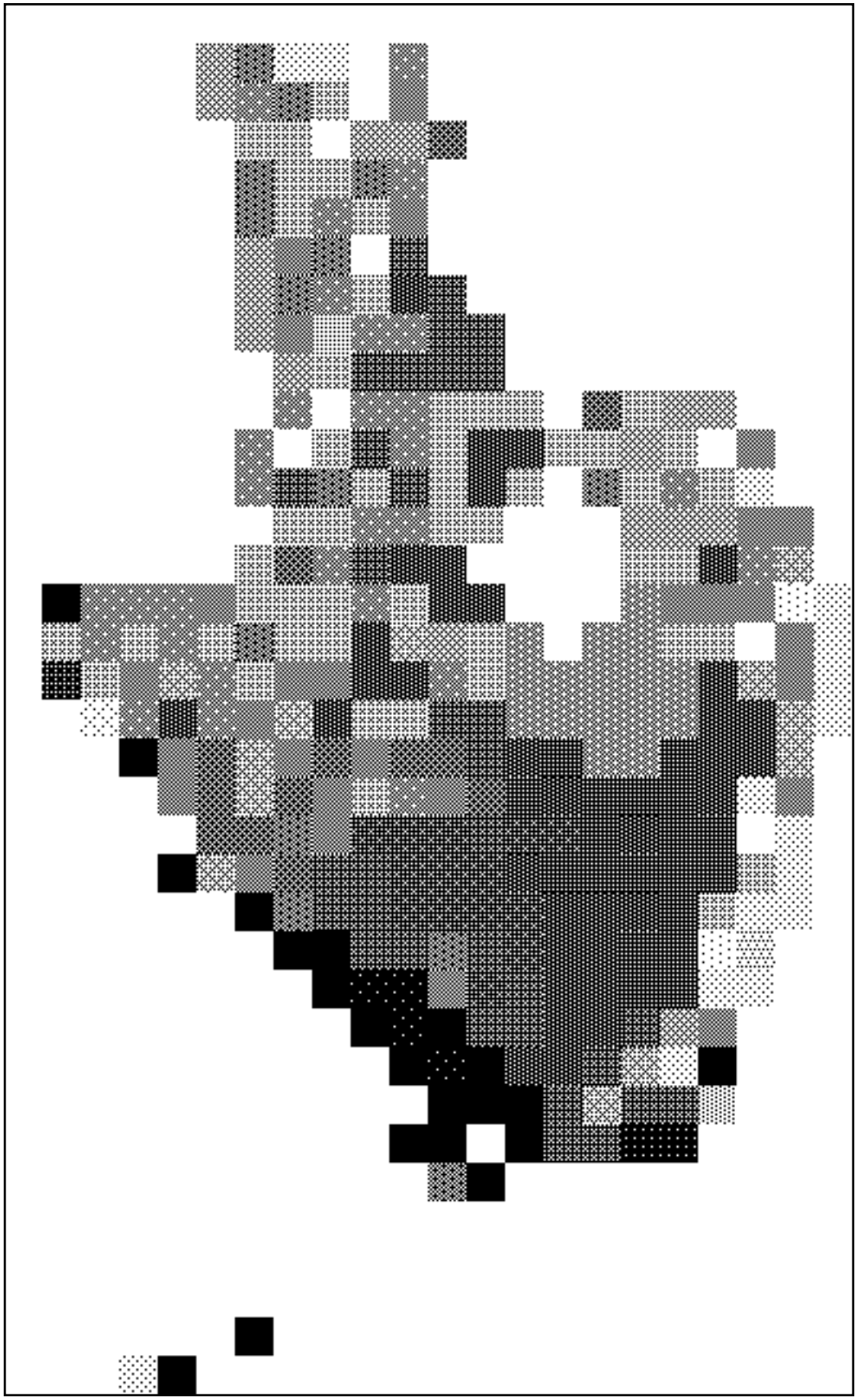

Figure 26e. South Florida at 0.005 cells/km$^2$.

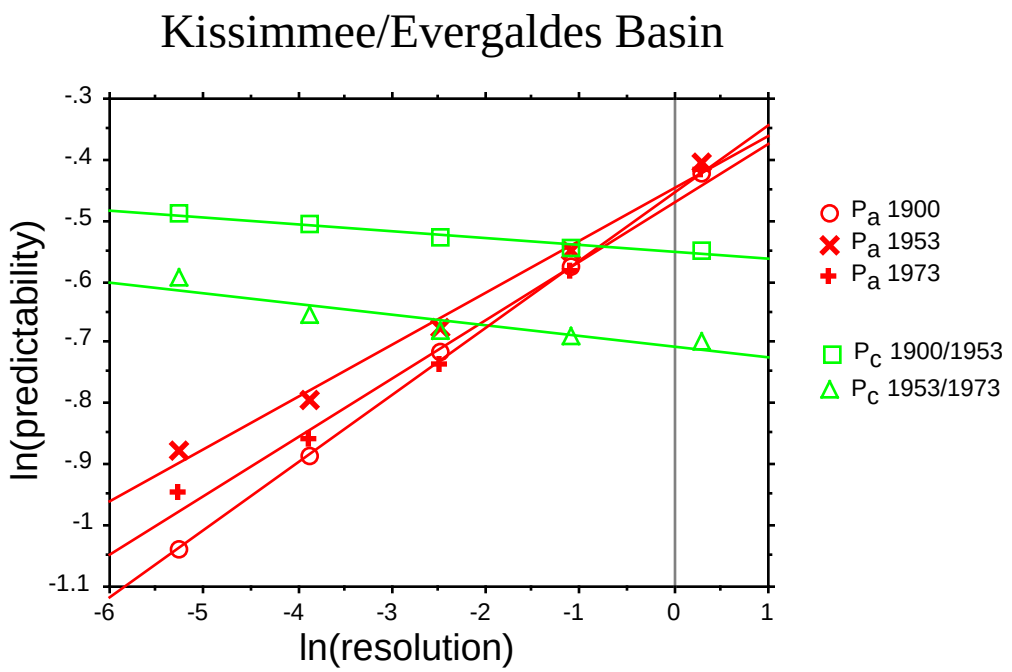


Figure 27. Log of resolution vs. log of predictability for the Kississmee/Everglades land use data. Plot shows both auto-predictability (AP) indicating internal pattern in the data for three different years, and cross-predictability (CP) indicating pattern matching between null models of prior land use maps and a particular map.

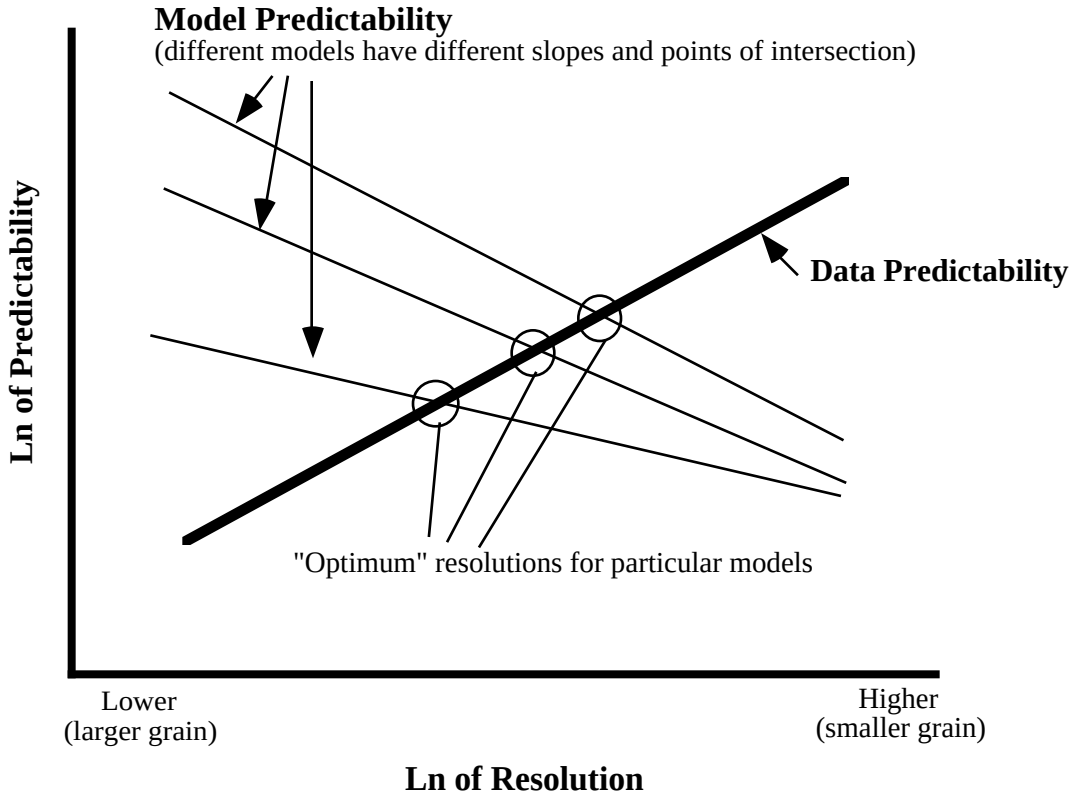


Figure 28. Hypothetical relationship between resolution and predictability of data and models. Data predictibility is the degree to which the uncertainty about the state of landscape pixels is reduced by knowledge of the state of adjacent pixels in the same map. Model predictability is the degree to which the uncertainty about the state of pixels is reduced by knowledge of the corresponding state of pixels in output maps from various models of the system.

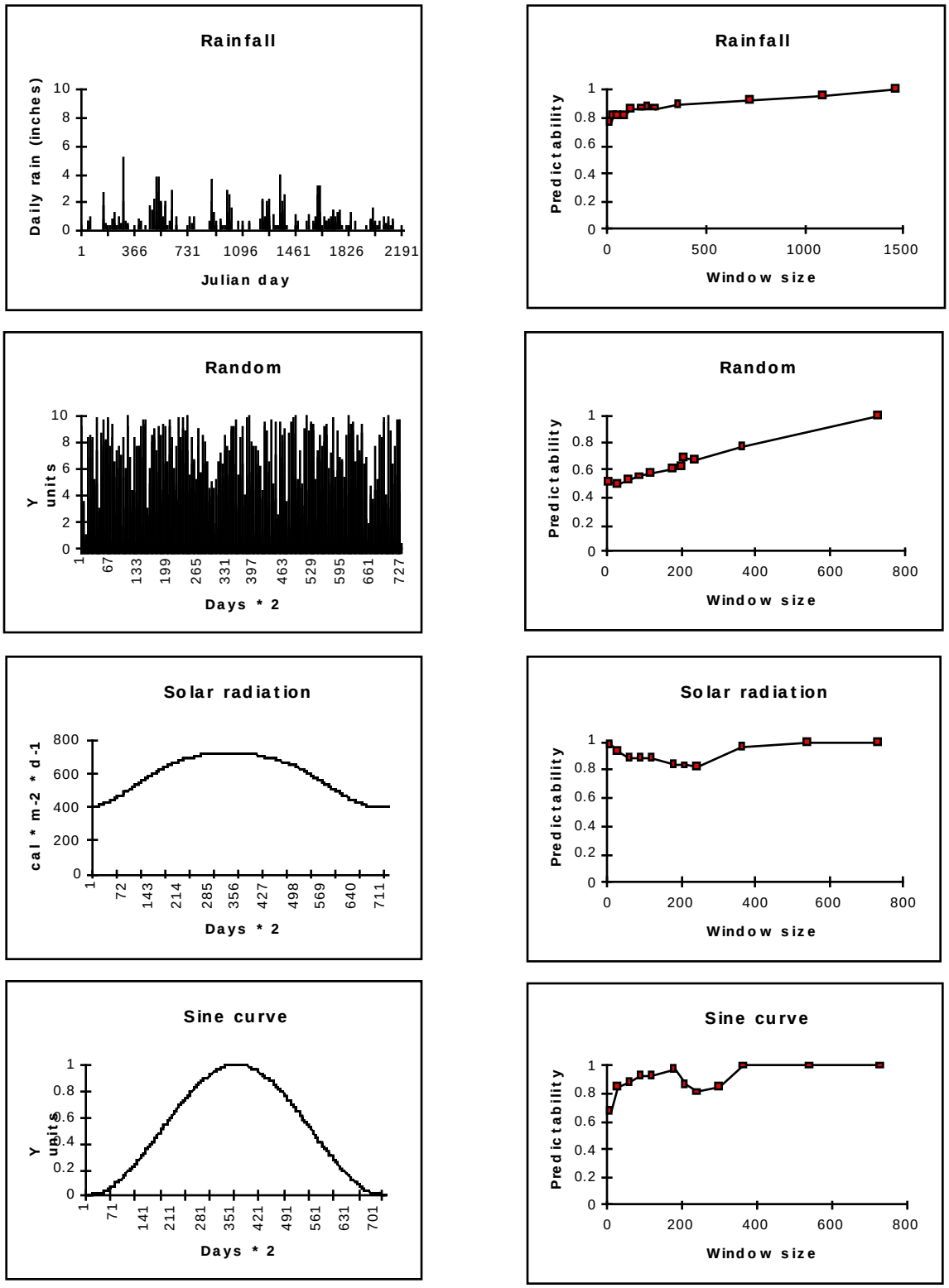


Figure 29. Raw time series data (left column) and the relation between predictability and resolution for each data set (right column).

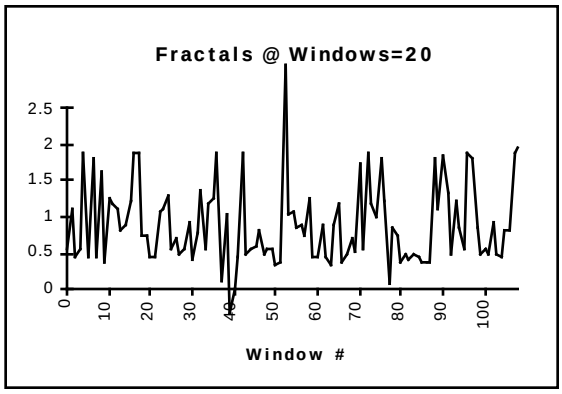
Fractals @ Windows=20
2.5
2
1.5
1
0.5
0
0
10
20
30
40
50
60
70
80
90
100
Window #

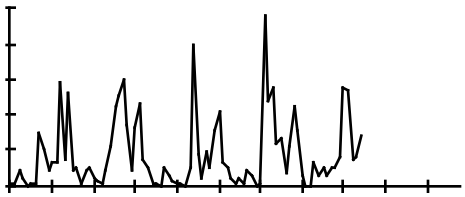

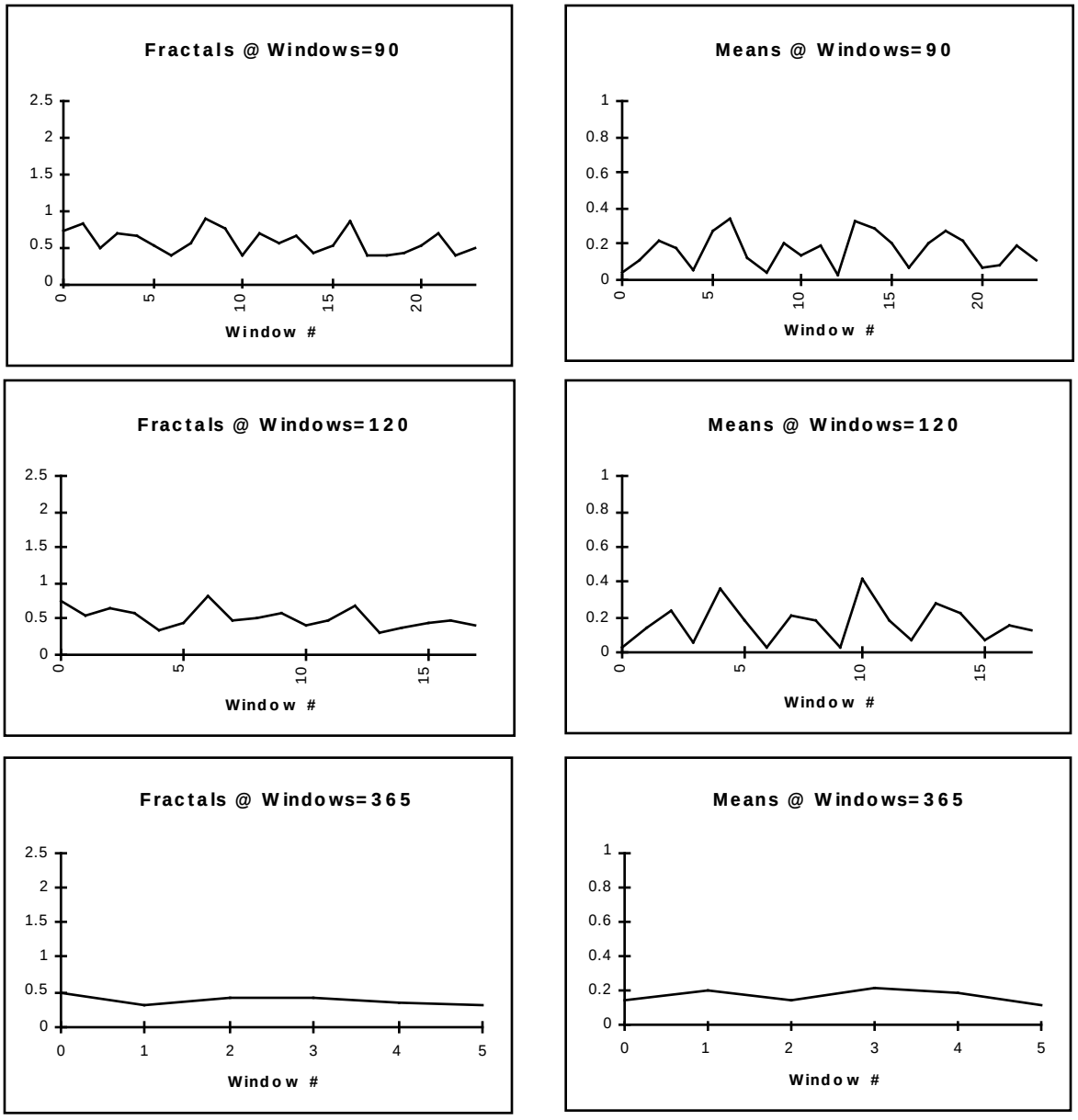


Figure 30b. Fractal dimensions of south Florida rainfall data.